THE PRECIPITATION EFFICIENCY OF WARM-SEASON MESOSCALE CONVECTIVE COMPLEXES IN THE UNITED STATES

by

JOSHUA D. DURKEE

(Under the Direction of Thomas L. Mote)

ABSTRACT

This study examines the precipitation efficiency of Mesoscale Convective Complexes (MCCs) during the "normal" year of 1982, drought year of 1983, and an anomalously wet year of 1993. The spatio-temporal patterns of MCC precipitation efficiency, as well as the synoptic environments conducive to MCC development and how they affect MCC precipitation efficiency are detailed. Results indicate that MCC precipitation efficiency is spatio-temporally dependent on the time of year, latitude of its occurrence, and storm dynamics. Ultimately, the time of year is the most significant factor in MCC precipitation efficiency because the latitude of the storm's development, and the synoptic patterns in which MCCs develop, are dependent on the time of season. However, the time of year only accounts for about 10 % of the variance in precipitation efficiency which indicates that other factors (e.g., wind shear, sub-cloud base moisture, etc.) may play a larger roll in determining MCC precipitation efficiency.

INDEX WORDS: Mesoscale Convective Complex, precipitation efficiency, precipitation rate, MCC storm type, storm dynamics

THE PRECIPITATION EFFICIENCY OF WARM-SEASON MESOSCALE CONVECTIVE COMPLEXES IN THE UNITED STATES

by

JOSHUA D. DURKEE

B.S., Western Kentucky University, 2000

A Thesis Submitted to the Graduate Faculty of The University of Georgia in Partial Fulfillment of the Requirements for the Degree

MASTER OF SCIENCE

ATHENS, GEORGIA

2003

THE PRECIPITATION EFFICIENCY OF WARM-SEASON MESOSCALE CONVECTIVE COMPLEXES IN THE UNITED STATES

by

JOSHUA D. DURKEE

Major Professor: Thomas L. Mote

Committee: Andrew J. Grundstein

Vernon G. Meentemeyer

Electronic Version Approved:

Maureen Grasso
Dean of the Graduate School
The University of Georgia
August 2003

DEDICATION

I would first and foremost like to dedicate this thesis to my child, who as of the time of writing this dedication, has only four weeks left before he or she is born. You are my striving factor for staying motivated, focused, and determined to accomplish such exciting, but difficult, tiring, stressful, and demanding tasks through all my studies, work, and in life. To my wife Becky, who has always loved, encouraged, and supported me throughout our ten years together. No words can describe my appreciation for you. This thesis is especially for you.

To my mom and dad, who helped me and encouraged me to pursue graduate school and to always pursue the challenges of life head on. Your love and support has made all of these challenges worthwhile. I dedicate this thesis to you. To my sister Kristen, her husband Jim, and my brother Colin, who have always been there for the much needed support and laughter. This thesis is for you. To my grandma and late grandpa, who have always loved, supported, and encouraged me throughout my life. This thesis is for you. And to my wife's parents, Lorraine and Dave, who have always shared their love and support. This thesis is for you.

And finally, to all of my friends and colleagues, who have always been there for the much-needed stress relieving times, whether it be storm chasing, traveling across the country just to catch a concert, sitting around playing music, laughing it up in the climate lab, or just hanging out at the house or apartment. Thank You.

ACKNOWLEDGEMENTS

I would like to thank the one person in my life who has helped me through my graduate work more than any, my wife Becky. Thank you for your strong will to put up with all the long hours I have spent away from you while working through my graduate studies, and particularly this thesis, and doing so while bearing our unborn child. Words cannot express my gratitude towards you. I love you and thank you for just being you.

I would like to thank Tom Mote who gave me his time and patience, and for lending me his expertise and extensive knowledge which helped guide me through much of my graduate studies, and particularly this thesis. I would also like to thank Tom for all the research and teaching opportunities he has given during my time here at The University of Georgia. For that, I am greatly appreciated. To Andrew Grundstein and Vernon Meentemeyer, thank you for all your insight and suggestions throughout my graduate studies, and particularly for this thesis. I too, am greatly appreciated.

Finally, I wish to thank Mace Bentley (Northern Illinois University), Randall Collander (Forecast Systems Laboratory/Cooperative Institute of Research in the Atmosphere), J. Michael Fritsch (Penn State University), and Richard Kane (National Weather Service -Pittsburgh) for the assistance of gathering data for this study and the suggestions they sent out.

To my good friends and colleagues, Jamie Dyer, for his willing effort to help me through the countless hours of computer programming, and Walker Ashley, for his extensive knowledge, help, and advice for much of this thesis.

TABLE OF CONTENTS

Page

LIST OF TABLES

Page

LIST OF FIGURES

Page

CHAPTER 1

INTRODUCTION

Since 1980, numerous studies have recognized the significance of precipitation contributed from mesoscale convective systems (MCSs). Among the classes of MCSs, attention has focused on the largest of all midlatitude convective weather systems, the mesoscale convective complex (MCC) (Rogers et al. 1985). MCCs are large, long-lived, highly organized type of meso-α scale[1] convective weather systems that exhibit a quasi-circular continuous cold cloud shield (Maddox 1980). Maddox (1980) defined MCCs based upon observable cloud-top characteristics in enhanced infrared (IR) satellite imagery that must meet specific temperature, spatial, and temporal criteria (Table 1.1.1). From the spatial and temporal thresholds set forth by Maddox (1980), MCCs are most significant in terms of their potential production of abundant amounts of rainfall over a large area (Tollerud et al. 1987; McAnelly and Cotton 1989).

Previous studies asserted that precipitation patterns of MCCs have significant social, economic, and agricultural effects across the Great Plains and Midwest. In particular, Rogers and Howard (1983) showed that a single MCC occurrence can produce enormous detrimental effects in terms of property and crop damage, injuries and deaths. MCCs have the ability to generate a variety of severe convective weather phenomena

---

[1] meso-α scale: length scales of 250-2500 km and duration of ≥ 6 h.

Table 1.1.1 Mesoscale Convective Complex Definition* from Maddox (1980). (Based on analyses of enhanced IR satellite imagery)

Mesoscale Convective Complex (MCC) Definition from Maddox (1980)		
Criterion	**Physical Characteristics**	
Size		Cloud shield with continuously low IR temperature -32°C must have an area 100,000 km^2
	B	Interior cold cloud region with temperature of -52°C must have an area 50,000 km^2
Initiation	Size definitions A and B are first satisfied	
Duration	Size definitions A and B must be met for a period of ≥ 6 hours.	
Maximum Extent	Contiguous cold-cloud shield (IR temperature -32°C) reaches maximum size.	
Shape	Eccentricity (minor axis/major axis) 0.7 at time of maximum extent.	
Terminate	Size definitions A and B no longer satisfied	
* some previous studies simplify this formal definition by removing size definition **A** or altering temperature thresholds.		

(e.g., high wind, large hail, and/or tornadoes), but undoubtedly, torrential rains and flash flooding are the most significant hazards produced from these systems (Maddox 1980). Annually, most convective storm fatalities in the United States occur from flash flooding events (Doswell et al. 1996).

Maddox (1980) found that one of five MCCs reported during 1978 produced injuries and/or deaths. Rogers and Howard (1983) found 27 of the 37 reported MCCs during 1982 were associated with heavy rain and/or flash floods that resulted in several injuries and deaths. Augustine and Howard (1988) indicated that 45 heavy rainfall/flash flood reports, 13 injuries, and 18 deaths were attributed to the 102 MCCs during 1986 and 1987. Of the 28 MCCs during 1993, 18 were associated with both the flash flooding and regional flooding in the central Plains (Anderson and Arritt 1998) that resulted in numerous injuries and deaths.

Knowledge of the spatio-temporal characteristics of MCC precipitation is crucial for understanding the impact these large rain-producing events have on society, and the agricultural communities that populate the Great Plains and Midwest. However, because of the detrimental effects MCC precipitation can cause, it is equally important to understand the capability of MCCs to process available water vapor in the form of precipitation for a given location and time of year. The concept of storm precipitation efficiency raises important questions:

- How does MCC precipitation efficiency change as the warm season progresses?
- How does precipitation efficiency change as MCCs develop further from the Gulf of Mexico (their primary source of moisture) (Tollerud et al. 1987 and Tollerud and Rogers 1991)?
- How does precipitation efficiency change with various synoptic patterns conducive to MCC development?
- Does higher (lower) MCC precipitation efficiencies contribute to "normal" and/or anomalous moisture conditions for a given year (e.g., drought vs. prolonged flooding)?
- What is the relationship between MCC precipitation efficiency and the intensity of the storm (i.e., rainfall rate)?

This thesis addresses the aforementioned questions by examining and determining the significance of the spatio-temporal characteristics of warm-season (defined here as April-August) MCC precipitation efficiency in the United States during the years 1982 ("normal" year), 1983 (drought year), and 1993 (anomalously wet year). Further, this thesis hypothesizes that MCC precipitation efficiency decreases as the warm season

progresses, as MCCs develop further away from the Gulf of Mexico, and as MCCs develop under weaker large-scale dynamics. Based on this hypothesis, MCC precipitation efficiency is dependent on the time of year, the location of the MCC's development, and the synoptic patterns in which they develop. The latitude, as well as the dynamics involved in a given MCC's occurrence are dependent on when the storm develops during the warm season. Therefore, MCC precipitation efficiency should be ultimately related to the time of year.

CHAPTER 2

BACKGROUND

A typical MCC produces at least 1 mm of precipitation encompassing an area of nearly 500,000 km^2 (i.e., approximately twice the size of Wyoming). The heaviest precipitation is associated with meso-β scale[2] regions of intense convection and tends to occur between storm initiation and maturation (Kane et al. 1987). MCC precipitation maxima are generally displaced 50 to 100 km equatorward of the cloud-shield centroid (McAnelly and Cotton 1989) in the southeast quadrant, followed by the northeast quadrant, indicating an asymmetrical precipitation pattern relative to storm motion (Kane et al. 1987). Collander and Tollerud (1993) suggested that the right flank is an area of preferential development due to the impinging southerly low-level jet relative to the storm's mean eastward motion. Kane et al. (1987) found that the southeast quadrant accounted for over half the heavy precipitation area. Knowledge of MCC precipitation characteristics is useful to meteorologists and hydrologists in forecasting heavy precipitation. A better understanding of flood control, soil moisture budgets, and water resource management could be quite beneficial for agricultural purposes (Kane et al. 1987).

---

[2] meso-β scale: length scales of 25-250 km and duration of < 6 h.

2.1 Characteristics Of MCC Precipitation

Aside from intense rainfalls and flash flooding, MCCs produce widespread beneficial precipitation required for the growing season in the region between the Rocky and Appalachian Mountains (Maddox et al. 1979; Fritsch et al. 1986; Tollerud and Collander 1993; Ashley et al. in press). Because MCC activity dominates this region during the warm season, the resultant precipitation can be valuable to the large agricultural community that thrives in this region (Ashley et al. in press).

Fritsch et al. (1986) found that mesoscale convective weather systems, including MCCs, accounted for 30 to 50% of the warm-season (seen here as April-September) rainfall in the region located between the Rocky Mountains and the Mississippi River. In a recent study, Ashley et al. (in press) compiled a 15-year MCC climatology (1978-1987, 1992, 1993, 1997-1999) and found that the average of 35 MCC occurrences a year contributed 8 to 18% of the annual warm-season (seen here as May-August) precipitation in this region. Additionally, Ashley et al. (in press) found that the MCC precipitation pattern exhibited an increase in both latitude and precipitation as the warm season progressed (Figure 2.1.1).

2.1.2 Effects Of MCC Seasonal Migration Patterns

The monthly MCC precipitation pattern illustrated by Ashley et al. (in press) concurred with previous studies and showed a typical poleward shift in MCC migration occurs as the warm season progresses (Augustine and Howard 1988). Kane (1985) indicated that MCC migration into the Midwest produces crucial July and August precipitation for the corn-growing season in Iowa. Fritsch et al. (1986) suggested that

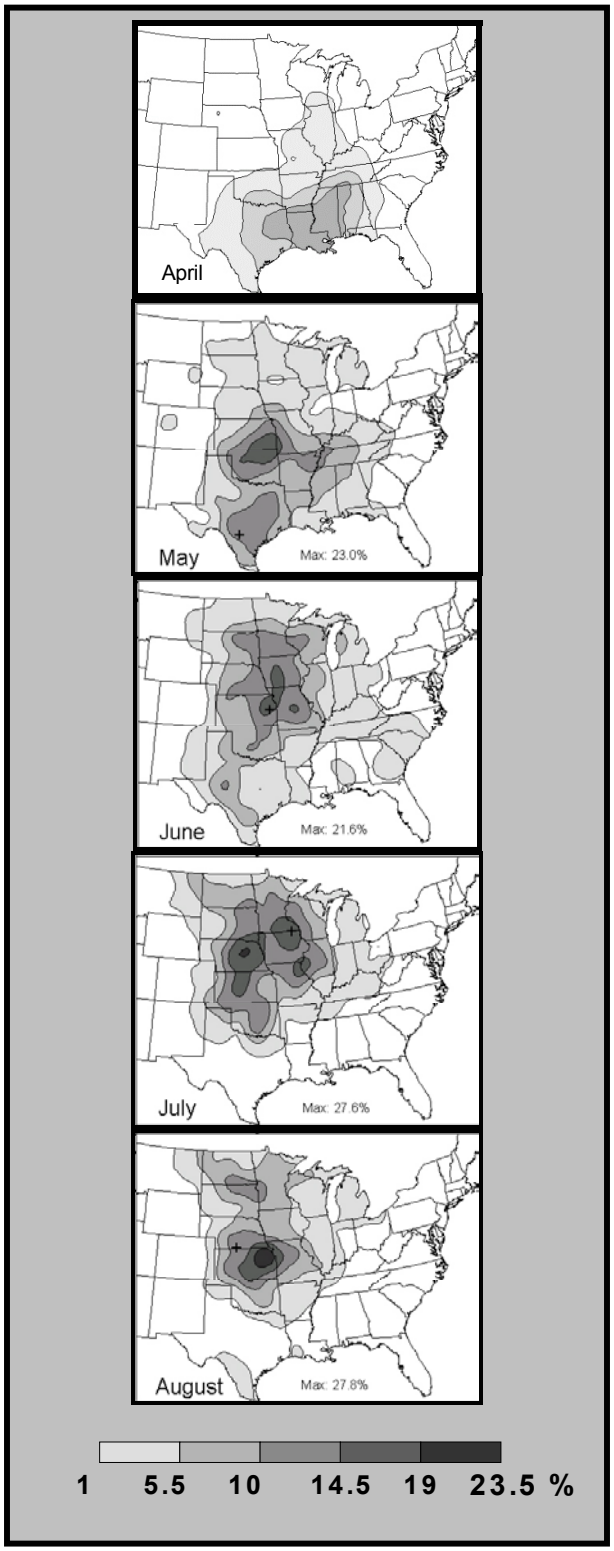

Figure 2.1.1. Spatial distribution of the average percentage of total MCC rainfall during April, May, June, July, and August. From Ashley et al. (in press).

MCC precipitation could hinder the onset of drought and help sustain a soil budget. For example, Kane (1985) found that despite below average MCC precipitation during 1983, the majority of Iowa's precipitation during the corn-growing season was still attributed to MCCs.

a. Frequency And Density

Previous literature illustrated that the mean MCC poleward migration throughout the warm season has significant effects on MCC size, duration, frequency, storm clustering, and precipitation totals. Ashley et al. (in press) found 34 MCC occurrences during April for a period between 1978 and 1999. The highest spatial density, represented by the concentration of -32ºC anvil cloud shield hours (see Table 1.1.1) over a given location, occurred over central Mississippi and western Alabama during this time. During May, 114 events occurred from 1978 to 1999, with a northwest shift in the highest density located over southeast Kansas, northeast Oklahoma, northwest Arkansas, and southwest Missouri, while a slightly smaller density maximum was also located over southern Texas. June marked the peak MCC occurrences of 133 with a slight northeastward migration of the density maximum into Missouri. Ashley et al. (in press) found MCC development in proximity to the Gulf of Mexico decreased whereas MCCs were more frequent in the Northern Plains and Upper Midwest during this time. The decline in MCC occurrences began with 125 in July with a density maximum over northern Iowa and southern Minnesota. A significant decline in MCC occurrences from 125 to 82 occurred in August. The density maximum during this time was located over the northeast corner of Kansas (Figures 2.1.2 and 2.1.3).

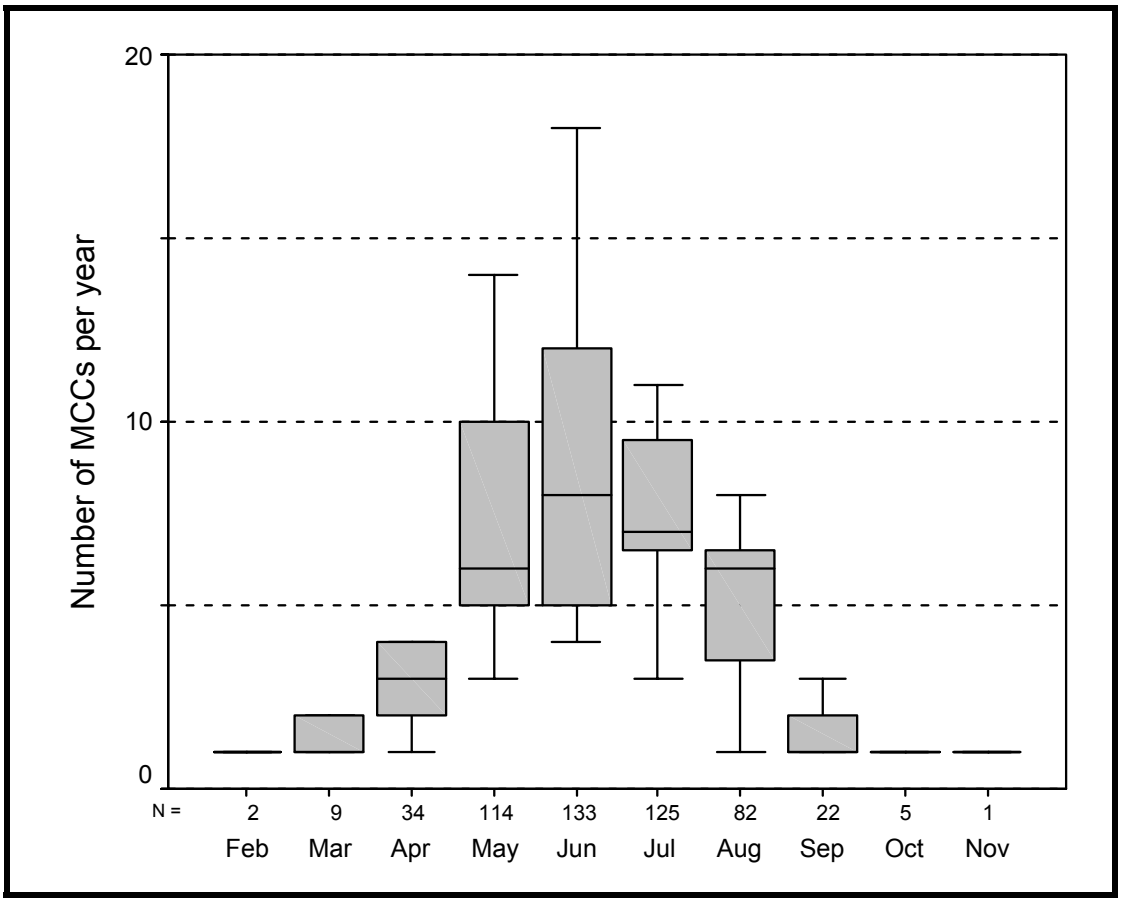

Figure 2.1.2. Box-and-whisker plot of annual MCC frequency derived from the 15-year dataset put forth by Ashley et al. (in press). The plots show the median (thick line), interquartile range (shaded), and outliers (i.e., the 10^{th} and 90^{th} percentile as whiskers) for the indicated months. Additionally, the total number of MCCs per month for all 15 years investigated is indicated along the x-axis. From Ashley et al. (in press).

As expected, the poleward migration of MCC density maxima corresponded with the monthly precipitation pattern previously mentioned. As MCCs developed further away from the Gulf of Mexico, not only did the frequency and density undergo changes, but also significant changes occurred in storm size, duration, and precipitation amounts.

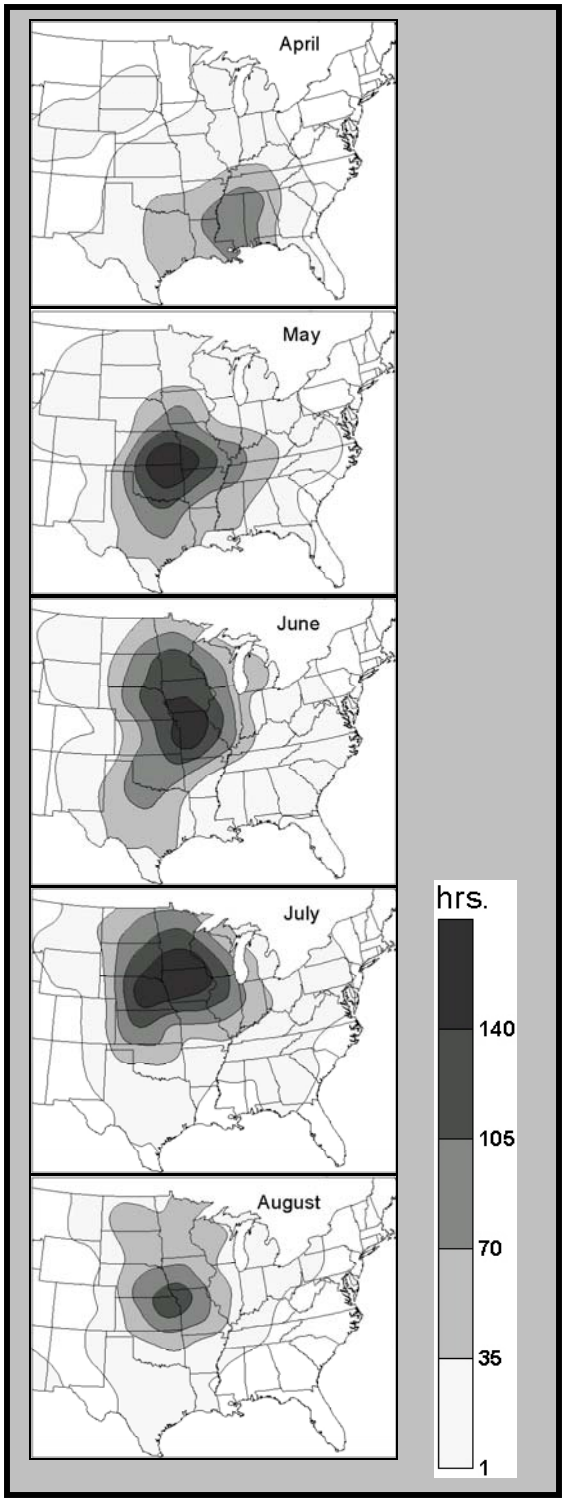

Figure 2.1.3. MCC densities derived from the total number of hours of -32°C cloud shield coverage for the warm season during 1978-1999. From Ashley et al. (in press).

b. Size, Duration, And Precipitation

Tollerud et al. (1987) and Ashley et al. (in press) found that MCCs with the largest areal extents generally developed in Gulf Coast states during April and May. Additionally, heavy precipitation was associated with these large spring MCCs containing maximum areal extents between 260,000 to 300,000 km^2. Tollerud and Rogers (1991) and Ashley et al. (in press) found MCCs that occurred in April were generally larger by nearly 50%, longer in duration by several hours, and produced greater than double the amount of total water volume. Although April and May had the highest variability in MCC size, duration, and rainfall amounts, the greatest extremes occurred in precipitation during these months. As the warm season progressed, the mean poleward shift in MCC migration corresponded well with both reductions in average size and mean precipitation amounts. Specifically, Tollerud and Rogers (1991) found that relatively low precipitation MCCs occurred during June. Interestingly, Ashley et al. (in press) found peak MCC frequency occurred in June (see Figure 2.1.2). Most MCCs in July and August had areal extents near 180,000 km^2 (Tollerud et al. 1987; Tollerud and Rogers 1991). Late season MCCs (July-August) were smaller than average early warm-season MCCs (April-May) with shorter life cycles (Figures 2.1.4 and 2.1.5).

Early warm-season MCCs generally had larger cloud shields, longer duration, produced more precipitation, and occurred less frequent when compared to the middle and latter portions of the warm season. However, despite the MCC characteristics previously mentioned, considerable monthly, annual, and interannual variability exists within each characteristic. Kane et al. (1987), Tollerud et al. (1987), and Tollerud and

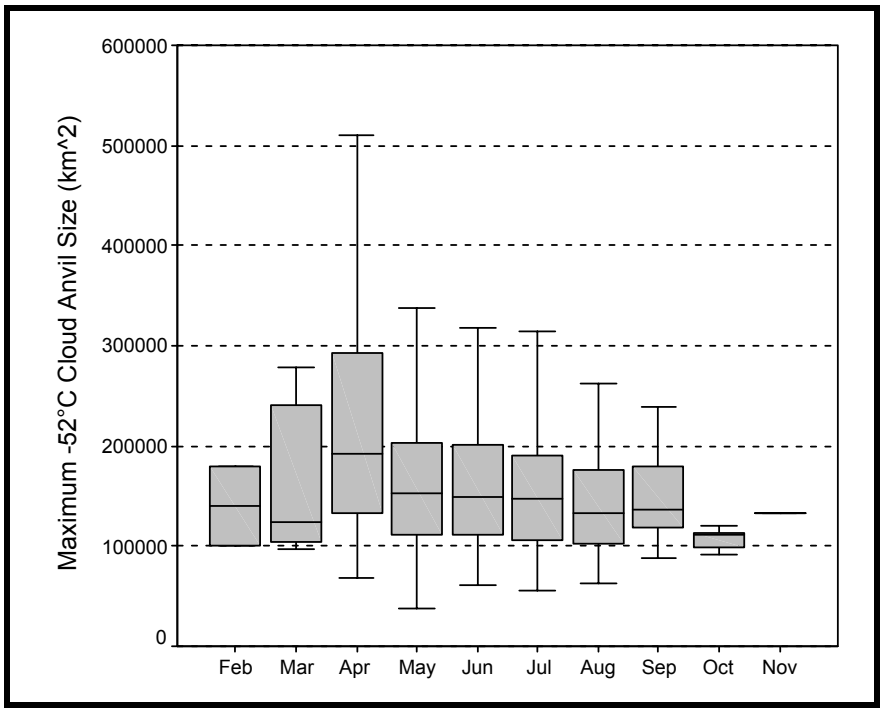

Figure 2.1.4. Box-and-whisker plot of the temporal distribution of maximum -52ºC anvil-cloud sizes for each month derived from the 15-year MCC dataset. From Ashley et al. (in press).

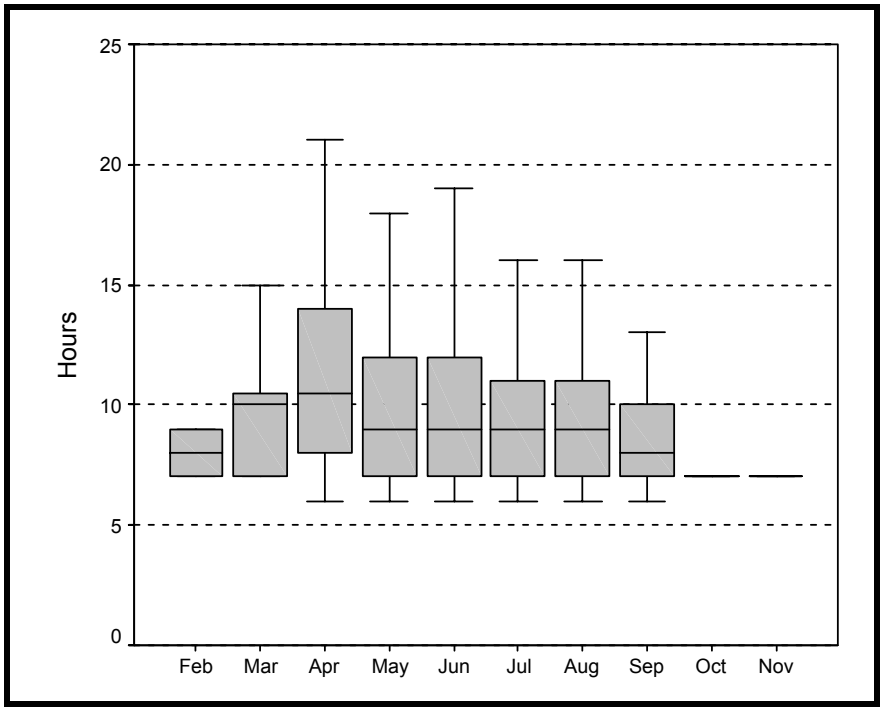

Figure 2.1.5. Box-and-whisker plot of the temporal distribution of MCC duration for each month derived from the 15-year MCC dataset. From Ashley et al. (in press).

Rogers (1991), Geerts (1998), and Ashley et al. (in press) have all attempted to explain the seasonal pattern of MCC location, size, duration, and precipitation.

2.1.2 Environments Conducive To MCC Development

Tollerud et al. (1987) and Tollerud and Rogers (1991) speculated that since moisture is the primary fuel source for MCC development, larger (smaller) MCCs may correspond with closer (further) proximity to the Gulf of Mexico. Therefore, heavier rain episodes could be expected closer to the Mississippi River basin, where ample moisture is available from the low-level jet. In addition to moisture supply, Geerts (1998) concurred with Tollerud and Rogers (1991) that MCC development during the early warm season is favorable due to rigorous baroclinic forcing from synoptic-scale circulations. In order to gain a better understanding of MCC precipitation characteristics and patterns, Kane et al. (1987) described four favorable synoptic settings for MCC development in relation to precipitation amount: *synoptic, mesohigh, frontal, extreme-right-moving (XRM).* For a thorough discussion of MCC and flash flood classifications, see Maddox (1979) and Merritt and Fritsch (1984).

a. MCC Storm Types

Synoptic MCCs generally develop during the earlier half of the warm season (April-June) along the warm side of a slow-moving or quasi-stationary cold front in advance of an upper-level long-wave trough. MCCs can often initiate deep within the warm sector beneath an area of strong upper-level diffluence (i.e., 250-200 hPa) (Kane et al. 1987). *Mesohigh* MCCs generally develop during July and August in the warm sector

apart from strong baroclinic zones (i.e., a time when large-scale dynamics are weak), just west of a 500 hPa long-wave ridge axis. However, *mesohigh* MCCs may develop near a frontal boundary and later propagate into the warm sector. Typically, *mesohigh* MCCs are initiated by an outflow boundary within a weak pressure gradient, in association with a weak upper-level short-wave trough (Kane et al. 1987). *Frontal* MCCs generally develop during the middle of the warm season along the cool side of a warm front or east-west quasi-stationary frontal boundary and are located west of a 500 hPa long-wave ridge axis (Kane et al. 1987). Finally, *XRM* MCCs, a subset of the *frontal* category, occur during the mid-to-late warm season under weak large-scale forcing (Kane et al. 1987). Although each MCC storm type favors certain dynamics and regions for development, with respect to the Great Plains and Midwest, an important feature common in all MCC development is the southerly flow of warm, moist, conditionally unstable air (Kane 1985; Kane et al. 1987; Maddox 1979).

b. MCC Storm-Type Precipitation

Kane et al. (1987) found considerable variability in precipitation amount among each storm type. For example, *synoptic* MCCs produced nearly twice the precipitation area and volume than *mesohigh* events. Precipitation contributed from frontal MCCs was between that of *synoptic* and *mesohigh* rainfall amounts. However, all MCCs in each category produced greater than 26 mm of average precipitation over an average area of 100,000 km^2. Since each category is present in specific regions and is temporally dependent, Kane et al. (1987) suggested that the difference in both precipitation area and magnitude may be indicative of the general weakening trend of large-scale dynamics

from the early-to-late warm season. As a result, the size of the MCC precipitation area during the latter portion of the warm season may have a greater dependence upon latent heat release and internal dynamics. Lastly, Ashley et al. (in press) suggested that large-scale changes in the atmospheric wave and jet-stream patterns might also affect the convective precipitation patterns within the region between the Rocky and Appalachian Mountains.

2.2 Precipitation Efficiency

Precipitation efficiency is defined as the ratio of mass water output (i.e., precipitation) to the influx of available water vapor mass into the cloud (Doswell et al. 1996). Precipitation efficiency is an important factor because it accounts for how capable MCCs are at depositing available moisture in the form of precipitation. With the tendency for MCCs to migrate poleward, become more frequent, and decline in size and duration as the warm season progresses, knowledge of how each characteristic affects the precipitation efficiency may lead to a better understanding of MCC behavior in certain regions (e.g., Gulf Coast vs. Northern Plains) during certain times of the year.

Storm frequency may have less effect on anomalous precipitation patterns when compared to a given storm's ability to process available moisture. Fritsch et al. (1986) found during a large-scale drought regime, mesoconvective weather systems, including MCCs, were just as frequent, but smaller than average with lower precipitation efficiencies. These results indicated that environmental factors (e.g., lower than average moisture supply) helped sustain the drought, regardless of average storm frequency. Likewise, Anderson and Arritt (1998) showed, by only considering 1993 events, high

storm density (i.e., reoccurring storms over the same area) and precipitation efficiency were significant factors in regional flooding, but not storm frequency. Previous studies have investigated the precipitation efficiency of various storm types including typical air-mass thunderstorms, squall lines, hail storms, winter storms, tropical storms, and MCSs (Braham 1952; Sellers 1965; Newton 1966; Auer and Marwitz 1968; Marwitz 1972; Foote and Fankhauser 1973; Fankhauser 1988; Doswell et al. 1996; Allen 2002). Numerous environmental factors (e.g., available moisture, wind shear, cloud-base area, cloud-base height) have also been suggested to influence the precipitation efficiency.

2.2.1 Previous Precipitation Efficiency Research

Braham (1952) represents one of the earliest attempts to quantify water and energy budgets of typical air-mass thunderstorms. Using both sounding and surface station data, Braham (1952) found the average total inflow was 8.9×10^8 kg with an average rainfall total of 10^8 kg. Based on these findings, typical air-mass thunderstorms had an average precipitation efficiency of approximately 11%.

Newton (1966) examined certain characteristics of internal circulations in large, sheared cumulonimbus clouds. In particular, Newton (1966) used rawinsonde data and radar observations to determine the water vapor flux through the updraft, as well as surface precipitation contributed from a passing squall line through Oklahoma City on 21 May 1961. The precipitation efficiency of the squall line was calculated at 50%, nearly five times that of the typical air-mass thunderstorm found by Braham (1952). Newton (1966) suggested a probable reason for higher efficiencies in larger storms such as squall lines, is the water vapor mass flux in the updraft is one to two orders of magnitude greater

compared to a typical air-mass thunderstorm. Additional reasons for greater efficiencies in storms of this type included longer life-cycles (in concurrence with McAnelly and Cotton 1989), upper-level divergence at lower pressures with smaller mixing ratios, and less entrainment leading to minimal evaporative loss near cloud edges (Newton 1966).

Auer and Marwitz (1968) examined the precipitation efficiency of eight hailstorms in northeast Colorado and South Dakota, using aircraft measurements from the cloud base. In their study, precipitation efficiency was defined as the ratio of the surface precipitation rate to moisture flux through the cloud base at the 800 mb level. The rainfall rate was measured using Plan Position Indicator (PPI) radar imagery and surface rain gauge reports. Auer and Marwitz (1968) found precipitation efficiencies ranged from 21-120%, with the latter exceeding 100% due to the lack of updrafts ingesting moisture into the storm. Simply put, instantaneous flux measurements can create a condition of infinite efficiency where moisture inflow ceases while precipitation continues (Fankhauser 1988). For example, Doswell et al. (1996) stated that at the beginning stage of a convective storm when updrafts dominate, no precipitation falls and precipitation efficiency is 0%. During the mature stage when both updrafts and downdrafts circulate, efficiency is between 0 and 100%. Once the storm begins to dissipate, downdrafts dominate, and inflow ceases, rainfall may continue rendering infinite efficiency. Therefore, instantaneous efficiency measures are not meaningful and makes sense to integrate the ratio over the storm's life cycle (Doswell et al. 1996; Fankhauser 1988) (Figure 2.2.1). A generalized view of how this ratio typically behaves during the life cycle of a precipitating thunderstorm is shown in Figure 2.2.2.

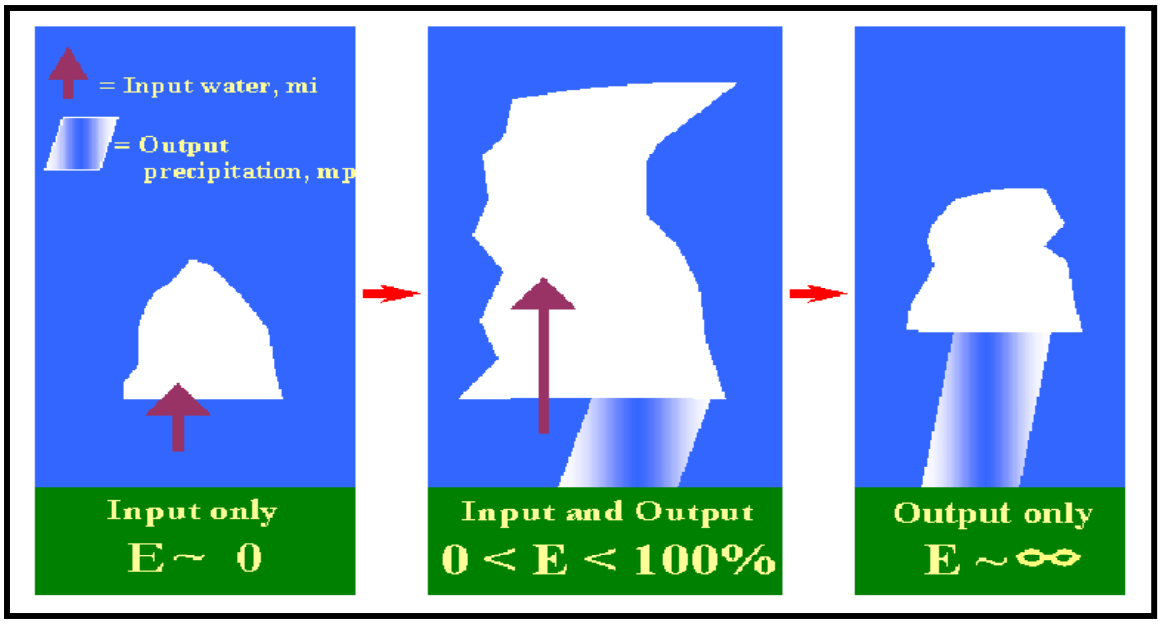

Figure 2.2.1. Schematic illustration of instantaneous precipitation efficiency during the growth and decay cycles throughout typical storm duration. From Allen (2002).

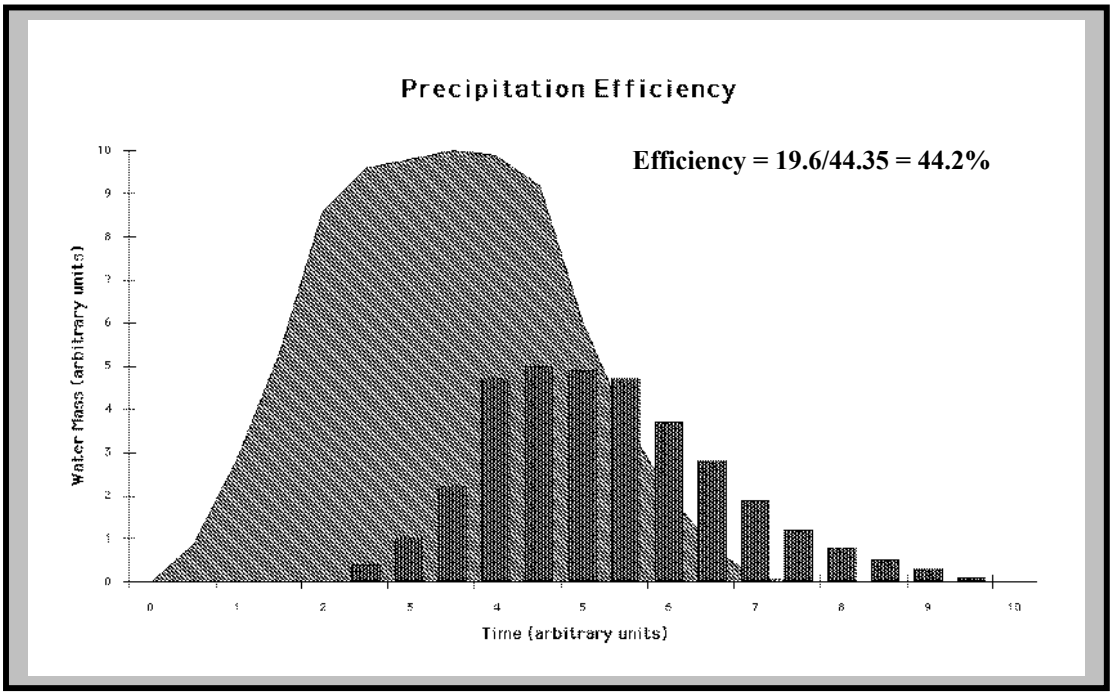

Figure 2.2.2. Schematic depiction of average water vapor flux (hatched area beneath the curve) and precipitation (vertical bars) during the life cycle of a precipitating system. For this illustration, the cumulus stage is represented by 0-3 time units, the mature stage is represented by 3-6 time units, and the dissipating stage is representative of 6-10 time units, where unit time is arbitrary. The resultant precipitation efficiency is approximately 44 percent. From Doswell (1996).

Marwitz (1972) adapted the same precipitation efficiency measurements as Auer and Marwitz (1968), along with results from previous studies, in an attempt to determine a relationship between environmental wind shear and precipitation efficiency. Results showed a negative correlation suggesting high (low) shear environments lead to less (more) efficient storms. Marwitz (1972) suggested storms that exhibit strong wind shear increase entrainment of cool dry air which acts to increase evaporation, erode cloud boundaries, and thus, decrease precipitation efficiency.

In a similar study to Auer and Marwitz (1968), Foote and Fankhauser (1973) considered the sub-cloud airflow and moisture budget of a northeast Colorado hailstorm on 22 July 1972. In their study, precipitation efficiency was calculated using the ratio of surface precipitation to moisture influx. Using a combination of radar, rawinsonde data, and a surface data, Foote and Fankhauser (1973) found the hailstorm to have a precipitation efficiency of 15%, low compared to the aforementioned findings. Foote and Fankhauser (1973) agreed with Marwitz (1972) that high wind shear acted to decrease the efficiency of the storm. Foote and Fankhauser (1973) indicated that storm precipitation efficiencies near 15% are most likely associated with supercell storms that develop in high-shear environments. However, this suggestion may only be applicable for unicellular storms, not merging cells in MCS formation (Allen 2002).

Data gathered through aircraft measurements, soundings, and a surface mesonetwork from the Convective Precipitation Experiment (CCOPE), were used in a comprehensive study by Fankhauser (1988) to compare the precipitation efficiency (defined as the ratio of surface precipitation to water vapor inflow) of seven mature-phase storms with several physical and environmental parameters. The precipitation efficiency

from the seven storms ranged from 19-47%. Since surface rainfall measurements were inadequate due to a low density rain gauge network, radar data was used for each event. Fankhauser (1988) indicated potentially important factors (e.g., microphysical processes, moisture inflow above the cloud base, etc.) are commonly neglected in precipitation efficiency measurements and further research is necessary for better efficiency measures.

To add to the statistical analyses performed by Marwitz (1972), Fankhauser (1988) examined other environmental factors that possibly influence precipitation efficiency. The results disagreed with Marwitz's (1972) results and showed wind shear did not have an inverse relationship with precipitation efficiency. However, a small dataset and low-to-moderate shear measurements showed a neutral relationship between wind shear and precipitation efficiency, indicating an inadequate sample. Further, a low (high) Bulk Richardson Number (R*), the ratio of convective available potential energy (CAPE) to kinetic energy (KE -associated with low-level wind shear), was anticipated to correlate with low (high) precipitation efficiency. Again, no relationship was established most likely due to a small dataset. Problems using the small dataset further led to an inability to establish any possible relationship between precipitation efficiency and CAPE. A positive correlation did exist between KE and precipitation efficiency. The association between the mean cloud-base area and precipitation efficiency also showed a positive correlation. The largest storms, most likely strongest dynamically, exhibited the highest precipitation efficiency. Lastly, increased cloud-base mixing ratios increased efficiency, whereas increased cloud-base height showed a negative correlation. The latter correlation is likely explained by greater evaporation with higher cloud-base heights. Although the research performed by Fankhauser (1988) investigated more environmental

factors (and how they affect precipitation efficiency) than prior studies, a larger dataset, accompanied by more statistical analyses, are required for a better representation of the relationship between precipitation efficiency and the various environmental factors.

To construct a climatology of average precipitation efficiency, Sellers (1965) calculated a ratio of mean daily precipitation to average precipitable water. In this form of the ratio, precipitable water, the amount of water vapor in a fixed, integrated vertical column of air extending from the surface to the upper levels of the atmosphere, represents the available moisture intake for a given storm to condense for rainfall production. Therefore, this ratio becomes a measure of average moisture that precipitates to the surface on an average day. However, it is important to note this definition does not take into account the cause of condensing water vapor (e.g., dynamic or microphysical processes). Instead, Sellers' (1965) definition demonstrates mean water vapor transports over a given time period (Allen 2002).

Sellers (1965) found a steady decline in average precipitable water values from the equator to the poles, as a result of poleward decreasing temperatures. Low water vapor content in the higher latitudes was generally accompanied by low precipitation rates. However, the correlation between a poleward decrease in low precipitation rates due to a decline in water vapor amounts becomes skewed over many desert regions that have relatively high quantities of water vapor. Therefore, other mechanisms for condensing water vapor must be considered. For example, low precipitation rates in areas containing higher quantities of water vapor might be accounted for by the stable atmosphere found in desert regions. The stability suppresses rising air and the resultant adiabatic cooling process. In contrast, the combination of instability, cyclonic motion,

and large-scale ascending air, provides an ideal condition for condensing large amounts of moisture. Moreover, Sellers (1965) illustrated that orographic effects acted to increase (decrease) precipitation efficiency on the windward side (lee side) of large mountain ranges.

Sellers (1965) found that precipitation efficiency is greatest (19%) between 30-40ºN. Spring (April-May) MCCs generally develop within this latitudinal band. Furthermore, precipitation efficiency between 40-50ºN latitude decreased to 15%, which coincides with Sellers' (1965) findings of comparatively low efficiencies during July – both a location and time when MCCs are near peak frequency.

Finally, Allen (2002) investigated the precipitation efficiency of warm-season MCSs in Missouri (and portions of the surrounding states) using Sellers' approach. Allen's (2002) results showed average precipitation efficiencies near 25%. Allen (2002) indicated that averaging storm-total precipitation might have led to lower efficiencies. For example, fast-moving systems such as those in Allen's (2002) study resulted in over smoothing of the data. In other words, six-hour average precipitation totals did not take into account high precipitation deposition at any given hour and led to lower efficiencies. Allen (2002) also analyzed environmental factors that have been theorized to influence precipitation efficiency. Findings included a positive correlation between sub-cloud-base relative humidity and precipitation efficiency. An inverse relationship was found between both convective inhibition (CIN) and wind shear, and efficiency. Allen (2002) is also the first to attempt a predictive equation for MCS precipitation efficiency for the improvement of quantitative precipitation forecasts (QPFs).

2.3 Summary

Previous studies (Maddox et al. 1982; Augustine and Howard 1988; Tollerud and Rogers 1991; Anderson and Arritt 1998; Anderson and Arritt 2001; Ashley et al. in press) have found MCCs are warm-season phenomena that primarily occur between the Rocky and Appalachian Mountains. In addition to the spatial and temporal MCC distributions, Maddox et al. (1979), Fritsch et al. (1986), Tollerud and Collander (1993), and Ashley et al. (in press) have determined the significance of MCC-induced precipitation on the overall hydroclimate of the eastern two-thirds of the United States.

MCC frequency and density is theorized to play a significant role in "normal" and anomalous precipitation patterns. While this is true, previous research (Braham 1952; Sellers 1965; Newton 1966; Auer and Marwitz 1968; Marwitz 1972; Foote and Fankhauser 1973; Fankhauser 1988; Doswell et al. 1996; Allen 2002) illustrated that an underlying mechanism that determines the amount of precipitation is the storm's efficiency. Because the intensity of a given storm's precipitation is dependent upon its ability to process the available moisture (Doswell et al. 1996), and with concerns of flash floods produced by MCCs, an examination of the precipitation efficiency within these types of storms is needed. Within the meteorological community, serious challenges can arise when trying to anticipate and quantify the magnitude of heavy precipitation and/or flash flood producing events (Doswell et al. 1996). Knowledge of average storm precipitation efficiencies, particularly by location and time of year, will aid in QPFs of such events. As the precipitation forecasts are improved, then regions dependent on MCC rainfall, as well as regions prone to flash flooding from MCC rainfall, will be better prepared for these types of convective mesoscale systems.

This thesis determines the significance of warm-season MCC precipitation efficiency in relation to the 1983 drought, anomalously wet period during 1993, and the maintenance of "normal" soil moisture levels during 1982, an average year. Specifically, MCC precipitation efficiencies during the early warm season (April-May) are compared to those during the latter portion of the warm season (June-August). This study also investigates the relationship between warm-season MCC precipitation efficiency and precipitation rates. Finally, the relationship between MCC storm-type classifications from Kane et al. (1987) and precipitation efficiency is established. Because MCCs typically exhibit latitudinal variation throughout the warm season, and the climatological trend of precipitation efficiency decreases both poleward between 30-50º latitude (approximately the latitudinal range of MCC development) and as the warm season progress, it is hypothesized that as MCCs develop further from the Gulf of Mexico, the precipitation efficiencies should decrease. Additionally, because MCC storm types are also specified by space and time, it is further hypothesized that stronger (weaker) dynamics correlate with higher (lower) MCC precipitation efficiency.

CHAPTER 3

DATA AND METHODOLOGY

Previous research illustrated that various methods have been applied for calculating precipitation efficiencies for numerous storm types. The results from these studies provided useful information about precipitation efficiency characteristics and the environmental factors that influence its measures. It is important to recognize that while the methods for calculating precipitation efficiency have commonly changed, the definition has remained the same. The methods in which precipitation efficiency was calculated depended on the focus of the research, and available data during both the study period and time the research was conducted. This study will determine MCC precipitation efficiency during the "normal" year of 1982, drought year of 1983, and the anomalously wet year of 1993, by using Sellers' (1965) efficiency equation.

3.1 Study Period

During 1982, there were 32 MCCs during April-August. Although portions of Missouri, Iowa, Texas, and Oklahoma received above average precipitation (7.5-30 cm, 3-12 inches), no large region within the central United States exhibited anomalous precipitation patterns (Figure 3.1.1). Further, the position of the Bermuda High allowed for a persistent southerly flow of warm moist air from the Gulf of Mexico into the central United States (Wagner 1983). In contrast, anomalously high temperatures and low

precipitation occurred during 1983 (Ludlum 1983). Although 28 MCCs occurred in the central United States, portions of Iowa, Missouri, Nebraska, Kansas, Oklahoma, and Texas received below average precipitation (5-20 cm, 2-8 inches) (Figure 3.1.2). An upper-level, large-scale anticyclonic ridge was positioned over much of central United States. As a result, the atmosphere was stabilized and the southerly flow of Gulf moisture was weakened. The feedback mechanisms produced from this synoptic pattern included strong convective inhibition, anomalously low precipitation, and higher than average temperatures (Fritsch et al. 1986).

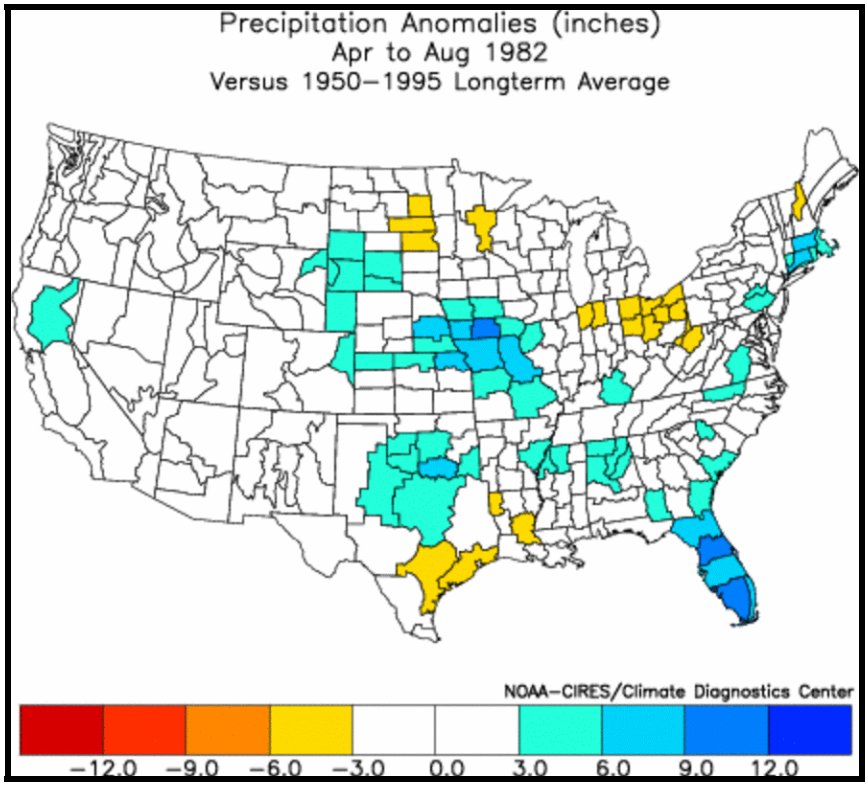

Figure 3.1.1. Precipitation anomalies by climate division from April-August during 1982 (http://www.cdc.noaa.gov/Usclimate/Usclimdiv.html).

Kunkel et al. (1994) characterized 1993 as having "the most devastating flood of modern times." This anomalously wet period was preconditioned by above-average

precipitation and saturated soils that began in July 1992. Following July 1992 were large areas of persistent heavy rainfall that fell along the upper Mississippi River basin throughout the warm season during 1993 (Kunkel et al. 1994). Anderson and Arritt (1998) found that these large areas of heavy rainfall were attributed to persistent elongated convective systems (PECS) and the 27 MCCs that occurred during April-August. An extensive region extending from North Dakota to Missouri and Wisconsin to Kansas received above average precipitation (5-20 cm, 2-8 inches) (Figure 3.1.3). The upper-level features included a high amplitude wave pattern with a ridge positioned over the Midwest, which allowed for sufficient moisture transport from the Gulf of Mexico into the Great Plains region (Anderson and Arritt 1998).

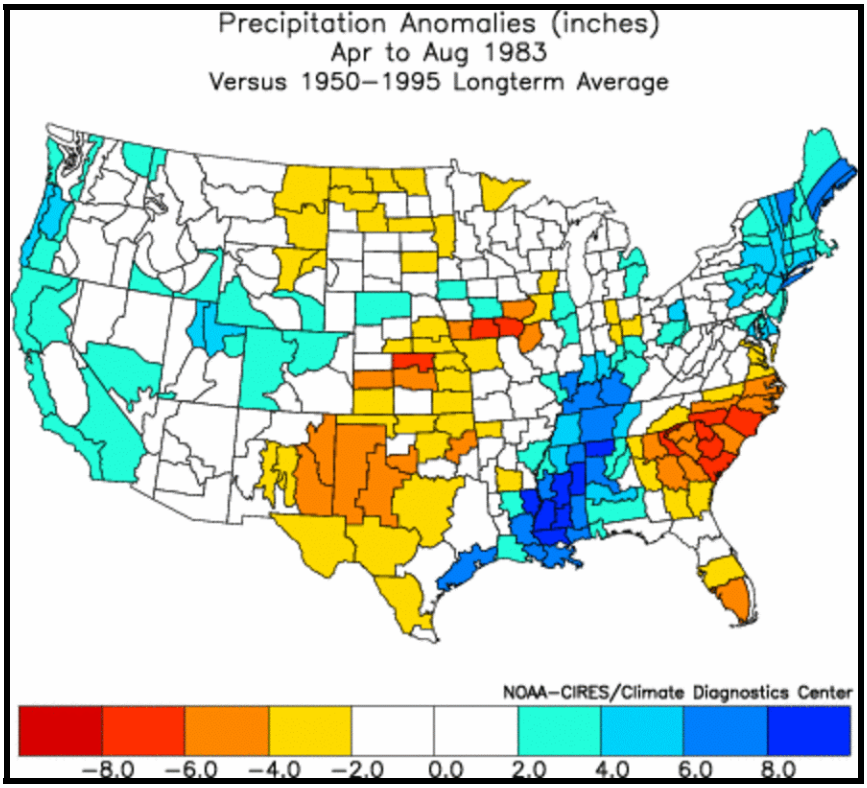

Figure 3.1.2. Precipitation anomalies by climate division from April-August during 1983 (http://www.cdc.noaa.gov/Usclimate/Usclimdiv.html).

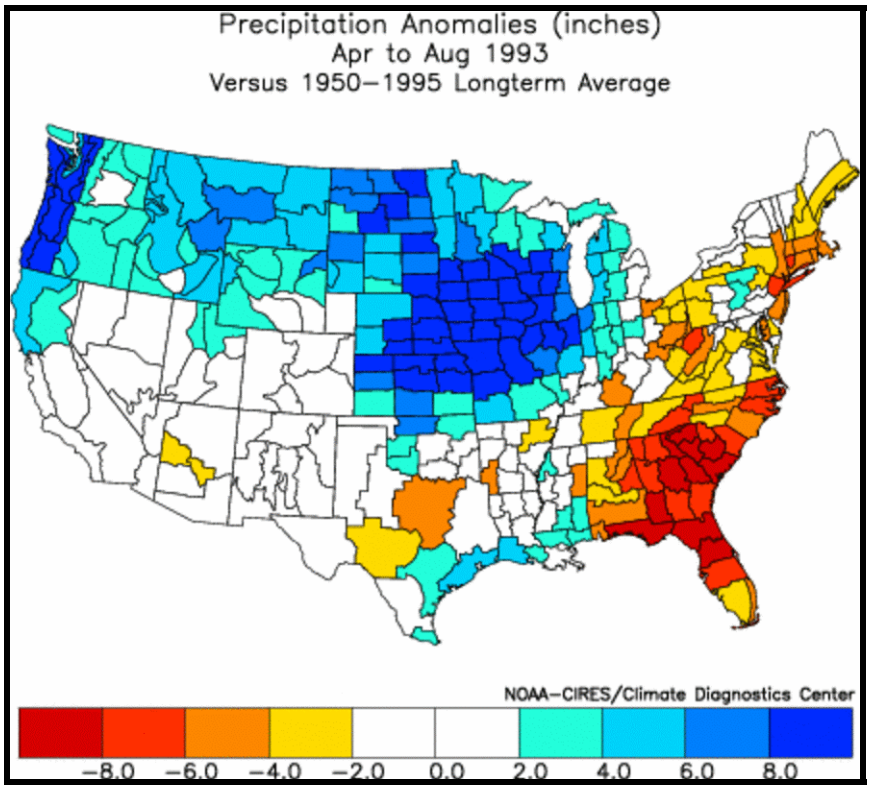

Figure 3.1.3. Precipitation anomalies by climate division from April-August during 1993 (http://www.cdc.noaa.gov/Usclimate/Usclimdiv.html).

3.2 Data

To determine and compare precipitation efficiencies of MCCs during 1982, 1983, and 1993, this study employed the 15-year MCC climatological dataset assembled by Ashley et al. (in press), that was originally derived from Ed Tollerud (NOAA Forecast Systems Laboratory) and Chris Anderson (Iowa State University). The MCC dataset includes the three critical stages of storm development (i.e., initiation, maximum areal extent, and termination), time each stage occurred, maximum extent of both size **A** and **B** definitions (see Table 1.1.1), and the location of the –32ºC anvil centroid during each stage (Table 3.2.1). Storm initiation commences once both size **A** and **B** criteria

Table 3.2.1. Example of MCC characteristics used in Ashley et al. (in press) study. This dataset employed from Tollerud (1993) includes number of MCCs during a given year, time during each critical stage (given by month, day, hour, and UTC), maximum areal extent of –32ºC and –52ºC cloud shield (km^2), and latitude and longitude of –32ºC anvil centroid during each critical stage.

YEAR	INIT.	MAX	TERMINATE	CLOUDTOP	CLOUDTOP	INIT.	INIT.	MAX	MAX	TERM.	TERM.
EVENT #	MDDHHMM	MDDHHMM	MDDHHMM	<32 km^2	<52 km^2	LON	LAT	LON	LAT	LON	LAT
8301	3150200	315930	3151230	178000	103000	99	41	95.5	43	93.5	44
8302	4010900	4011200	4011700	495000	233000	96	37.5	92.5	38	89	39.5
8303	4050030	4050600	4051800	420000	248000	90.5	34	87.5	36.5	84.5	35.5
8304	4061600	4061800	4070130	255000	69000	89.5	32.5	88.5	33	87	32.5
8305	4271500	4271800	4280500	223000	108000	96	39.5	94.5	39.5	86	41.5

(Maddox 1980) are met, while termination is when the MCC no longer exhibits the size criteria. Due to an incomplete dataset, "first storms", initial storm cells that later merge for subsequent MCC formation, were not compiled by Ashley et al. (in press) and thus, were not used in this study. For the years 1982, 1983, and 1993, 95 MCCs were documented during the warm season (April-August).

3.2.1 Precipitation Data

Additional data includes hourly MCC precipitation totals for each event. Ashley et al. (in press) compiled hourly precipitation data (including both MCC and non-MCC precipitation) using a network of National Weather Service (NWS) Cooperative Observer Program (COOP) and first-order stations from the National Climatic Data Center's (NCDC) TD-3240 (HPD; Hammer and Steurer 2000). Ashley et al. (in press) have taken into account the errors using this dataset described by Groisman and Legates (1994) and Brooks and Stensrud (2000). Such errors included precipitation underestimation, lack of objectivity when trying to ascertain if large precipitation amounts were produced from

inaccurate data, and ineffective areal-mean estimates in orographic regions. These sources of error did not significantly affect Ashley et al. (in press) results since the fraction of MCC to non-MCC precipitation (i.e., not precipitation totals) was utilized, precipitation was spatially averaged, and most MCC precipitation occurred within the Great Plains and Midwest.

3.2.2 Precipitable Water Data

NOAA-CIRES Climate Diagnostics Center's NCEP/NCAR reanalysis data provided instantaneous, four-times daily (i.e., 0Z, 6Z, 12Z, and 18Z) precipitable water values at a 2.5º latitude by 2.5º longitude resolution. One limitation of using precipitable water is that it is a volumetric measurement of water vapor of an entire atmospheric column, whereas moisture is usually available to a storm at lower levels (i.e., below the inflow region). However, since water vapor in the upper levels is very low to negligible due to lower temperatures and reduced moisture of less dense air, precipitable water approximates the available moisture at low levels (Allen 2002). Another disadvantage is the relatively low spatial resolution of the reanalysis dataset. The low spatial resolution may also not fully capture the variability of precipitable water surrounding a given MCC. Nevertheless, the reanalysis data represents the only available precipitable water dataset with a sufficiently long time series and spatial coverage to meet the requirements of this study.

3.3 Precipitation Efficiency Equation

The methods performed by Ashley et al. (in press) gave MCC tracks with approximate anvil centroids, areal extents, motion, and precipitation amounts at any given hour during the entire MCC life cycle. To accurately measure a given storm's precipitation efficiency, a time-average of the storm's life cycle should be taken into account (Doswell et al. 1996). Therefore, this study used Sellers' (1965) precipitation efficiency equation given by:

$$\overline{PE} = \left[\frac{\overline{P}_{LC}}{\overline{PW}_{LC}} \right] \cdot 100\% \qquad \textbf{(3.3.1)}$$

where $\overline{P}_{LC}$ is the mean precipitation over the storm's life cycle and $\overline{PW}_{LC}$ is the mean precipitable water over the storm's life cycle. The result gives an average precipitation efficiency ($\overline{PE}$) for the entire event. Sellers' (1965) equation represented the only approach to calculating *storm-average* precipitation efficiencies.

3.4 Methodology

To calculate MCC precipitation efficiency, this study used hourly average precipitation totals and hourly average precipitable water data. Therefore, Sellers' (1965) efficiency equation was adjusted to calculate the average MCC precipitation efficiency for each hour during the storm's lifecycle and ultimately, for the entire event. This form of the equation was employed to add to the extensive MCC hourly dataset previously compiled by Ashley et al. (in press), which allows for a consistent dataset for future MCC research.

3.4.1 Anvil Cloud Track Interpolation And Precipitation

To determine MCC precipitation, Ashley et al. (in press) applied a simple interpolation method. Since –32ºC anvil centroids during each critical stage were identified by latitude and longitude for a specific time, anvil centroids, centroid tracks, and areal extents were interpolated in a linear fashion for each hour between stages. The result gave an average storm vector for each event (Figure 3.4.1). This method was based on Collander and Tollerud's (1993) study, which found that MCC movement was linear and cloud expansion/contraction rates between each stage monotonic. Additionally, this method was further supported by McAnelly and Cotton (1989). MCC precipitation was determined by the amount of precipitation recorded beneath the –32ºC anvil cloud shield. The dilemma with this method was no data for the –32ºC cloud shields existed after 1992. Therefore, Ashley et al. (in press) derived an average ratio of 1.31 from the –32ºC to –52ºC cloud shield radii during 1978 to 1987 to calculate an estimated area of the –32ºC cloud shields for MCCs from 1978 to 1999.

The cloud-track technique put forth by Ashley et al. (in press) assumed MCC precipitation fell exclusively beneath the circular –32ºC cloud shields, along linear centroid tracks. Given these assumptions, the validity of this interpolation method was tested by overlaying NASA Marshall Space Flight Center's Global Hydrology Resource Center (GHRC) 8-km, 15-minute reflectivity data with 28 isolated events during 1997 to 1999. Ashley et al. (in press) found that isolated events better illustrated the spatial and temporal precipitation boundaries and could therefore be objectively determined. Additional testing included using an expanded radius by increasing –32ºC anvil cloud shield by a fraction of 1.4. Observations were also spatially weighted onto a 1º latitude

by 1º longitude grid. Finally, the differences between the –32ºC cloud shield and the expanded radius were examined. Results from these tests showed that the majority of areas that received heavier MCC precipitation were accounted for, and thus, the area beneath the –32ºC cloud shield was sufficient for calculating MCC precipitation (Figure 3.4.2).

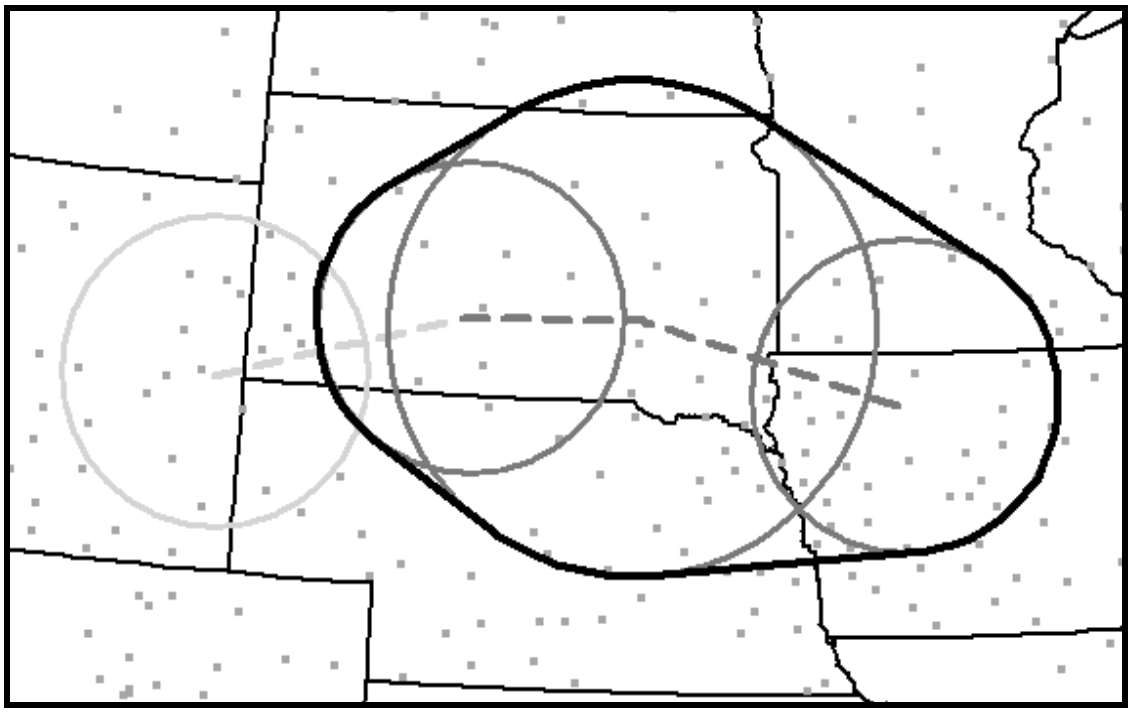

Figure 3.4.1. Schematic representation of the cloud-track technique put forth by Ashley et al. (in press), that was used to determine MCC-related precipitation observations across the Central and Northern Plains during 4 June 1982. The circles represent the -32°C anvil during the three critical stages of the MCC's life cycle. For this example, the initial storm cells (westernmost circle) are illustrated. Subsequent circles include storm initiation, maximum areal extent, and termination (see Table 1.1 for MCC criteria). The hourly precipitation dataset used in this study are indicated by the gray dots. All observations positioned beneath the black outline, representative of the anvil track, were included in the event's precipitation totals (after Tollerud and Collander 1993). From Ashley et al. (in press).

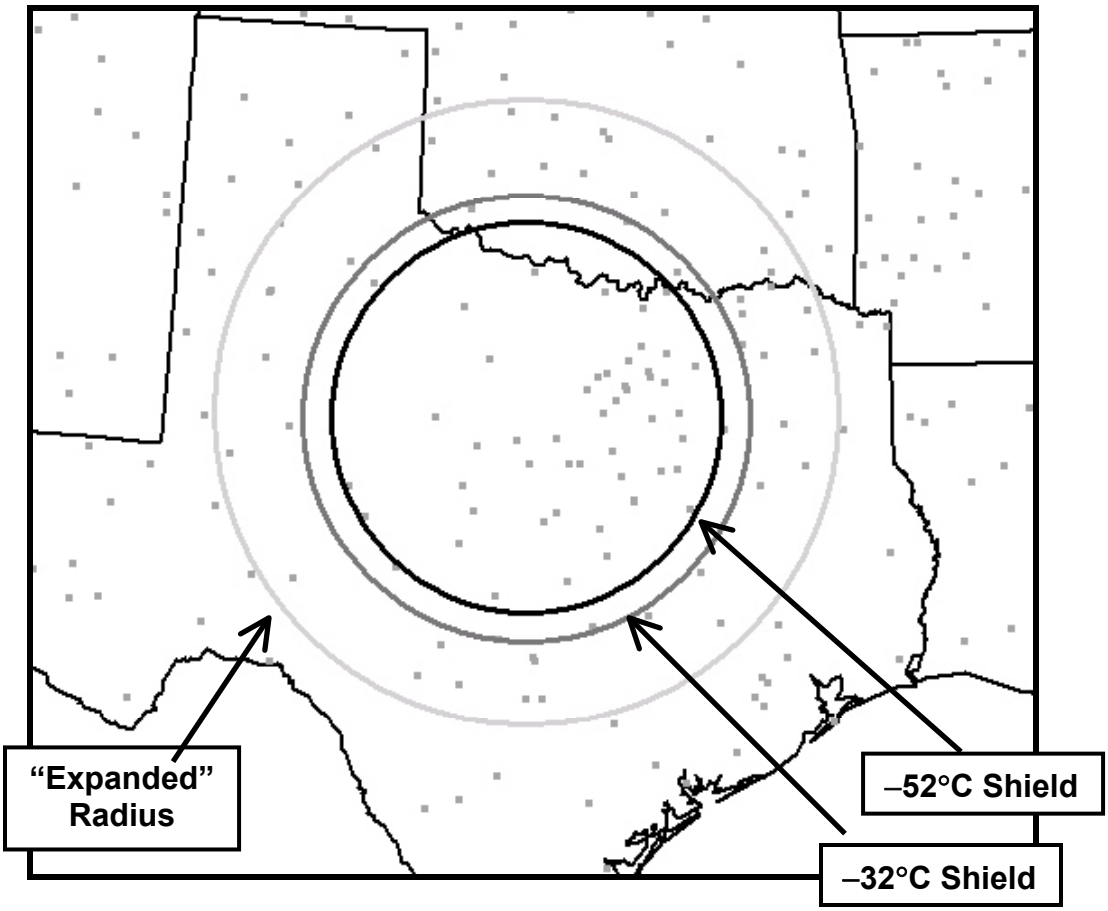

Figure 3.4.2. As in Figure 3.4.1, except illustrating the various radii utilized in testing the MCC cloud-track technique. The radius of the -32°C cloud shield, radius of the -52°C cloud shield, and the expanded radius (i.e., 1.4 times the -32°C cloud shield radius) are based on the averages for the 527 events in the 15-year dataset. Hourly precipitation dataset stations with precipitation data used in this study are indicated by the gray dots. From Ashley et al. (in press).

3.4.2 Precipitable Water Interpolation

In order to determine the coordinates of the four-dimensional precipitable water matrix during each critical stage, the longitudinal and latitudinal range of centroid locations, as well as the areal coverage range of the –32ºC cloud shields were considered. It is assumed that water vapor mass input exhibits a quasi-sinusoidal pattern between three consecutive six-hour instantaneous precipitable water values (e.g., 06Z – 12Z –

18Z) (see Figure 2.2.2). Therefore, hourly precipitable water was interpolated between each six-hour measurement using a three-point sine curve interpolation method give by:

Minimum– Maximum

$$\overline{PW} - \left(PW_{\max} - \overline{PW}\right)\sin\left[\frac{\pi}{2} + \left(n_i \frac{\pi/2}{n/2}\right)\right] \qquad \textbf{(3.4.1)}$$

Maximum – Minimum

$$\left(PW_{\max} - \overline{PW}\right)\sin\left[\frac{\pi}{2} + \left(n_i \frac{\pi/2}{n/2}\right)\right] + \overline{PW} \qquad \textbf{(3.4.2)}$$

where $PW_{\max}$ is the maximum precipitable water for each grid point for three consecutive six-hour measurements, $\overline{PW}$ is the mean precipitable water for each grid point for three consecutive measurements, n is the number of time steps (i.e., hours of duration), and n_i is the i^{th} time step for each MCC. Although the three-point sine curve interpolation method smoothes the water vapor mass input curve presented by Doswell et al. (1996), changes in water vapor measures were negligible.

Once hourly precipitable water matrices were compiled, the grids were re-sampled and smoothed from a 2.5º grid to a 0.25º grid resolution using a minimum-curve-surface interpolation method. As a result of the low spatial resolution, it was necessary to regrid the precipitable water fields to a much higher spatial resolution in order to extract only those observations within the circular –32°C cloud shield for a given

MCC. For each hour, the anvil cloud shields were overlaid the interpolated grid matrices and hourly average precipitable water ($\overline{PW}_h$) beneath the anvil cloud shield was calculated using the following expression:

$$\overline{PW}_h = \frac{\sum_{i=1}^{n}\sum_{j=1}^{m} PW_{i,j}}{n \cdot m} \qquad \textbf{(3.4.3)}$$

where $PW_{i,j}$ is the precipitable water value at a given latitude and longitude coordinate, and *n* and *m* are the total number of coordinates. The results rendered an hourly spatial average of precipitable water beneath each MCC –32ºC cloud shield. Therefore, the hourly averaged precipitable water corresponded with hourly averaged precipitation totals and hourly precipitation efficiencies (PE_h) were determined by:

$$PE_h = \left[\frac{\overline{P_h}}{\overline{PW}_h} \right] \cdot 100\% \qquad \textbf{(3.4.4)}$$

where $\overline{P_h}$ is the average MCC precipitation observed beneath the –32ºC cloud shield for a given hour. The average precipitation efficiency of an MCC over its entire life cycle ($\overline{PE}_{MCC}$) is then:

$$\overline{PE}_{MCC} = \frac{\sum_{h=1}^{s} PE_h}{s} \qquad \textbf{(3.4.5)}$$

where *S* is the number of hourly calculated precipitation efficiencies and $\overline{PE}_{MCC}$ is the average precipitation efficiency for the entire event. An example calculation of

Table 3.4.1. An example of the interpolated average precipitable water (PW) beneath the –32ºC cloud shield, average precipitation totals, and average precipitation efficiency (PE) for each hour during the 18 June 1982 MCC. For this event, the average precipitation efficiency was 4.11%.

Precipitation efficiency of the 18 July 1982 MCC				
Hour (UTC)	***n****	**Interpolated PW (mm) ***	**Precipitation Total. mm**	**PE% ***
6	0	45.0	4.5	10.06
7	1	46.3	0.8	1.77
8	2	46.5	0.9	1.94
9	3	48.3	2.5	5.15
10	4	50.2	3.0	5.98
11	5	51.4	2.4	4.69
12	6	52.0	2.2	4.29
13	7	51.6	1.3	2.60
14	8	50.1	1.4	2.73
15	9	48.5	1.3	2.72
16	10	46.8	1.1	2.33
Average Precipitation Efficiency = 4.11%				
**n* is the number of time steps (i.e., hours of duration)				

precipitation efficiency for the 18 July 1982 MCC is shown in Table 3.4.1. For this event, the average precipitation efficiency was 4.11%.

3.4.3 Statistical Analysis

A visual comparison of the MCC temporal and spatial means can only suggest potential significance and/or patterns of MCC precipitation efficiency. The independent t-test was used in this study to account for the total number of occurrences that make up a mean value and determined whether the mean within a certain group for one dependent variable (e.g., *synoptic* vs. *frontal* precipitation efficiency) is unique. Additionally, a regression analysis was used to determine whether latitude or the time of year was a

better predictor in estimating MCC precipitation efficiency. For this study, a 95% confidence interval was used.

CHAPTER 4

TEMPORAL ANALYSIS OF 1982, 1983, AND 1993 WARM-SEASON MCCs

This chapter illustrates the monthly distribution of MCCs and MCC storm-type (e.g., *synoptic*, *mesohigh*, *frontal*) characteristics during the warm season for the entire study period. Such characteristics include storm frequency, duration, maximum areal extent, precipitable water, precipitation efficiency, precipitation rate, and precipitation amount. MCC characteristics during each year are further discussed in order to compare results between anomalous and "normal" moisture conditions.

4.1 Monthly Analysis Of All MCCs During 1982, 1983, And 1993

4.1.1 Frequency

For the entire study period, 87 events occurred between April-August. The greatest number of 32 MCCs occurred during 1982, followed by 28 events in 1983 and 27 events in 1993. The monthly frequency pattern closely resembles the pattern in the 15-year MCC climatology derived by Ashley et al. (in press) (see Figure 2.1.2). April had the lowest frequency of 11 events, while June marked the peak with 23 events (Figure 4.1.1).

This pattern is indicative of the increased heat and humidity in the lower troposphere during the mid-to-late warm season which increases the atmospheric

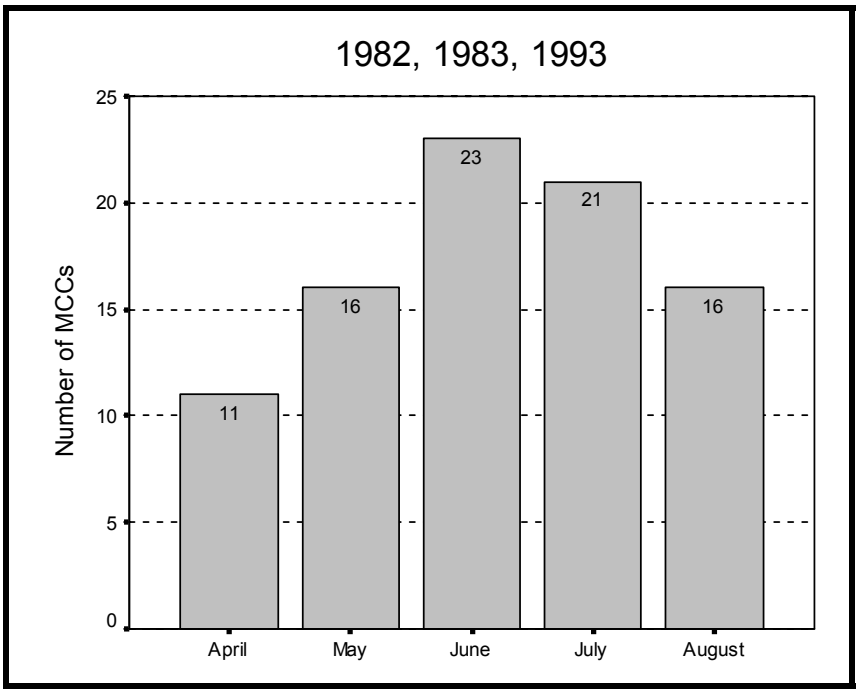

Figure 4.1.1. Bar graph of the monthly MCC frequency for 1982, 1983, and 1993.

instability enough to spawn such large, convective mesoscale systems. During the transition season, thermal energy is decreased and cyclonic motion is increased which acts to develop more linear convective patterns (i.e., less confinement in a broader region containing less convective inhibition when compared to the mid-to-late warm season).

4.1.2 Duration

The mean duration for all MCCs during 1982, 1983, and 1993 was 11.4 hours. Tollerud et al. (1987), Tollerud and Rogers (1991), and Ashley et al. (in press) illustrated that April and May MCCs typically exhibit longer lifecycles. For this study, the peak mean MCC duration occurred in April (14.7 hours) –nearly three hours greater than the second highest mean duration (June , 12.1 hours). The shortest mean duration occurred in

August (10.1 hours) (Figure 4.1.2). With the exception of June having a mean duration greater than May by nearly 30 minutes, the mean monthly MCC duration in this study concurs with Kane et al. (1987), Tollerud et al. (1987), and Tollerud and Rogers (1991), Geerts (1998), and Ashley et al. (in press) results –as the warm season progresses, MCC life-spans decrease.

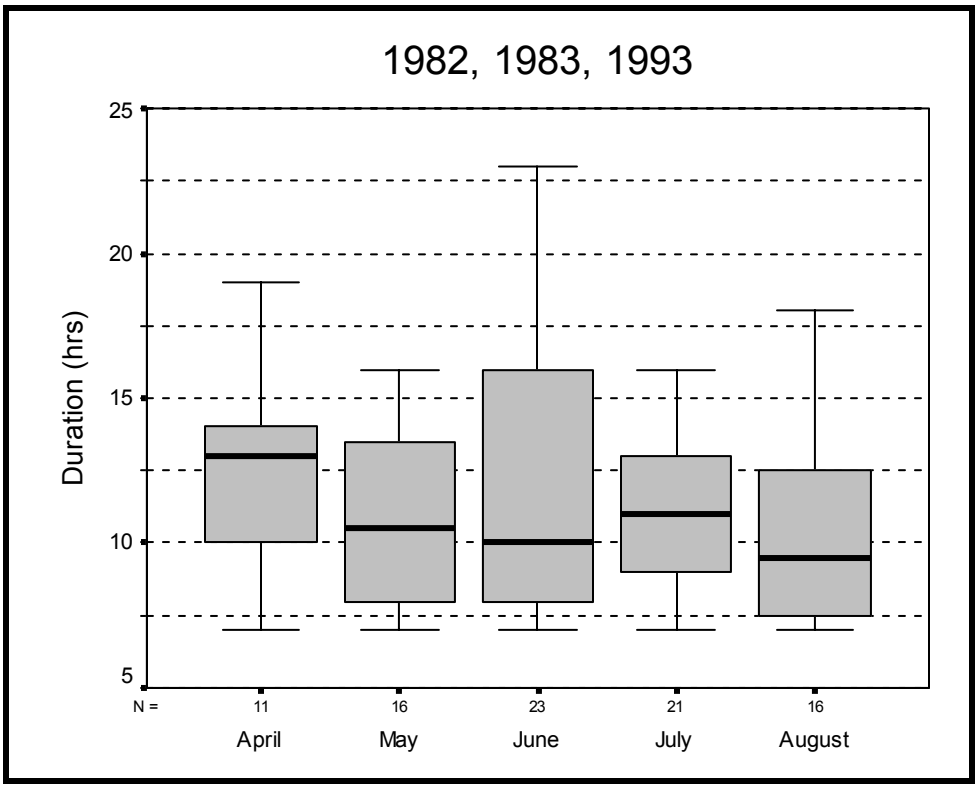

Figure 4.1.2. Box-and-whisker plot of the monthly MCC duration for 1982, 1983, and 1993. The plots show the median (thick line), interquartile range (shaded), and outliers (i.e., the 10th and 90th percentile as whiskers) for the indicated months. Additionally, the total number of MCCs per month for all 3 years investigated is indicated along the x-axis.

4.1.3 Maximum Anvil cloud Size

The mean maximum -52°C cloud shield for all MCCs was nearly 175,600 km^2 (i.e., approximately twice the size of Minnesota). Tollerud et al. (1987), Tollerud and

Rogers (1991), and Ashley et al. (in press) found that April events typically exhibit the largest areal extents. Thereafter as the warm season progress, cloud shield sizes generally decrease. The monthly mean -52°C cloud shield sizes in this study coincide with the seasonal pattern described in Tollerud et al. (1987), Tollerud and Rogers (1991), and Ashley et al. (in press) results. April -52°C cloud shields were well above the mean of 175,600 km^2 with a mean areal extent of nearly 225,300 km^2 (i.e., nearly twice the size of Nevada), respectively. Mean -52°C cloud shields decreased throughout the warm season to a mean areal extent of approximately 143,000 km^2 (i.e., nearly twice the size of Washington) in August (Figure 4.1.3).

4.1.4 Precipitable Water And Precipitation Totals

For the entire study period, there were 11 MCCs recorded during April. However, due to missing precipitation data for the 7 April 1993 MCC, this event was excluded from the remainder of analyses performed in this study (i.e., all yearly, monthly, and/or storm-type analyses that included precipitable water, precipitation efficiency, precipitation amount, and precipitation rate).

The mean precipitable water, measured beneath -32°C cloud shields, for all MCCs was 36.3 mm. The mean precipitation total, measured beneath -32°C cloud shields, was 14.8 mm. The monthly analysis for mean precipitable water and precipitation also illustrated a seasonal trend. The mean precipitable water for April MCCs was 30.3 mm. As the warm season progressed, mean precipitable water increased each month to 43.1 mm in August (Figure 4.1.4). In contrast, precipitation totals decreased each month from 18.5 mm in April to 11.6 mm in August (Figure 4.1.5).

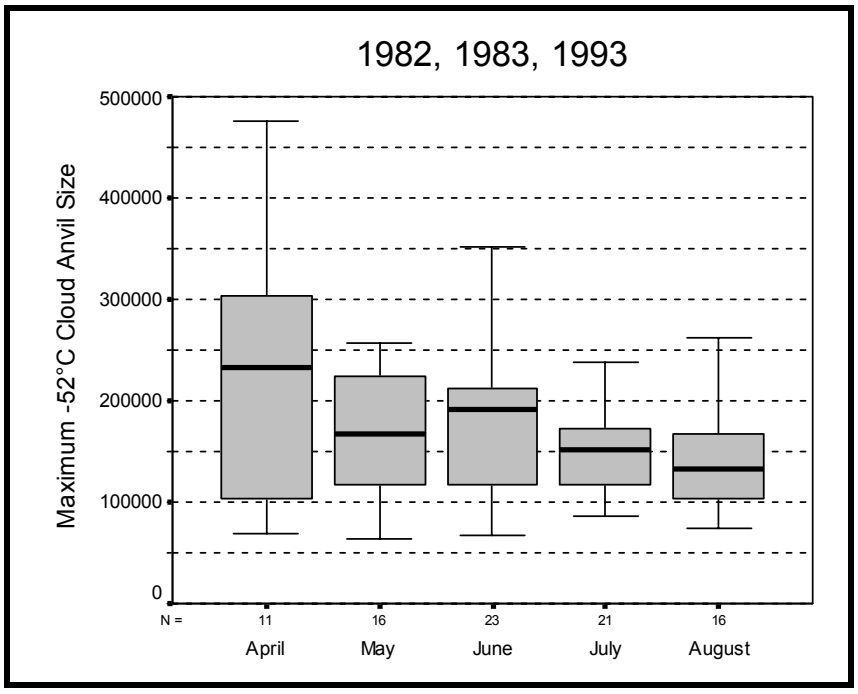

Figure 4.1.3. Box-and-whisker plot of the monthly maximum -52ºC anvil-cloud sizes for 1982, 1983, and 1993.

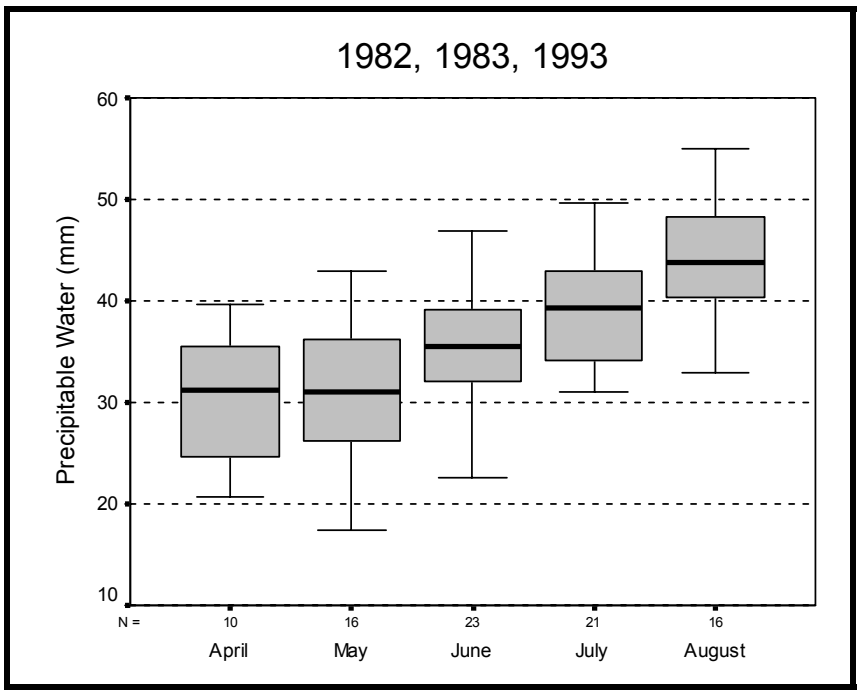

Figure 4.1.4. Box-and-whisker plot of the monthly distribution of precipitable water vapor for 1982, 1983, and 1993.

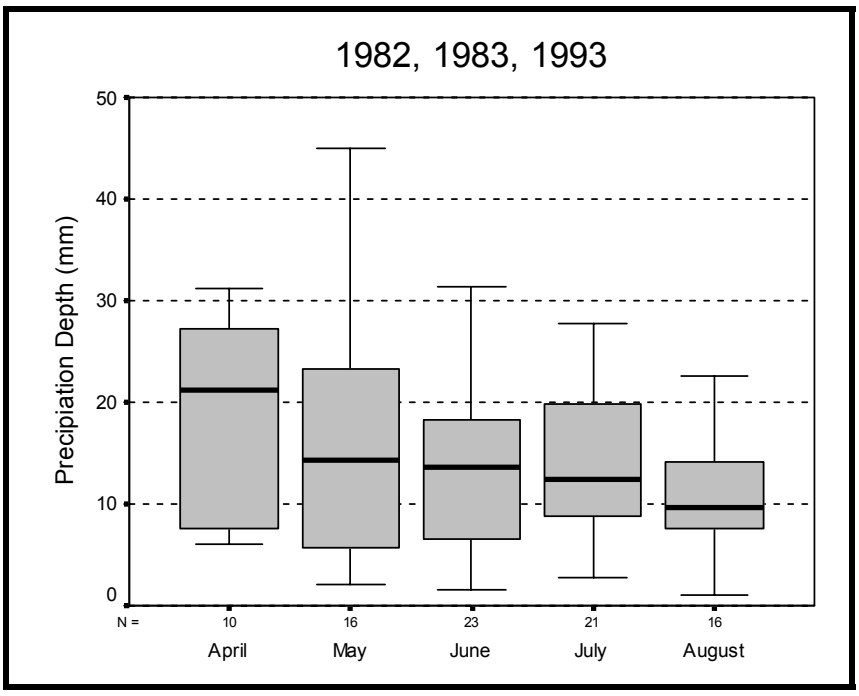

Figure 4.1.5. Box-and-whisker plot of the monthly distribution of precipitation totals for all MCCs during 1982, 1983, and 1993.

4.1.5 Precipitation Efficiency and Precipitation Rate

The mean precipitation efficiency and precipitation rate for all MCCs was 3.67% and 1.3 mm hr $^{-1}$. The monthly mean precipitation efficiency analysis further illustrated a seasonal trend. April MCCs had the highest mean precipitation efficiency of 4.87%. For each consecutive month thereafter, precipitation efficiency steadily decreased to 2.59% in August (Figure 4.1.6). The results of the monthly mean precipitation rates closely resemble the seasonal distribution of mean precipitation efficiency. April MCCs had the highest mean precipitation rate of 1.6 mm hr $^{-1}$ and decreased each month to 1.1 mm hr $^{-1}$ in August (Figure 4.1.7). The independent t-test showed that the precipitation efficiency during April was significantly higher than that for July. The efficiency during April and May was also significantly higher than for August (Table 4.1.1).

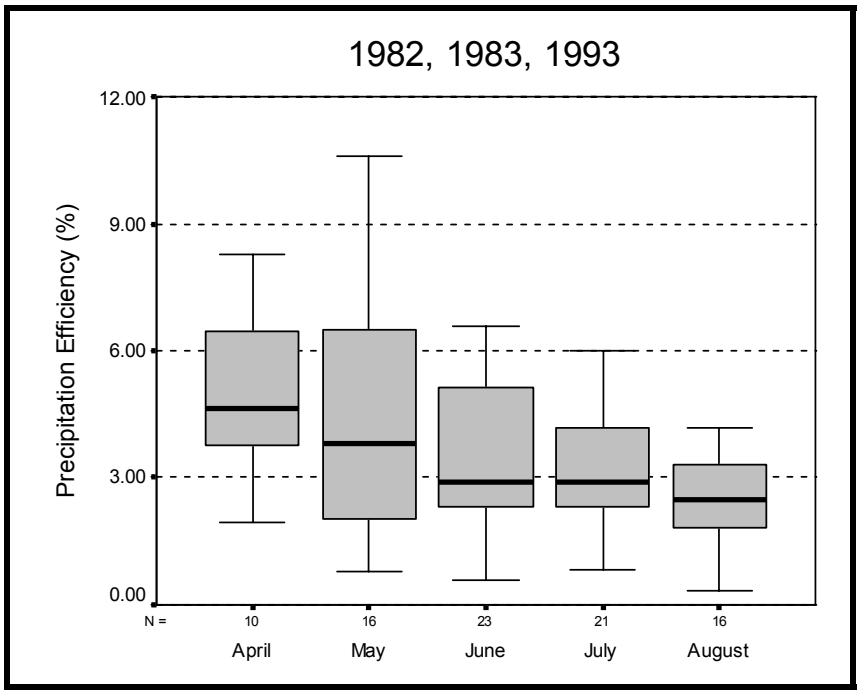

Figure 4.1.6. Box-and-whisker plot of the monthly distribution of precipitation efficiency for all MCCs during 1982, 1983, and 1993.

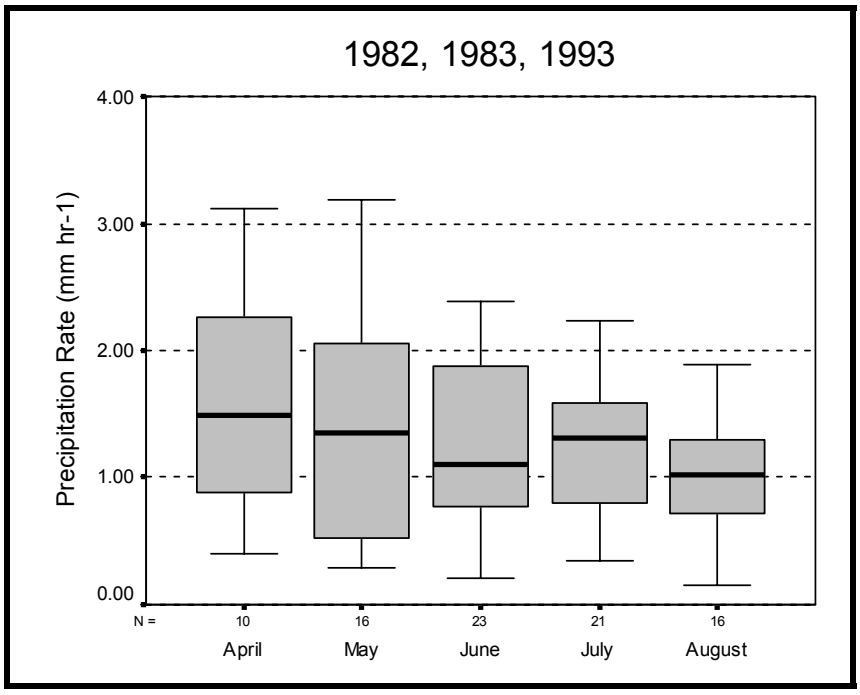

Figure 4.1.7. Box-and-whisker plot of the monthly distribution of precipitation rate for all MCCs during 1982, 1983, and 1993.

Table 4.1.1. Independent t-test results showing the number of MCCs in April, July, and August (N), mean precipitation efficiency (PE) in each month, significance (two-tailed) (sig.), and t-score (t) with a 95% confidence interval.

Month	N	mean PE	t	sig.
April	10	4.87	2.55	.023
July	21	3.18		

Month	N	mean PE	t	sig.
April	10	4.87	3.42	.004
August	21	2.59		

Month	N	mean PE	t	sig.
May	16	4.30	2.20	.039
August	16	2.59		

4.2 Monthly Storm-Type Analysis For All MCCs During 1982, 1983, And 1993

The discussion in subsection 2.1.2 highlighted four favorable *synoptic* settings conducive to MCC development: *synoptic*, *mesohigh*, *frontal*, and *extreme-right-moving* (*XRM*). Since *XRM* events were considered a subtype of the *frontal* classification and rarely occurred compared to other storm types, this study only observed *synoptic*, *mesohigh*, and *frontal* events. Storm types were subjectively categorized by performing surface analyses of sea-level pressure (SLP), surface station plots, and surface streamline winds. From the information provided from the surface analysis, a surface frontal analysis was performed. Upper-air analyses included an examination of 500 hPa isohypes, 500 hPa wind field, and 250-200 hPa divergence. By plotting the location of MCC development in relation to frontal boundaries, upper-air long and short-wave troughs and ridges, and upper-air divergence, each MCC was assigned a storm type. To

ensure this process of storm type categorization was reasonable and accurate, results from the surface and upper-air analyses were later compared to storm-type analyses performed by Kane et al. (1987) and Corfidi (1994). Examples of the surface and upper-air analyses used to determine each storm type are shown for a typical *synoptic* MCC during 17 May 1982 in Figures 4.2.1 and 4.2.2; *mesohigh* MCC during 19 July 1982 in Figures 4.2.3 and 4.2.4; and *frontal* MCC during 30 June 1982 in Figures 4.2.5 and 4.2.6.

4.2.1 Frequency

For the 87 MCCs that occurred during April-August, there were 31 *synoptic*, 19 *mesohigh*, and 37 *frontal* events. Kane et al. (1987) found that *synoptic* events generally have peak frequencies during April-June, *mesohigh* events in July and August, and *frontal* events in June. The results from the monthly storm-type analysis in this study concur with Kane et al. (1987). The highest frequencies of *synoptic* events occurred during April-June with a peak of 10 events in May (Figure 4.2.7). *Mesohigh* events had higher frequencies in July and August with a peak of 7 events in August (Figure 4.2.8), while *frontal* events were predominant in June with 12 events (Figure 4.2.9).

4.2.2 Duration

From subsection 4.1.2, longer-lived MCCs occurred in the early warm season and progressively became shorter-lived into the late warm season. *Synoptic* events generally occurred during the early warm season and had the longest mean duration of 13.3 hours. *Frontal* events peaked in June and had the second longest mean duration of 12.0 hours.

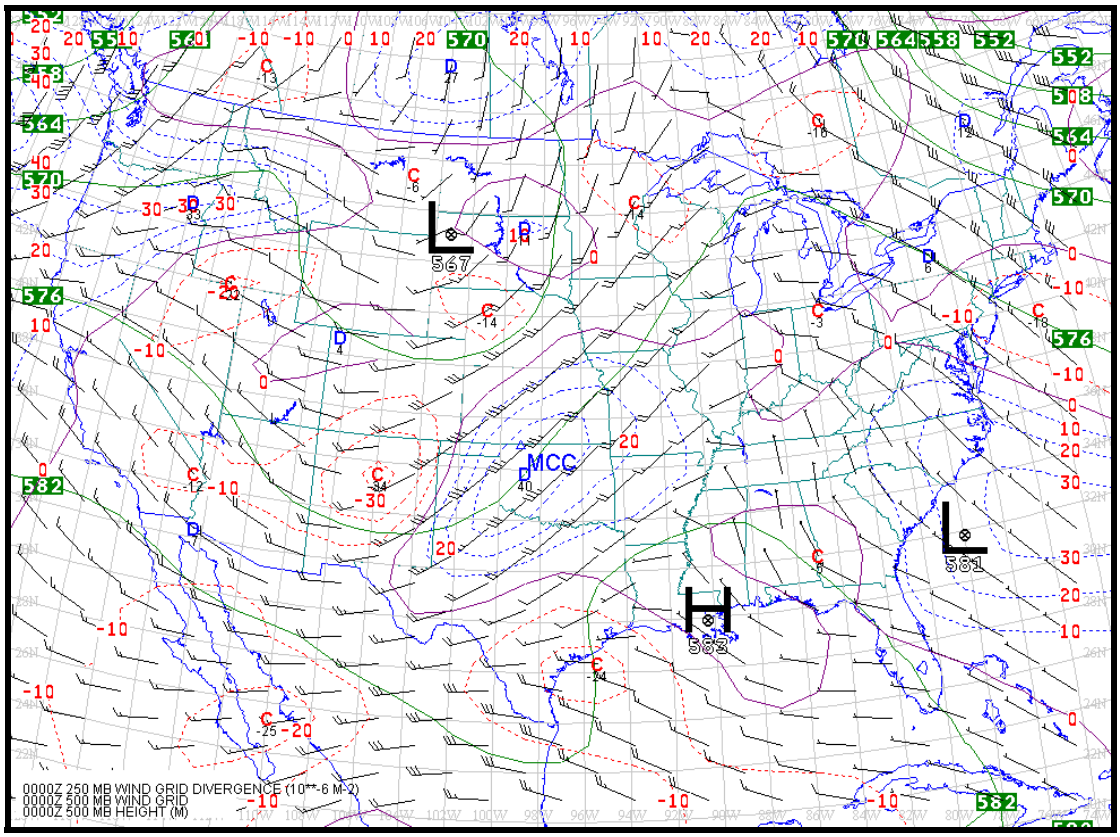

Figure 4.2.1. Illustration of a *synoptic* MCC which developed on the central border of Oklahoma and Kansas during 17 May 1982 at 00Z in advance of a 500 hPa trough beneath an area of strong upper-level divergence. This upper-air map displays conditions for 00Z.

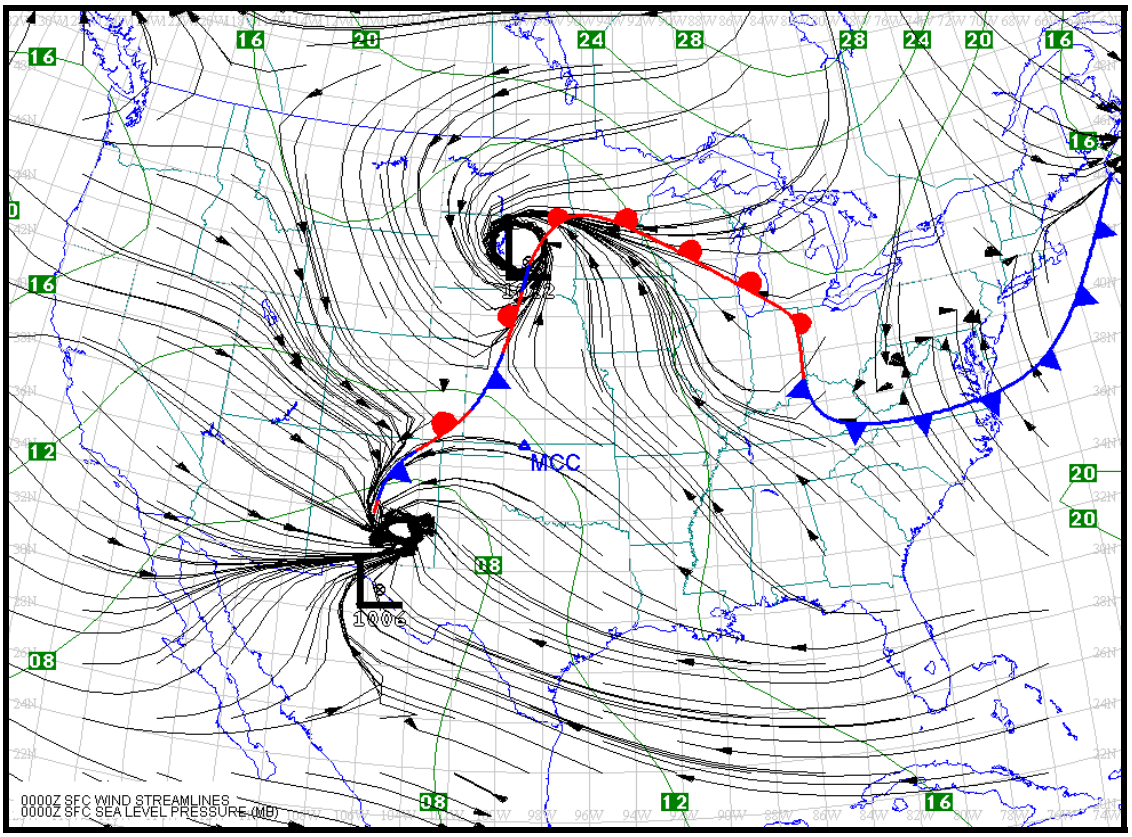

Figure 4.2.2. As in Figure 4.2.1 except for a surface analysis illustrating the MCC's development on the warm side of a stationary cold front. This surface map displays conditions for 00Z.

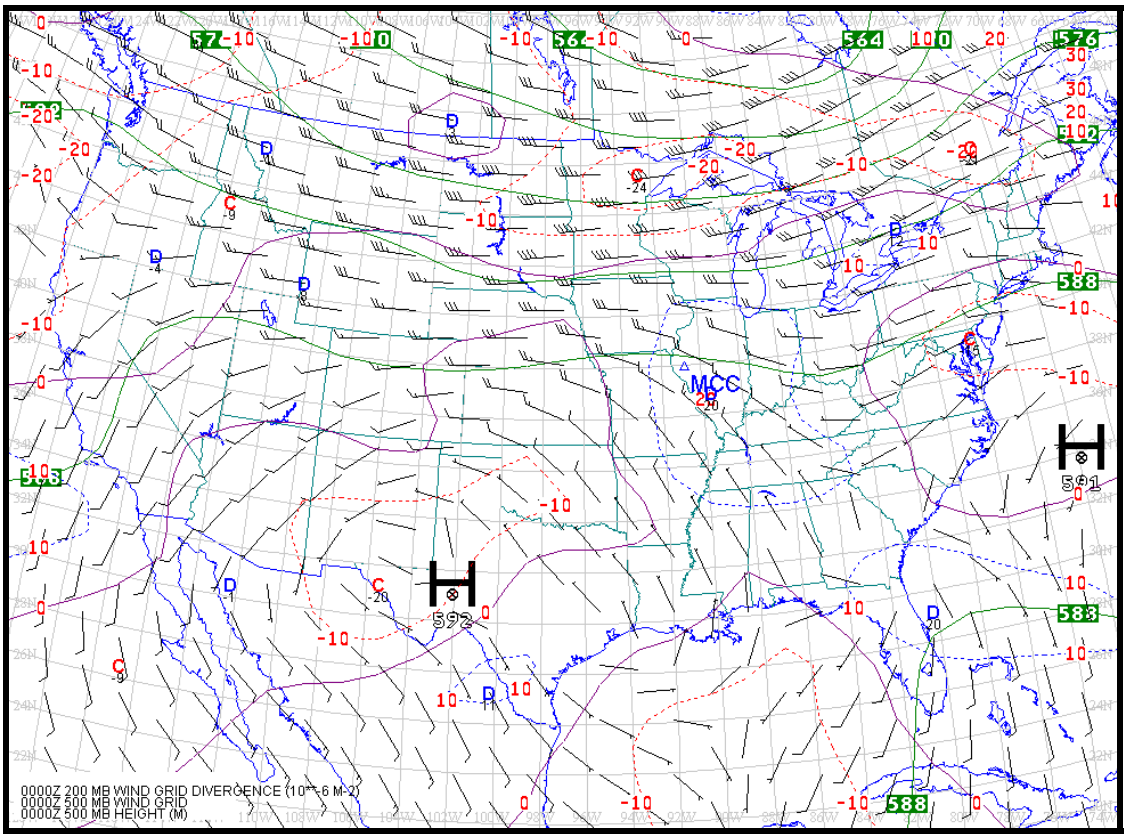

Figure 4.2.3. Illustration of a *mesohigh* MCC which developed in western-central Illinois on 19 July 1982 at 04Z just west of a 500 hPa trough in association with an upper-level short wave. This upper-air map displays conditions for 00Z, but the MCC is plotted according to the time of its development.

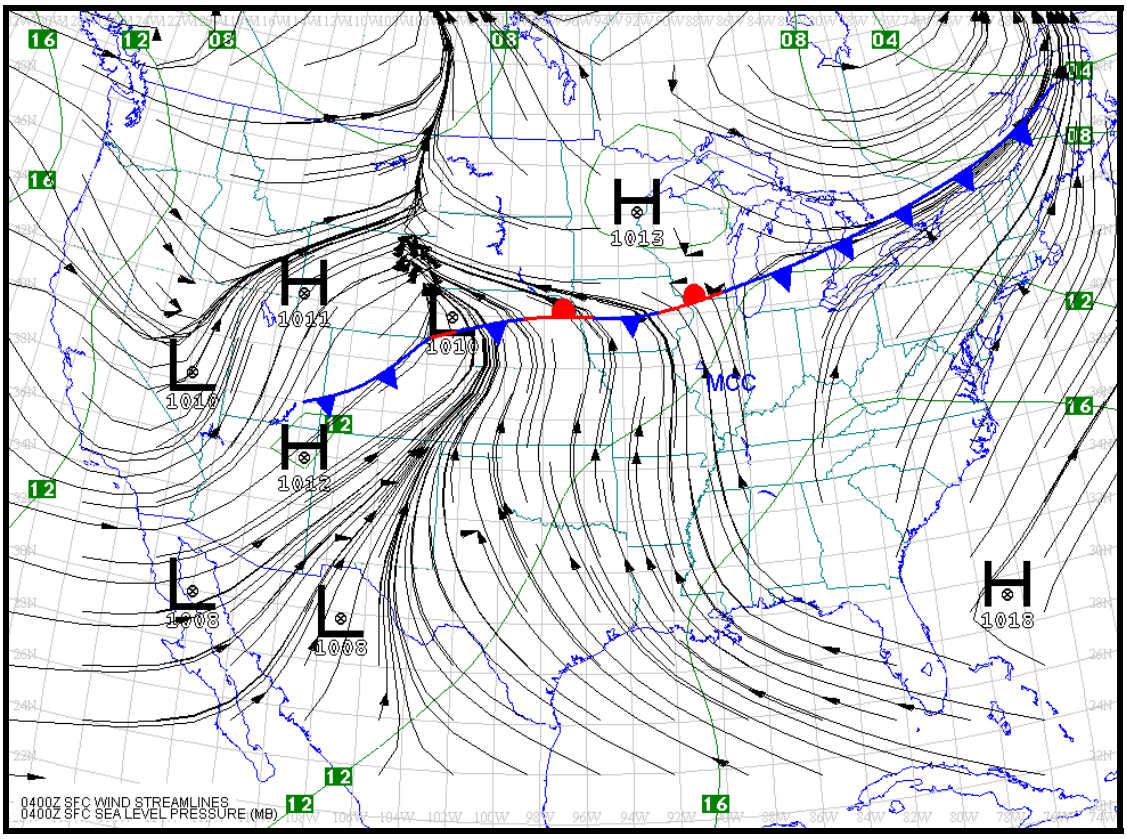

Figure 4.2.4. As in Figure 4.2.3 except for a surface analysis illustrating the MCC's development in the warm sector near a slow moving or quasi-stationary cold front in association with a weak surface pressure gradient. This surface map displays conditions for 04Z.

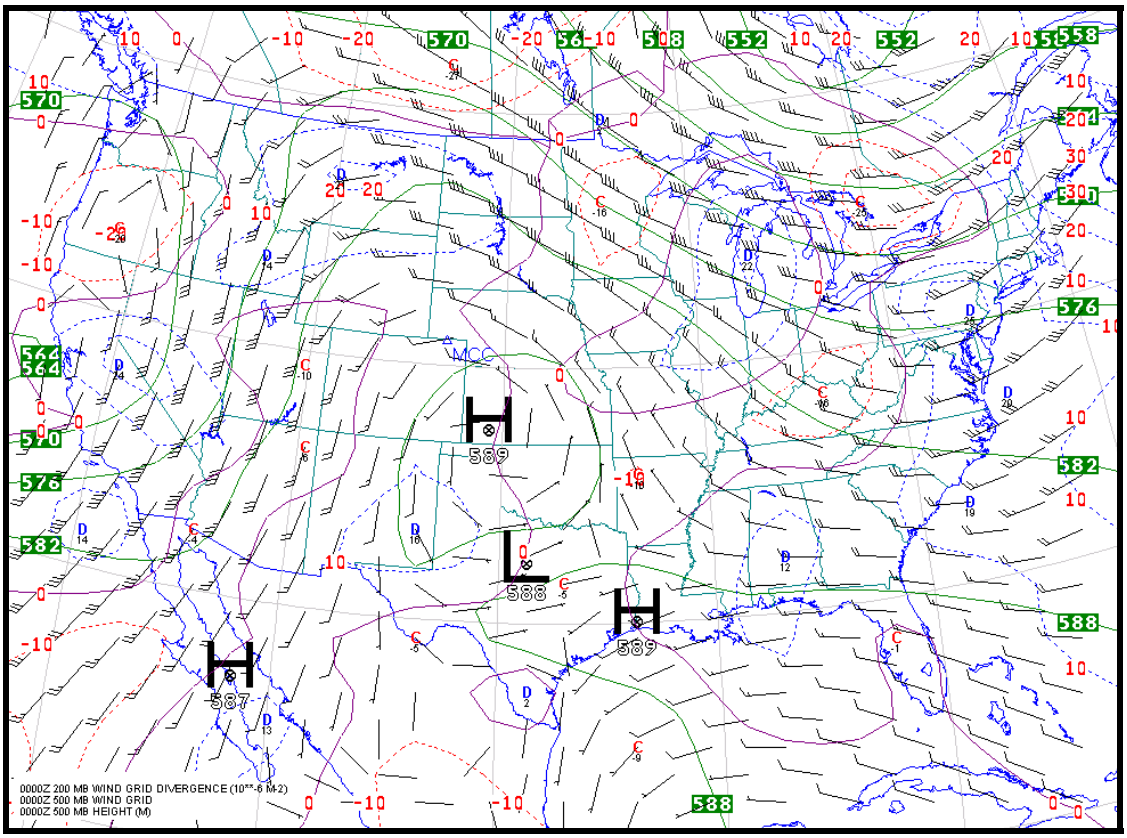

Figure 4.2.5. Illustration of a *frontal* MCC which developed on the border of northeast Colorado and the central panhandle of Nebraska during 30 June 1982 at 00Z west of a 500 hPa trough. This upper-air map displays conditions for 00Z.

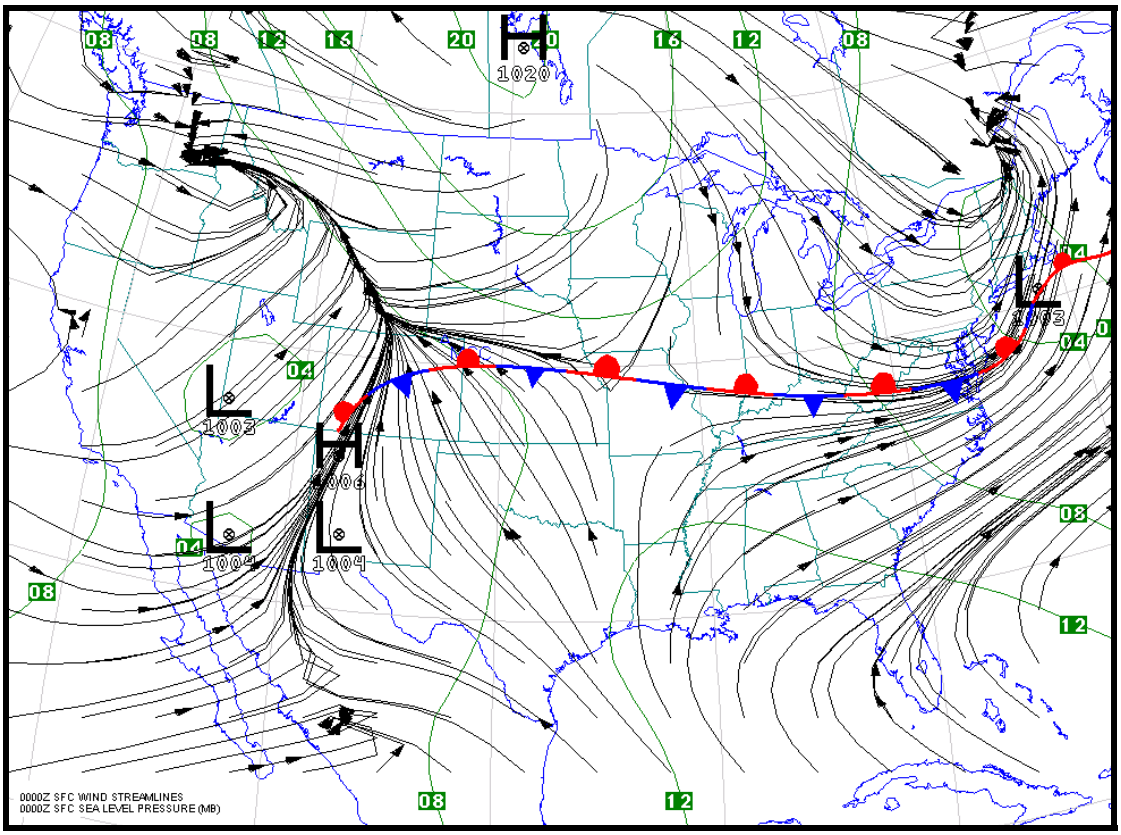

Figure 4.2.6. As in Figure 4.2.5 except for a surface analysis illustrating the MCC's development on the cool side of a quasi-stationary frontal boundary. This surface map displays conditions for 00Z.

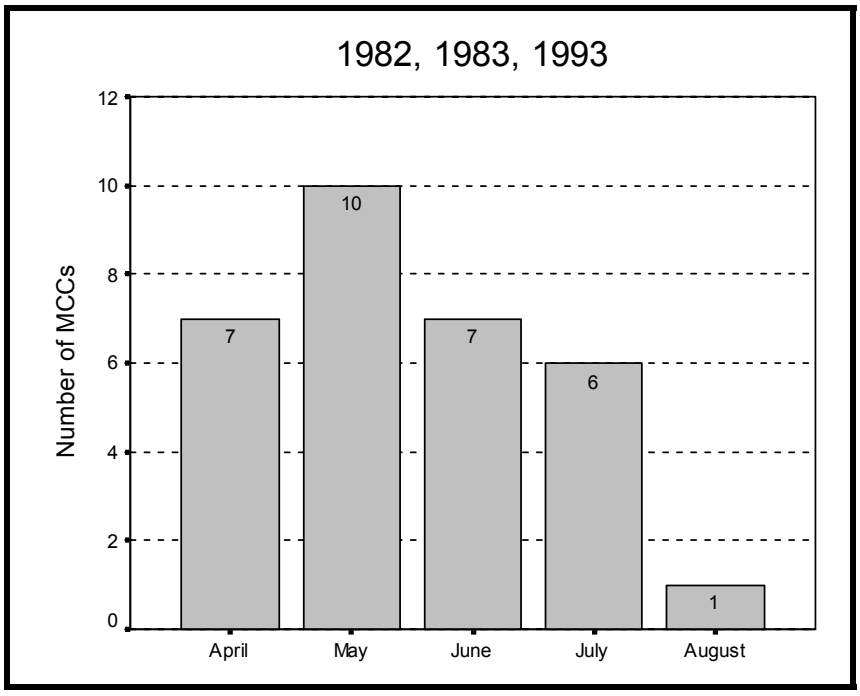

Figure 4.2.7. Bar graph of the monthly frequency for all *synoptic* MCCs during 1982, 1983, and 1993.

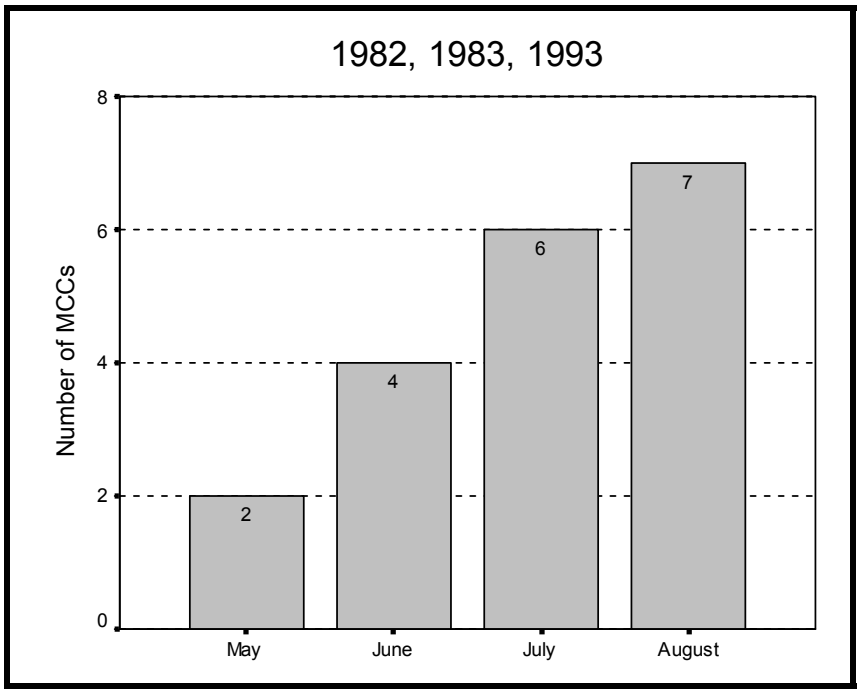

Figure 4.2.8. Bar graph of the monthly frequency for all *mesohigh* MCCs during 1982, 1983, and 1993.

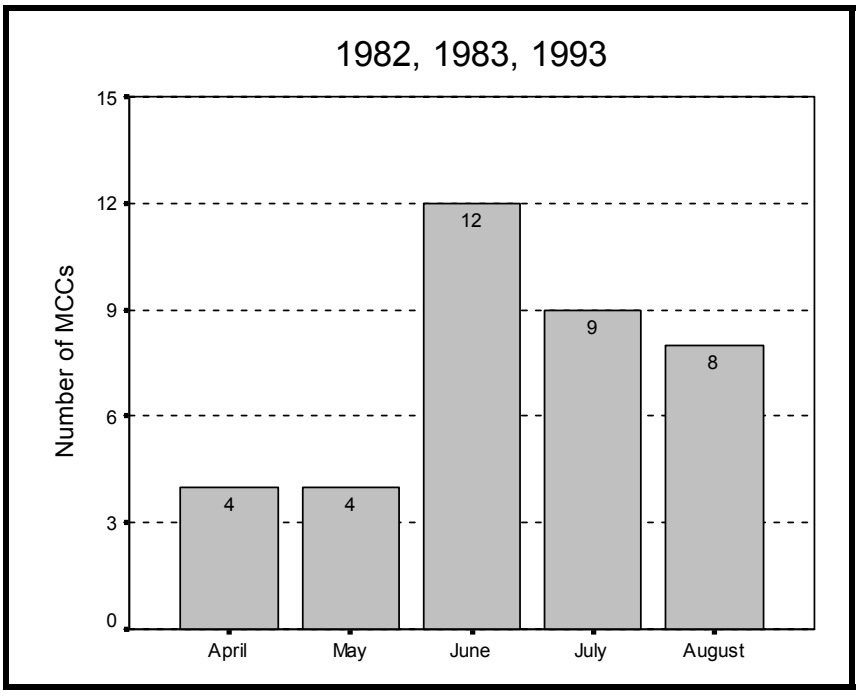

Figure 4.2.9. Bar graph of the monthly frequency for all *frontal* MCCs during 1982, 1983, and 1993.

Mesohigh events peaked in the latter portion of the warm season with a mean duration of 8.89 hours.

For *Synoptic* MCCs, the longest mean duration occurred in April (16.7 hours), followed by June (12.6 hours), and May (12.5 hours) (Figure 4.2.10). The *mesohigh* peak mean duration occurred in July (9.5 hours), followed closely by August (9.1 hours) (Figure 4.2.11).The peak mean *frontal* duration occurred in June (13.2 hours), followed by July (12.2 hours) and April (11.3 hours) (Figure 4.2.12).

4.2.3 Maximum Anvil cloud Size

From subsection 4.1.3, larger MCCs occurred in the early warm season and progressively became smaller into the late warm season. *Synoptic* events had the mean

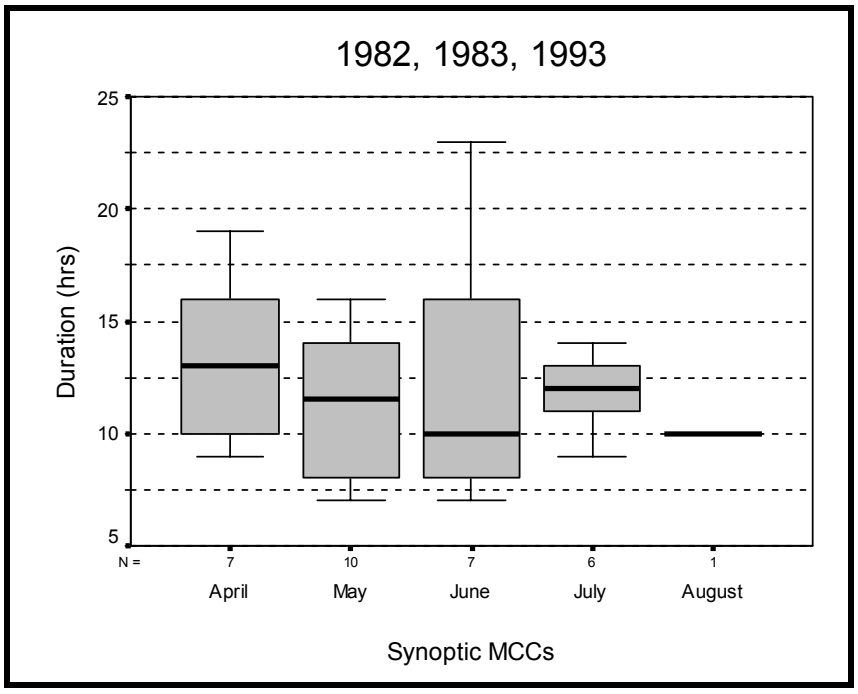

Figure 4.2.10. Box-and-whisker plot of the monthly duration for all *synoptic* MCCs during 1982, 1983, and 1993.

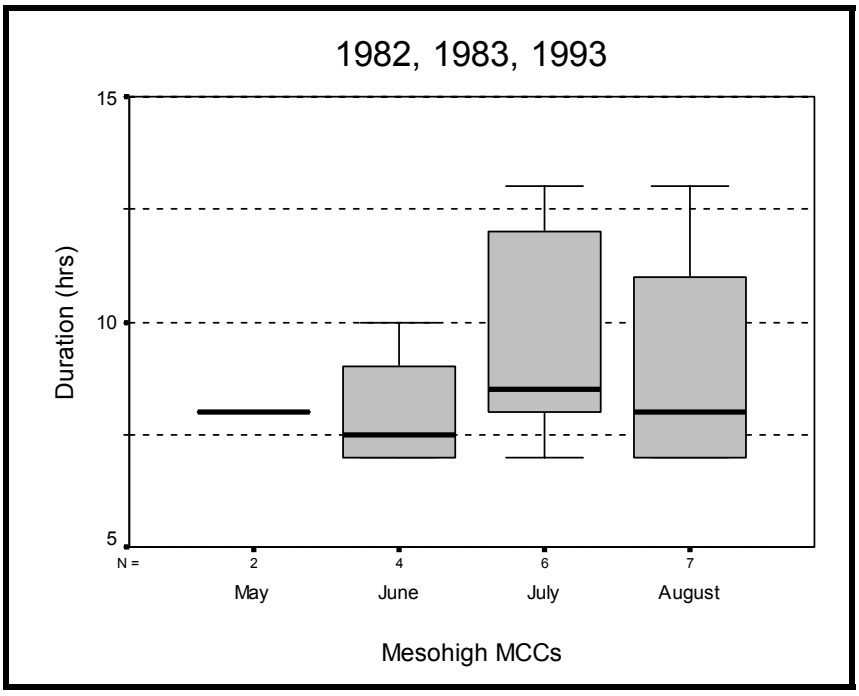

Figure 4.2.11. Box-and-whisker plot of the monthly duration for all *mesohigh* MCCs during 1982, 1983, and 1993.

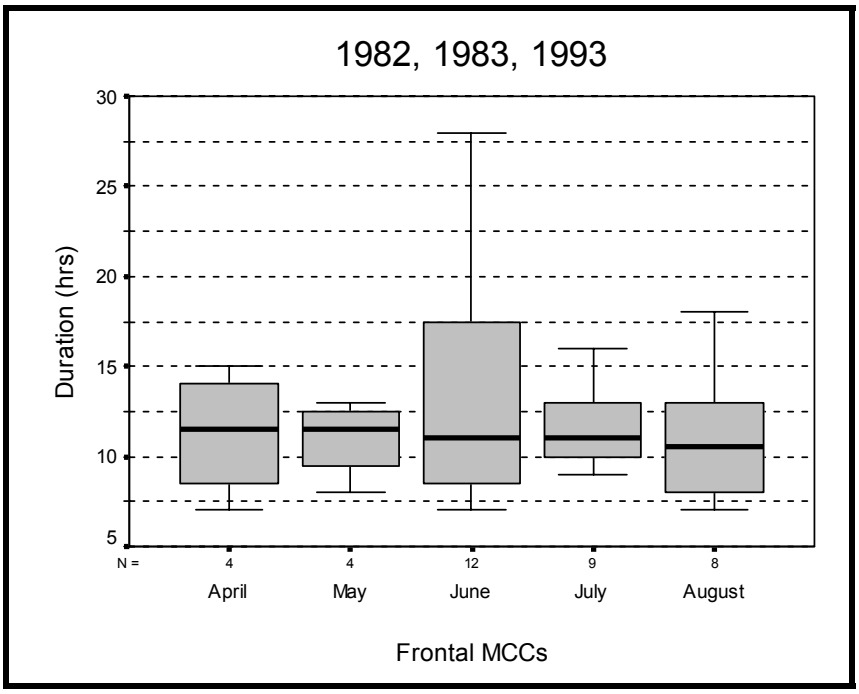

Figure 4.2.12. Box-and-whisker plot of the monthly duration for all *frontal* MCCs during 1982, 1983, and 1993.

largest anvil cloud size (203,100 km^2), followed by *frontal* events (181,100 km^2) and *mesohigh* events (120,000 km^2).

The -52°C anvil cloud shield for *synoptic* MCCs were largest in April (270,300 km^2), followed by July (196,300 km^2) and June (194,000 km^2), but there was a large range in anvil size during most months (Figure 4.2.13). The -52°C anvil cloud shield for *mesohigh* MCCs were largest in August (132,800 km^2), followed by July (120,500 km^2) (Figure 4.2.14). The peak *frontal* mean anvil cloud size occurred in May (261,800 km^2) but only includes two events, followed by June (191,500 km^2) and July (170,700 km^2) (Figure 4.2.15).

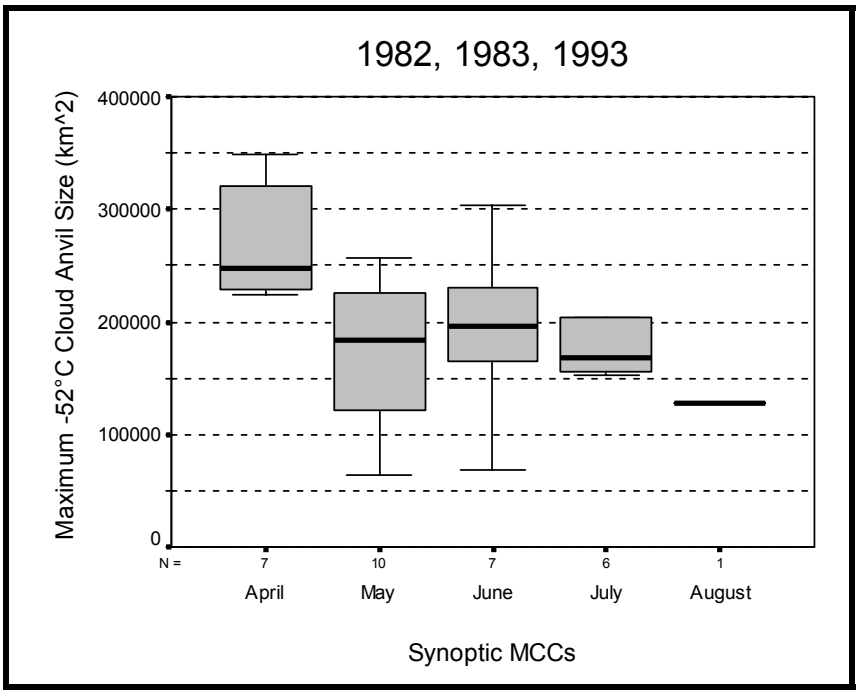

Figure 4.2.13. Box-and-whisker plot of the monthly maximum -52ºC anvil-cloud sizes for all *synoptic* MCCs during 1982, 1983, and 1993.

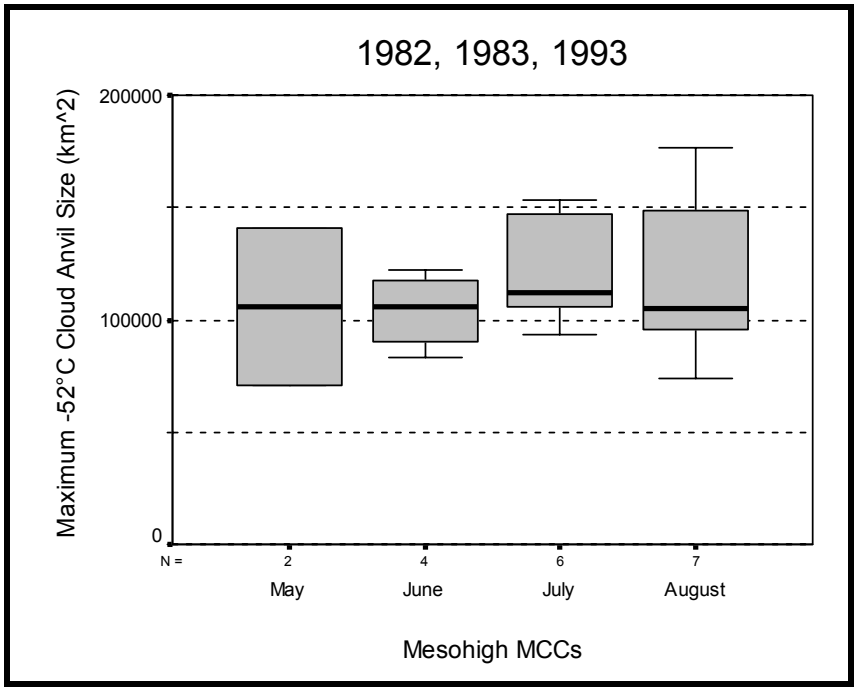

Figure 4.2.14. Box-and-whisker plot of the monthly maximum -52ºC anvil-cloud sizes for all *mesohigh* MCCs during 1982, 1983, and 1993

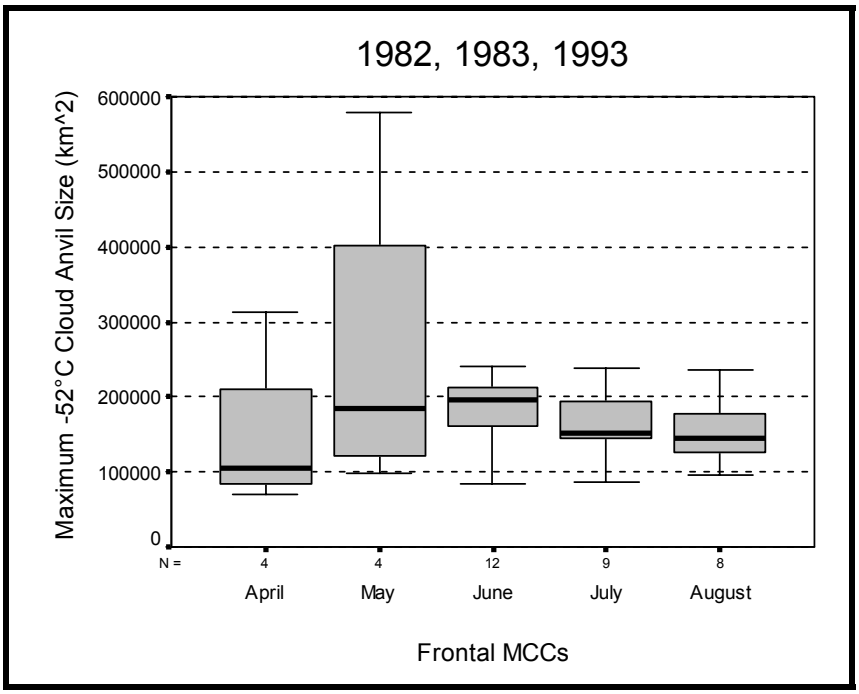

Figure 4.2.15. Box-and-whisker plot of the monthly maximum -52ºC anvil-cloud sizes for all *frontal* MCCs during 1982, 1983, and 1993.

4.2.4 Precipitable Water and Precipitation Total

From subsection 4.1.4, precipitable water was least in the early warm season and progressively became greater into the late warm season. In contrast, precipitation totals were greatest in the early warm season and progressively became smaller into the late warm season. *Synoptic* events had the least mean precipitable water (34.2 mm), followed by *frontal* events (36.3 mm) and *mesohigh* events (39.8 mm). However, the highest mean precipitation totals occurred from *synoptic* MCCs (17.9 mm), followed by *frontal* events (13.8 mm) and *mesohigh* events (11.7 mm). The mean *synoptic* precipitable water gradually increased each month from May (27.9 mm) to August (45.4 mm) (Figure 4.2.16).

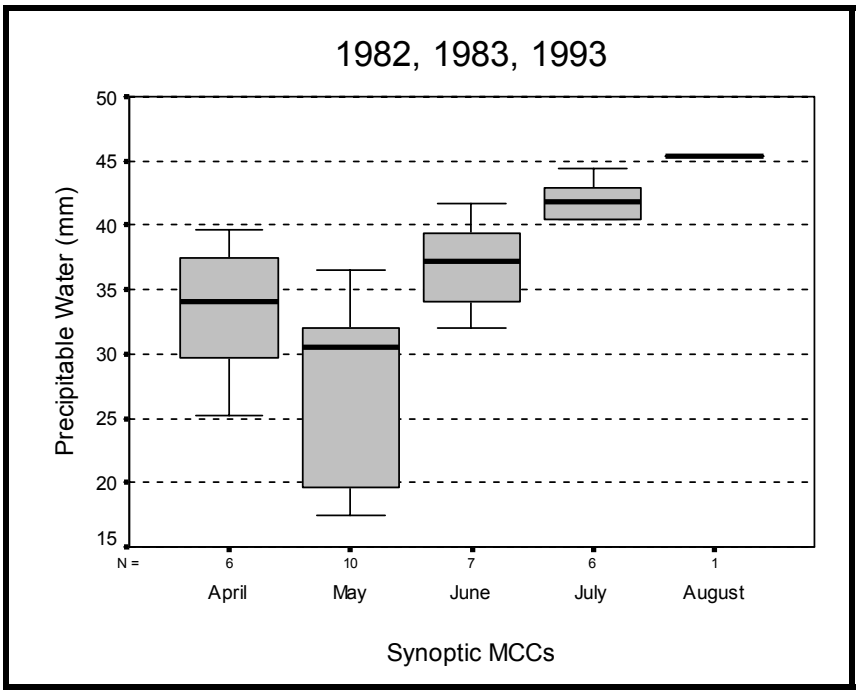

Figure 4.2.16. Box-and-whisker plot of the monthly distribution of precipitable water vapor for all *synoptic* MCCs during 1982, 1983, and 1993.

Mean *synoptic* precipitation totals decreased each month (with the exception of May) from April (23.9 mm, the highest mean precipitation total of all storm types) to August (9.7 mm) (Figure 4.2.17). Mean *mesohigh* precipitable water showed a seasonal increase in precipitable water from May (33.5 mm) to August (41.8 mm) (no April *mesohigh* events were recorded) (Figure 4.2.18). The mean *mesohigh* precipitation totals showed a seasonal decrease from May (14.1 mm) to August (10.0 mm) (Figure 4.2.19). Mean *frontal* precipitable water and precipitation amount had less seasonal variation. Mean *frontal* precipitable water increased from April (25.6 mm) to August (44.0 mm) (with the exception of May which only had two events) (Figure 4.2.20). However, there was no apparent seasonal trend with the mean *frontal* precipitation totals (Figure 4.2.21).

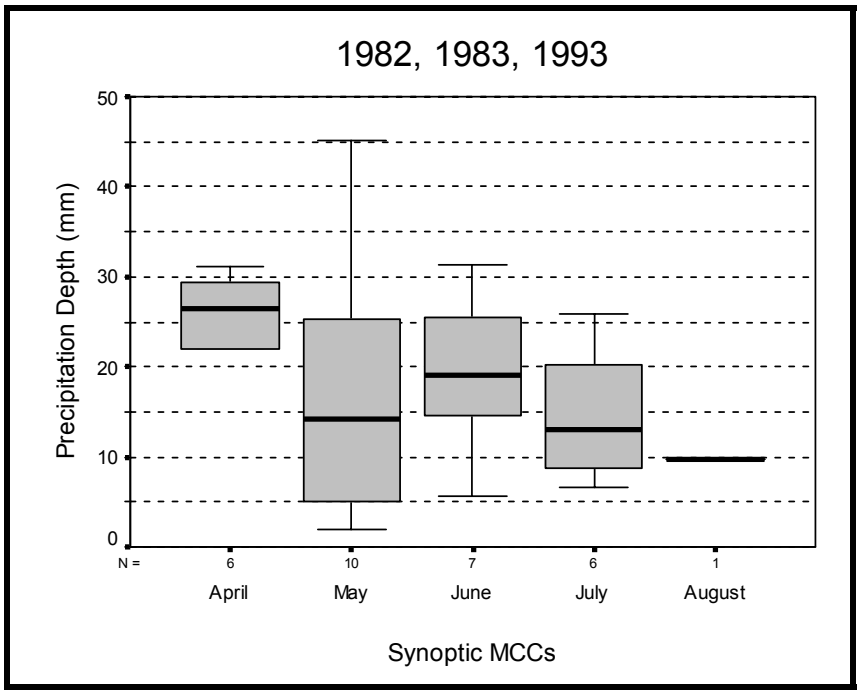

Figure 4.2.17. Box-and-whisker plot of the monthly distribution of precipitation totals for all *synoptic* MCCs during 1982, 1983, and 1993.

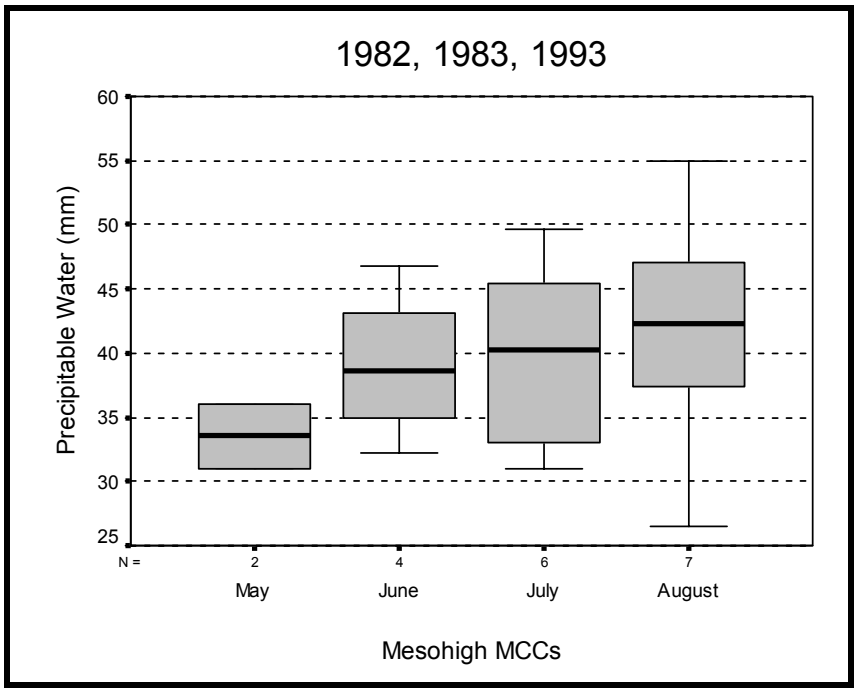

Figure 4.2.18. Box-and-whisker plot of the monthly distribution of precipitable water vapor for all *mesohigh* MCCs during 1982, 1983, and 1993.

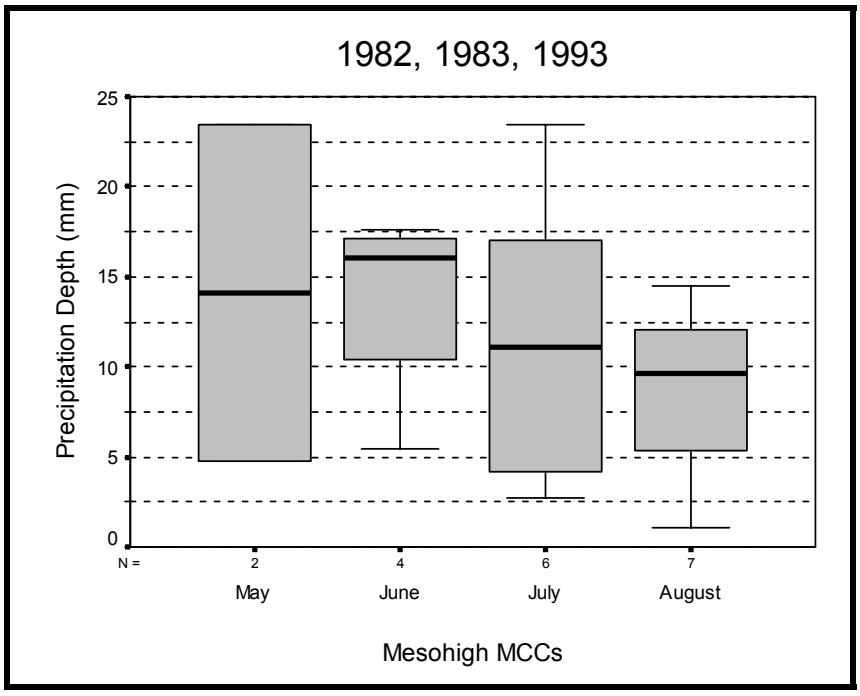

Figure 4.2.19. Box-and-whisker plot of the monthly distribution of precipitation totals for all *mesohigh* MCCs during 1982, 1983, and 1993.

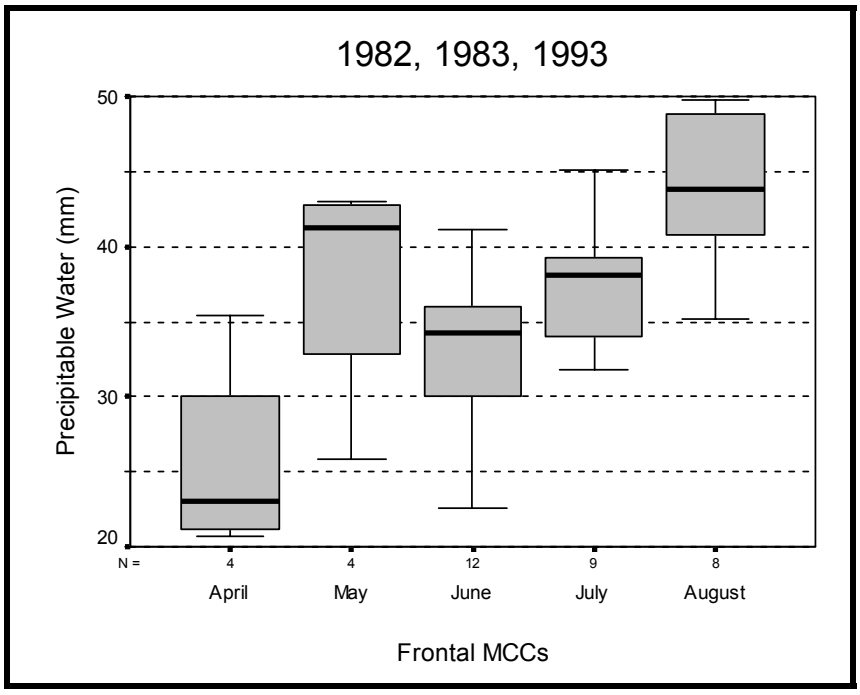

Figure 4.2.20. Box-and-whisker plot of the monthly distribution of precipitable water vapor for all *frontal* MCCs during 1982, 1983, and 1993.

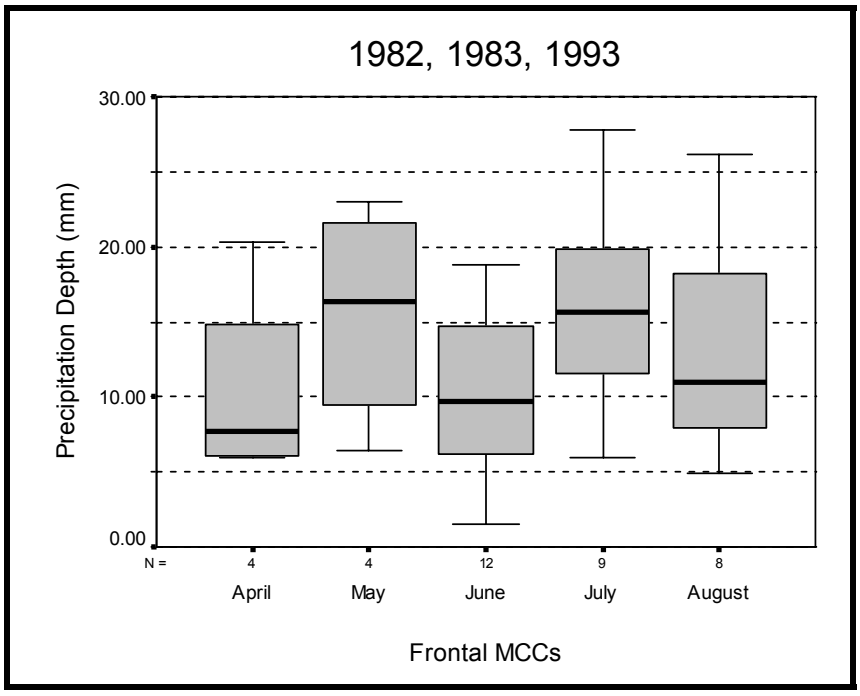

Figure 4.2.21. Box-and-whisker plot of the monthly distribution of precipitation totals for all *mesohigh* MCCs during 1982, 1983, and 1993.

4.2.5 Precipitation Efficiency and Precipitation Rate

From subsection 4.1.5, precipitation efficiency and precipitation rate was greatest in the early warm season and progressively became smaller into the late warm season. *Synoptic* events had the highest mean precipitation efficiency of 4.38%. However, *mesohigh* events had a higher mean precipitation efficiency than *frontal* events by just 0.10% with a mean efficiency of 3.36%. *Synoptic* events also had the highest mean precipitation rate of 1.5 mm hr $^{-1}$. *Mesohigh* events had a higher mean precipitation rate than *frontal* events with a rate of 1.3 mm hr $^{-1}$. However, the independent t-test showed for each storm type, *synoptic* precipitation efficiency was only significantly higher than that of *frontal* efficiency (Table 4.2.1).

Table 4.2.1. Independent t-test results showing the number of *synoptic* and *frontal* MCCs (N), mean precipitation efficiency (PE) in each storm type, significance (two-tailed) (sig.), and t-score (t) with a 95% confidence interval.

Storm Type	N	mean PE	t	sig.
synoptic	30	4.38	2.01	.050
frontal	37	3.26		

The mean *synoptic* precipitation efficiency decreased each month from April (5.74%) to August (2.11%) (with the exception of May) (Figure 4.2.22). The mean *synoptic* precipitation rate resembled the same seasonal trend as *synoptic* precipitation efficiency. The independent t-test showed that *synoptic* precipitation efficiency during April was significantly higher than that for July (Table 4.2.2). The mean *synoptic* precipitation rate decreased each month from April (2.0 mm hr $^{-1}$) to August (0.97 mm hr $^{-1}$) (with the exception of May) (Figure 4.2.23). Mean *mesohigh* precipitation efficiency showed a seasonal decrease from May (5.12%) to August (2.42%) (Figure 4.2.24). However, there was no significant difference of means in *mesohigh* precipitation efficiency by month**.** Mean *mesohigh* precipitation rate also showed a seasonal decrease from May (1.76 mm hr $^{-1}$) to August (1.02 mm hr $^{-1}$) (Figure 4.2.25).

Mean *frontal* precipitation efficiencies were much lower and showed less seasonal variation than mean *synoptic* and *mesohigh* efficiencies. With the exception of the mean of July (3.41%), *frontal* precipitation efficiency decreased from April (3.58%) to August (2.80%) (Figure 4.2.26). However, there was no significant difference of means from *frontal* precipitation efficiency by month. The monthly mean *frontal* precipitation rate

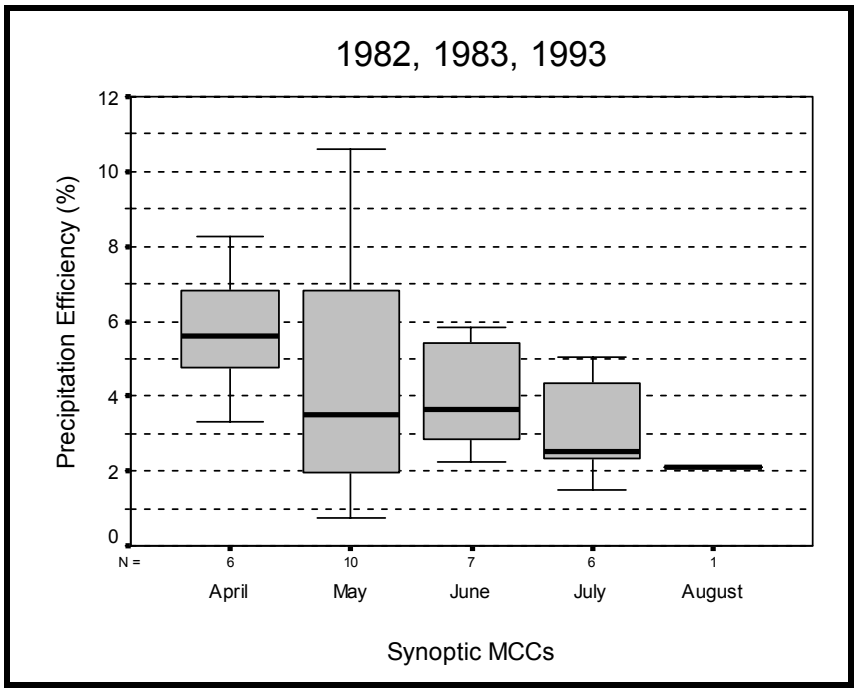

Figure 4.2.22. Box-and-whisker plot of the monthly distribution of precipitation efficiency for all *synoptic* MCCs during 1982, 1983, and 1993.

Table 4.2.2. Independent t-test results showing the number of *synoptic* MCCs (N) during April and July, mean precipitation efficiency (PE) in each month, significance (two-tailed) (sig.), and t-score (t) with a 95% confidence interval.

***Synoptic* MCCs**	**N**	**mean PE**	**t**	**sig.**
April	6	5.74	2.94	.016
July	6	3.04		

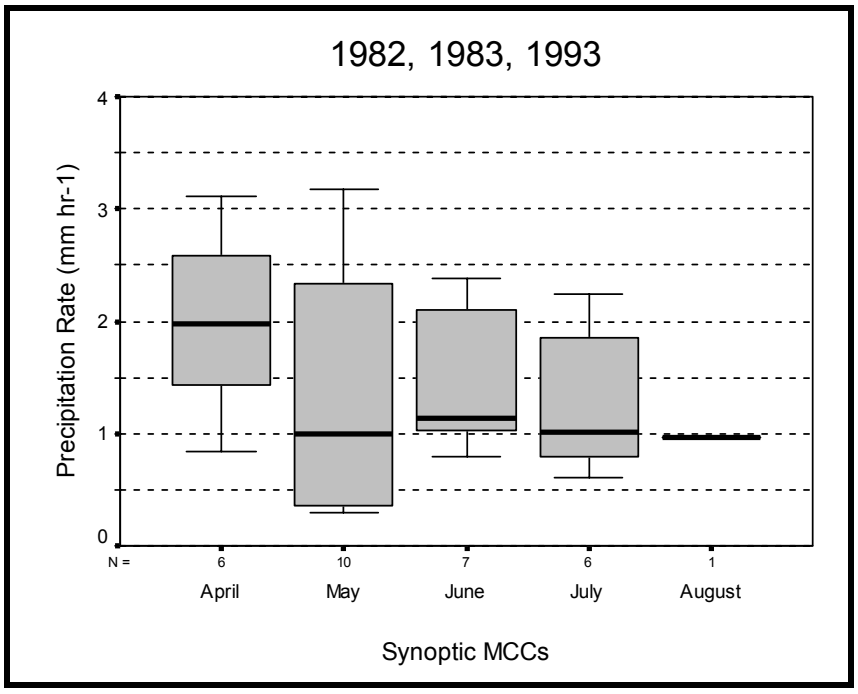

Figure 4.2.23. Box-and-whisker plot of the monthly distribution of precipitation rates for all *synoptic* MCCs during 1982, 1983, and 1993.

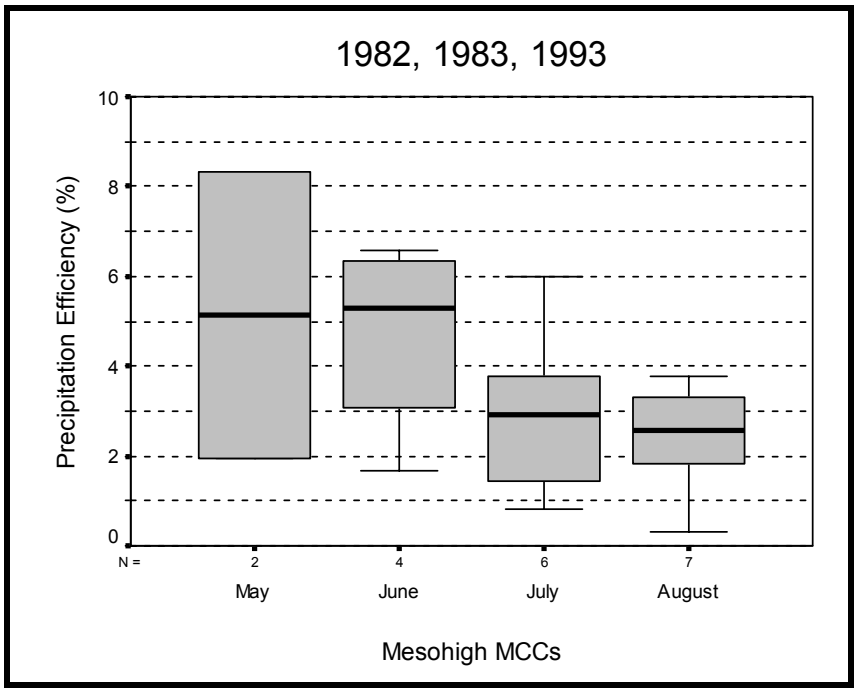

Figure 4.2.24. Box-and-whisker plot of the monthly distribution of precipitation efficiency for all *mesohigh* MCCs during 1982, 1983, and 1993.

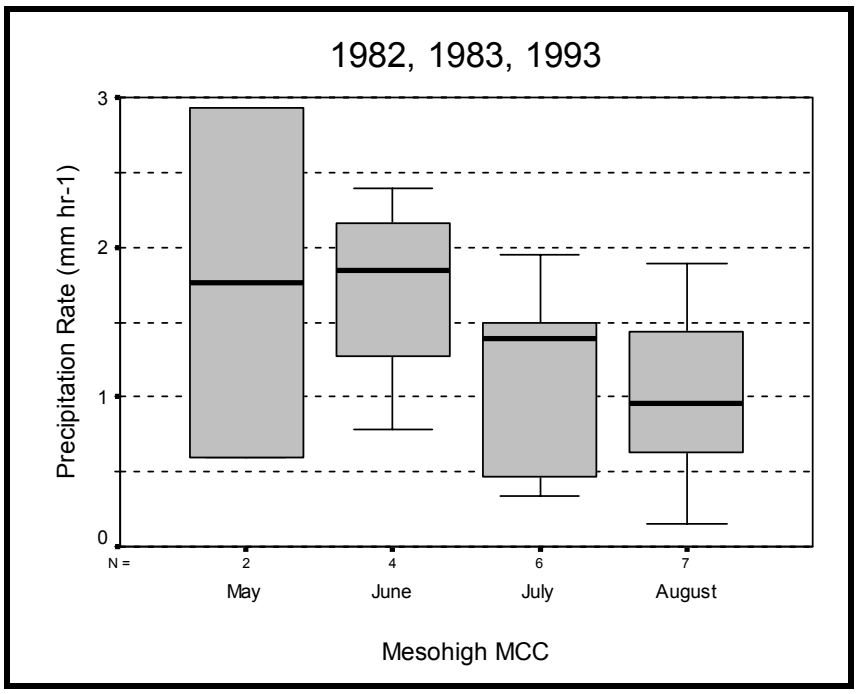

Figure 4.2.25. Box-and-whisker plot of the monthly distribution of precipitation rates for all *mesohigh* MCCs during 1982, 1983, and 1993.

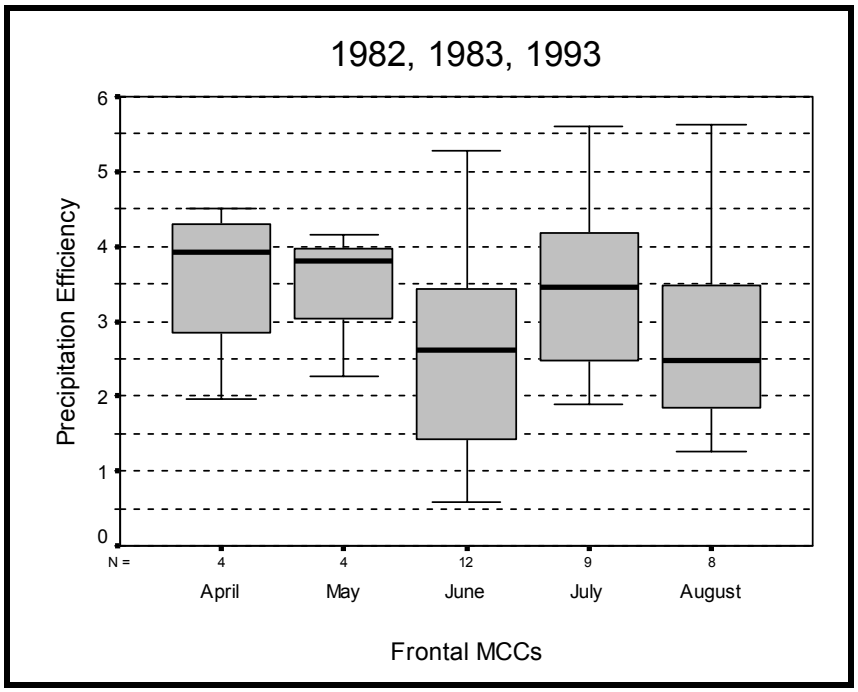

Figure 4.2.26. Box-and-whisker plot of the monthly distribution of precipitation efficiency for all *frontal* MCCs during 1982, 1983, and 1993.

had less variability than the mean *synoptic* and *mesohigh* precipitation rates. The peak mean *frontal* precipitation rate occurred in May (1.4 mm hr $^{-1}$), followed by July (1.3 mm hr $^{-1}$) and August (1.2 mm hr $^{-1}$) (Figure 4.2.27).

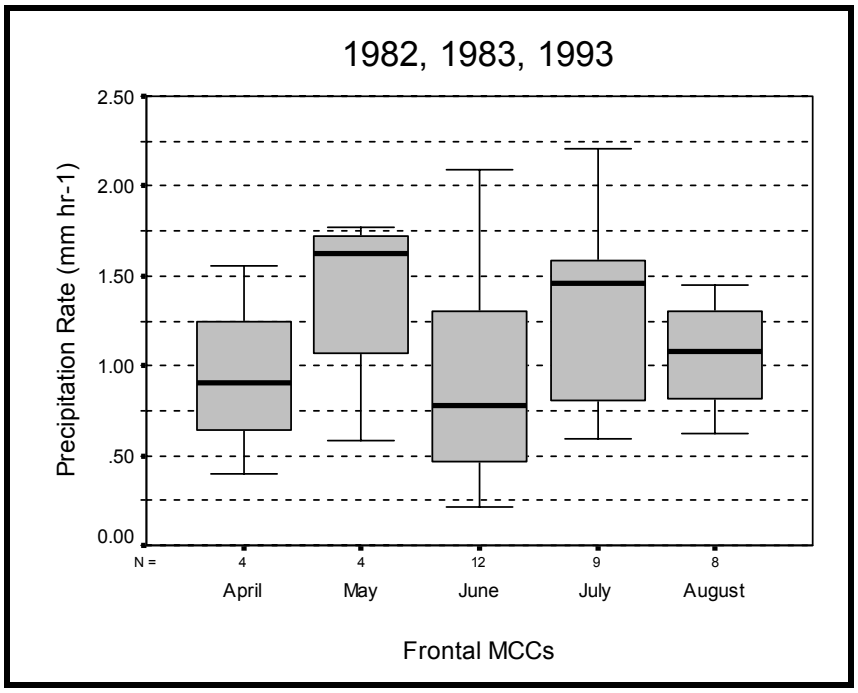

Figure 4.2.27. Box-and-whisker plot of the monthly distribution of precipitation rates for all *frontal* MCCs during 1982, 1983, and 1993.

4.3 Annual/Monthly Analysis By Year

The annual MCC analysis for the "normal" year of 1982 showed that on average, storm lifecycles were 10.3 hours with an anvil cloud size of 183,500 km^2, and storm precipitable water of 39.0 mm. The mean storm precipitation efficiency during this time was 3.71%, and produced a precipitation total of 13.3 mm at a rate of 1.4 mm hr $^{-1}$. The monthly analyses during 1982 showed that although April had the largest mean duration, mean largest anvil cloud size, and the highest mean precipitation rate and total. However, the highest mean efficiency occurred in May.

The annual analysis for the drought year of 1983 showed that on average, MCC lifecycles slightly increased 0.70 hours above the 1982 average to 11.0 hours. The anvil cloud size decreased by nearly 25,700 km^2 below 1982. Storm precipitable water also decreased by nearly 2.0 mm below 1982. However, the mean precipitation efficiency had a negligible difference (increased by only 0.04%), and produced 1.5 mm more precipitation than 1982. The monthly analysis for 1983 showed that the mean largest anvil cloud size, second longest mean duration, and the highest mean precipitation efficiency, rate, and total occurred during May.

The annual analysis for the anomalously wet year 1993 showed that on average, MCC duration increased 4.61 hours above 1982 to 14.7 hours. The anvil cloud size decreased by nearly 10,000 km^2 below 1982. The precipitable water also decreased below 1982 by nearly 6.0 mm. However, the precipitation efficiency decreased by only 0.17%, and produced 3.2 mm more precipitation on average than 1982 (with a rate of only .30 mm hr^{-1} below 1982). For 1993, the monthly analysis showed less variability. The longest-lived storms occurred in April, June, and August. Similarly, so did the mean largest anvil cloud sizes, mean precipitation efficiency, and mean precipitation totals. However, rather than showing a general decreasing trend throughout the warm season in the mean precipitation rate (as in 1982 and 1983), mean precipitation rate increased. This may be indicative of recycled moisture from the above-average precipitation and saturated soils that began in July 1992 and the persistent heavy rainfall that fell along the upper Mississippi River Basin throughout the warm season during 1993 (Kunkel et al. 1994). The month-to-month comparison further revealed that 1993 MCCs generally had longer mean lifecycles with mean larger anvil cloud shields compared to 1982 and 1983.

Interestingly, the drought year had the highest mean precipitation efficiency whereas the anomalously wet year had the lowest efficiency (although there was no significant difference of means). The years 1982 and 1983 had similar mean precipitation rates, whereas 1993 had the lowest mean precipitation rate, but the greatest precipitation amount. Additionally, 1983 had a higher mean precipitation total than 1982. In other words, the drought year had a higher precipitation total than the "normal" year, but with a lower precipitation rate than average. These results suggest that monthly storm-type characteristics must be examined further to understand whether a particular type of MCC (e.g., *synoptic*) had a greater influence on the precipitation characteristics during each year.

4.4 Annual/Monthly Storm-Type Analysis By Year

During the "normal" year of 1982, *frontal* MCCs were the longest-lived systems, followed by *synoptic* events. However, *synoptic* MCCs were more efficient and produced higher precipitation amounts than *frontal* events. During April and May, *synoptic* events had the highest mean precipitation efficiency, rate, and amount. The highest mean precipitation efficiency, rate, and amount were due to *mesohigh* events in June, followed by *frontal* events. In contrast, *frontal* events had the highest mean precipitation efficiency, rate, and amount during July, followed by *mesohigh* events. Although *mesohigh* MCCs were the most efficient with the highest precipitation rate, *frontal* events produced more precipitation in August.

During the drought year of 1983, *synoptic* MCCs were the most efficient storms that produced the greatest precipitation at the highest precipitation rate, followed by

mesohigh events. *Synoptic* events were the most efficient systems with the highest precipitation rate and amount during April and July. During May, June, and August, *mesohigh* events had the highest mean precipitation efficiency, precipitation rate, and precipitation amount.

During the wet period of 1993, *synoptic* events were the least efficient with the lowest precipitation rate and precipitation amount. Although *frontal* and *mesohigh* events had similar efficiencies (a difference of 0.13%), average *frontal* precipitation totals were higher, but with a lower rain rate. *Synoptic* events were the most efficient systems that produced the greatest amount of precipitation with the highest precipitation rate during April and May. Although *frontal* MCCs were the most efficient during June, *synoptic* events produced the greatest amount of precipitation. During August, *frontal* events had a slightly higher precipitation efficiency, rate, and amount than *mesohigh* events.

4.5 Summary

Overall, the temporal observations suggest that MCC precipitation efficiency was primarily related to the time of year. The examination of the monthly storm-type variability showed that on average, larger, longer-lived storms were not always the most efficient systems. However, what was common between each storm type was the general decreasing trend in precipitation efficiency throughout the warm season. These results suggested that the seasonal component played a larger roll in the overall efficiency of the storm. Although the type of MCC may have influenced the overall efficiency, the synoptic regime in which each storm type typically developed was still at least partially related to the time of year. In other words, regardless of when each storm type initiated,

storm-type efficiency was highest earlier in the warm season and generally decreased as the warm season progressed.

The comparison of MCC precipitation efficiency between anomalous and "normal" moisture conditions showed interesting results in that the "wet" year of 1993, MCCs were larger, longer-lived and produced higher amounts of precipitation than MCCs during the drought year of 1983. However, 1983 MCCs had a higher mean precipitable water, precipitation efficiency, and precipitation rate. Furthermore, MCCs during the drought year of 1983 had a higher mean duration, precipitation efficiency and precipitation total than 1982.

On average, during 1982 and 1983 there was a general decrease in MCC precipitation efficiency throughout the warm season. Mean precipitation efficiency within each storm-type during 1982 had less month-to-month variability (i.e., no seasonal pattern was apparent). During 1983, mean *mesohigh* precipitation efficiency showed a distinct monthly decrease as the warm season progressed. Mean *synoptic* precipitation efficiency showed a more indistinct seasonal decrease than *mesohigh* events, whereas *frontal* events did not exhibit a clear seasonal trend in precipitation efficiency. However, the independent t-test showed that there was no significant difference in mean precipitation efficiency between each storm type between 1983 and 1993. Precipitation efficiency during 1993 was unique in that the mean monthly efficiency showed a slight increase throughout the warm season.

The results of the higher mean precipitation efficiency during the drought year of 1983 compared to the lower efficiency during the wet period of 1993, raised more important questions:

- How do MCC and MCC storm-type frequency, precipitation efficiency, and precipitation rate change by latitude?
- How do MCC and MCC storm-type precipitation efficiency and precipitation rate change by latitude for each month?
- How might the clustering of MCCs be associated with drought years vs. wet years?

These questions are addressed in the following chapter by examining the spatio-temporal attributes of precipitation efficiency.

CHAPTER 5

SPATIO-TEMPORAL ANALYSIS OF 1982, 1983, AND 1993 WARM-SEASON MCCs

This chapter illustrates overall MCC and MCC storm-type precipitation efficiency in relation to latitude during the warm season for the "normal" year of 1982, drought year of 1983, and the anomalously wet year of 1993. Latitudinal precipitation efficiency characteristics within each year are further discussed in order to compare results between anomalous and "normal" moisture conditions. Finally, the relationship between spatial storm density (i.e., the concentration of MCC occurrences based on storm duration), precipitation efficiency, and anomalous and "normal" moisture conditions is described.

5.1 Latitudinal Analysis Of 1982, 1983, 1993 MCCs

5.1.1 Frequency

Augustine and Howard (1988) and Ashley et al. (in press) found as the warm season progressed, MCC frequency increased and generally exhibited a poleward migration. For the 87 events that occurred between April-August during 1982, 1983, and 1993, the poleward migration described by Augustine and Howard (1988) and Ashley et al. (in press) is illustrated in Figure 5.1.1. The monthly mean MCC latitude of initiation increased from April (34.9°N) to July (42.5°N), followed by a slight decrease in August

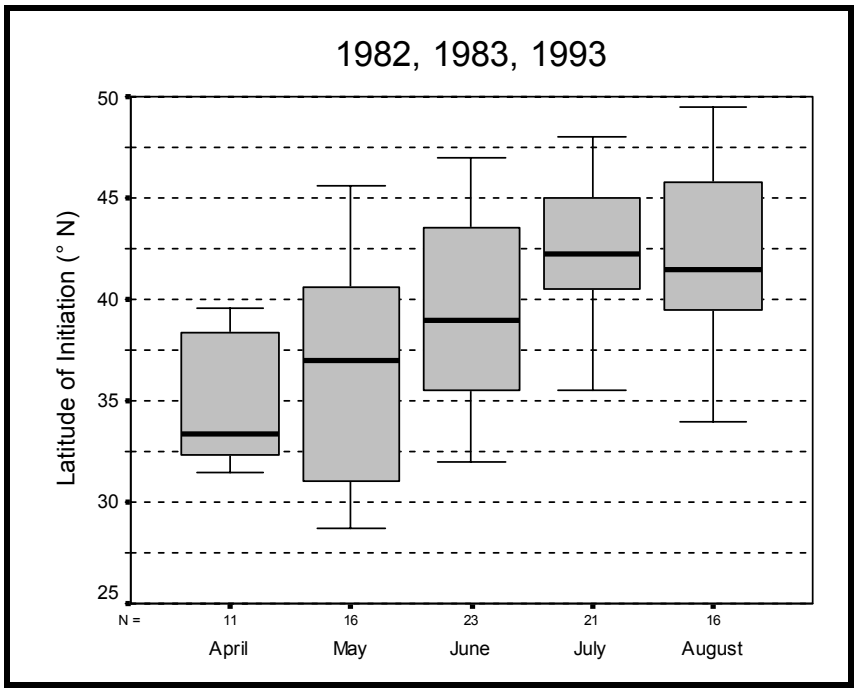

Figure 5.1.1. Box-and-whisker plot of the MCC latitude of initiation for each month during 1982, 1983, and 1993. The plots show the median (thick line), interquartile range (shaded), and outliers (i.e., the 10^{th} and 90^{th} percentile as whiskers) for the indicated months. Additionally, the total number of MCCs per month for all 15 years investigated is indicated along the x-axis.

(42.3°N). MCC frequency also increased between 25-45°N. The peak MCC frequency was 29 events between 40-45°N (Figure 5.1.2) The independent t-test showed that MCC latitude of initiation for April was significantly lower than that for June, July, and August. The latitude of initiation for May and June were also significantly lower than that of July and August (Table 5.1.1).

5.1.2 Precipitation Efficiency

With increasing latitude, the mean precipitation efficiency pattern was not as consistent as the monthly efficiency pattern. For example, precipitation efficiency

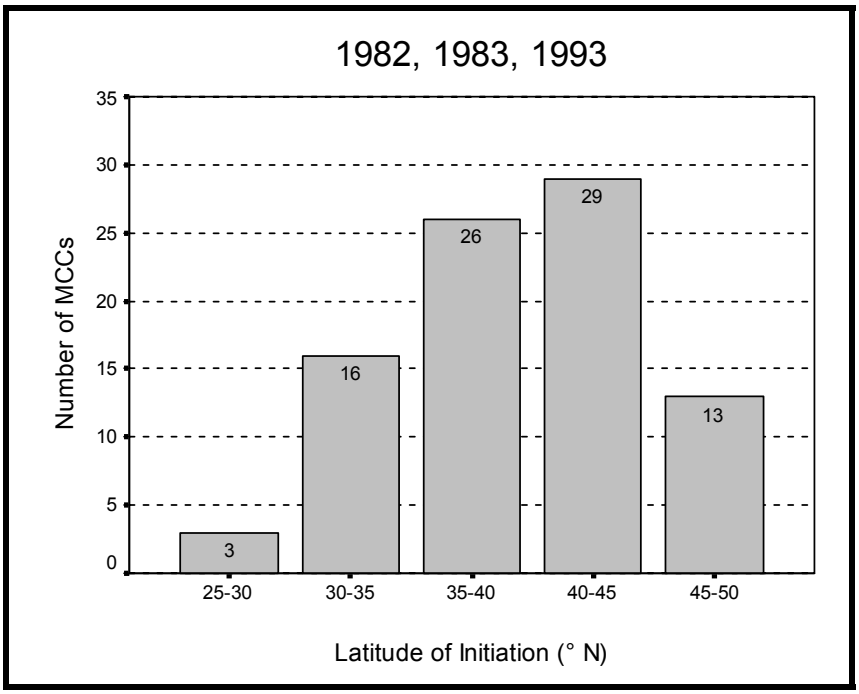

Figure 5.1.2. Bar graph of the storm frequency in each latitude band during 1982, 1983, and 1993.

Table 5.1.1. Independent t-test results showing the number of MCCs in April, May, June, July, and August (N), mean latitude of initiation (LAT) in each month, significance (two-tailed) (sig.), and t-score (t) with a 95% confidence interval.

Month	N	mean Lat	t	sig.
April	11	34.89	-3.1	.023
June	23	39.26		

Month	N	mean Lat	t	sig.
April	11	34.89	-6.2	.000
July	21	42.54		

Month	N	mean Lat	t	sig.
April	11	34.89	-5.1	.000
August	16	42.28		

Month	N	mean Lat	t	sig.
May	16	36.58	-4.0	.001
July	21	42.54		

Month	N	mean Lat	t	sig.
May	16	36.58	-3.4	.002
August	16	42.28		

Month	N	mean Lat	t	sig.
June	23	39.26	-2.7	.012
July	21	42.54		

Month	N	mean Lat	t	sig.
June	23	39.26	-2.1	.046
August	16	42.28		

decreased each month from April (4.87%) to August (2.59%) (see Figure 4.1.6). However, precipitation efficiency by latitude band showed that the second highest efficiency occurred between 25-30°N (4.72%), while the third highest occurred between 45-50°N (3.91%). But between 30-45°N, where 80% of all MCCs occurred, mean precipitation efficiency decreased with increasing latitude (Figure 5.1.3). The independent t-test showed that precipitation efficiency between 30-35°N was significantly higher than that between 40-45°N (Table 5.1.2).

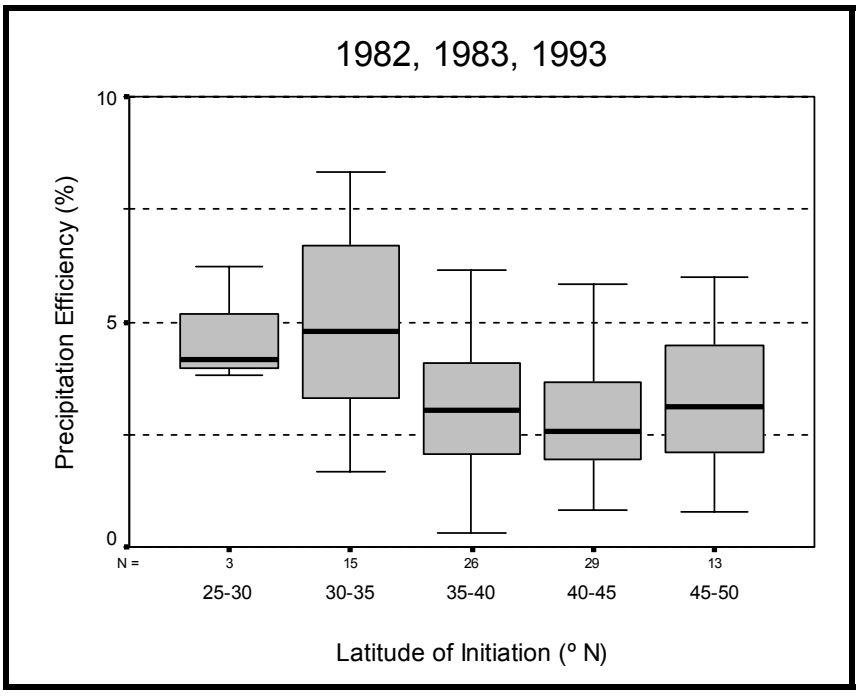

Figure 5.1.3. Box-and-whisker plot of the precipitation efficiency in each latitude band during 1982, 1983, and 1993.

Table 5.1.2. Independent t-test results showing the number of MCCs in the latitude bands of 30-35°N and 40-45°N (N), mean precipitation efficiency in each latitude band (PE), significance (two-tailed) (sig.), and t-score (t) with a 95% confidence interval.

Latitude Band	N	mean PE	t	sig.
30-35°N	15	5.05	3.75	.001
40-45°N	29	2.81		

Table 5.1.3. Linear regression results showing the significant relationship of MCC precipitation efficiency with the time of year (Month) and latitude of initiation (Lat_i). Parameters include total number of events (N), coefficient of determination (R^2), slope coefficient (B), t-score (t), and significance (two-tailed) (sig.) with a 95% confidence interval.

Independent	N	R^2	B	t	sig.
Month	86	.106	-2.17E-7	-3.15	.002
Lat_i	86	.072	-0.12	-2.55	.013

As the warm season progressed, mean precipitation efficiency decreased. As MCCs developed further from the Gulf of Mexico, mean precipitation efficiency also decreased. Since the mean precipitation efficiency decreased as MCCs migrated northward throughout the warm season, lower mean efficiency values at higher latitudes were expected. However, the linear regression analysis showed that the time of year (given by month) predicts 10.6% of the variance in MCC precipitation efficiency. Latitude predicts 7.2% of the variance in MCC precipitation efficiency. The time of year and latitude both were negatively correlated, but the slope for the time of year had a greater magnitude (i.e., greater response) (Table 5.1.3). Additionally, precipitation efficiency predicts 81.2% of the variance in precipitation rates, and 67.9% of the variance in precipitation totals (Table 5.1.4). This indicates that precipitation efficiency has a significant linear relationship between a given storm's intensity and rain rate.

To determine whether MCC precipitation efficiency was more dependent on time or space, an examination of mean monthly precipitation efficiency by latitude was necessary.

Table 5.1.4. Linear regression results showing the significant relationship of MCC precipitation efficiency with precipitation rate (PR) and precipitation amount (Precip.). Parameters include total number of events (N), coefficient of determination (R^2), slope coefficient (B), t-score (t), and significance (two-tailed) (sig.) with a 95% confidence interval.

Independent	N	R^2	B	t	sig.
PR	86	.81	2.61	19.06	.000
Precip.	86	.68	0.19	13.34	.000

During April, the mean precipitation efficiency decreased from 5.93% to 3.28% between 30-40°N. There were only three MCCs that occurred between 25-30°N. These three events occurred in May and had a mean efficiency of 4.7%. Between 30-50°N, mean efficiency decreased from 6.30% to 0.77% during May. Of the 24 MCCs that occurred in June, the mean precipitation efficiency of 21 events decreased from 3.78% to 3.10% between 30-45°N. The remaining three events had a mean efficiency of 6.30% between 45-50°N. The highest mean efficiency during July was 3.70% between 45-50°N, followed by 3.54% between 35-40°N and 2.9% between 40-45°N and thus, no clear spatial pattern was evident for July. With the exception of 30-35°N (2.26%), the mean precipitation efficiency increased in August between 35-50°N (1.91% - 3.29%).

MCCs that developed at lower latitudes during April and May had higher mean efficiencies compared to storms at higher latitudes. During June and July, the most efficient storms occurred between 45-50°N, not the lower latitudes. August MCCs became more efficient as latitude increased. These results showed that during the early warm season, precipitation efficiency was highest at lower latitudes. In contrast, higher efficiencies occurred at higher latitudes during the mid-to-late warm season. The

precipitation rate patterns were identical. These results suggest that both latitude and the time of year may play a role in the variation of MCC precipitation efficiency.

5.1.3 Storm-Type Precipitation Efficiency

On average, *synoptic* MCCs occurred at 38.5°N with a precipitation efficiency of 4.38%. An examination of *synoptic* precipitation efficiency by latitude showed that mean efficiency decreased from 6.21% to 2.44% between 25-50°N (Figure 5.1.4). The independent t-test showed that *synoptic* efficiency between 30-35°N had significantly higher mean efficiencies than that between 45-50°N (Table 5.1.5). The monthly *synoptic* analysis showed that April and May efficiency decreased as latitude increased. May was the only month when *synoptic* events occurred between 25-50°N. No *synoptic* precipitation efficiency pattern was evident during June-August.

Mesohigh events occurred at 40.1°N with a precipitation efficiency of 3.36%. The latitudinal range for *mesohigh* events was 30-50°N. The two highest mean *mesohigh* efficiencies were 4.70% between 30-35°N and 3.76% between 45-50°N (Figure 5.1.5). The independent t-test showed that there was no significant difference of means in *mesohigh* precipitation efficiency by latitude. The monthly *mesohigh* analysis showed that mean June precipitation efficiency was highly variable and no efficiency pattern was evident. The mean July *mesohigh* efficiency increased from 1.43% to 6.01% between 35-50°N. The mean August *mesohigh* efficiency was similar to June and no efficiency pattern was determined. Only one *mesohigh* event occurred during May.

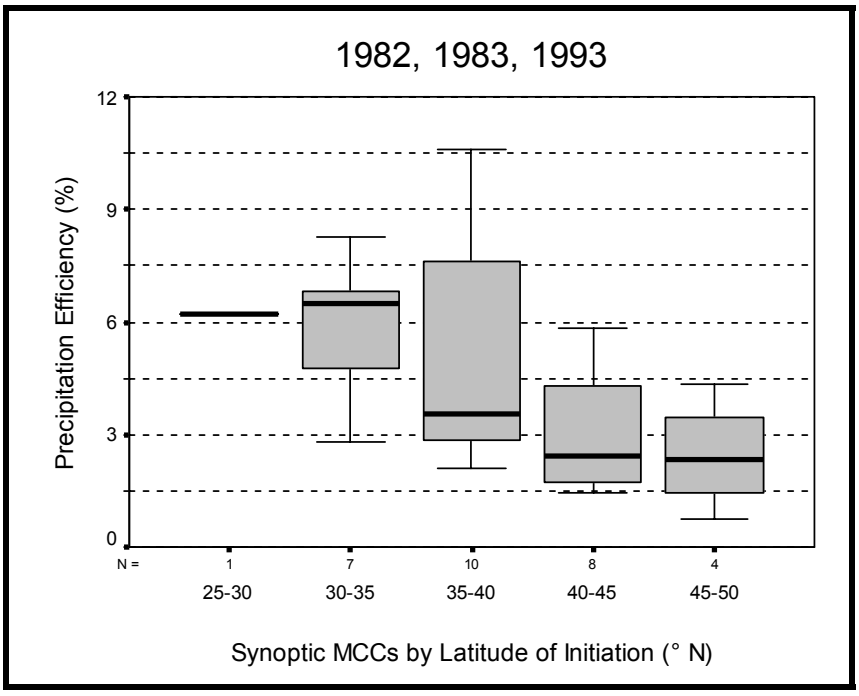

Figure 5.1.4. Box-and-whisker plot for all *synoptic* precipitation efficiency in each latitude band during 1982, 1983, and 1993.

Table 5.1.5. Independent t-test results showing the number of *synoptic* MCCs in the latitude bands of 30-35°N and 45-50°N (N), mean precipitation efficiency in each latitude band (PE), significance (two-tailed) (sig.), and t-score (t) with a 95% confidence interval.

Latitude Band	N	mean PE	t	sig.
30-35°N	7	5.82	3.35	.011
45-50°N	4	2.45		

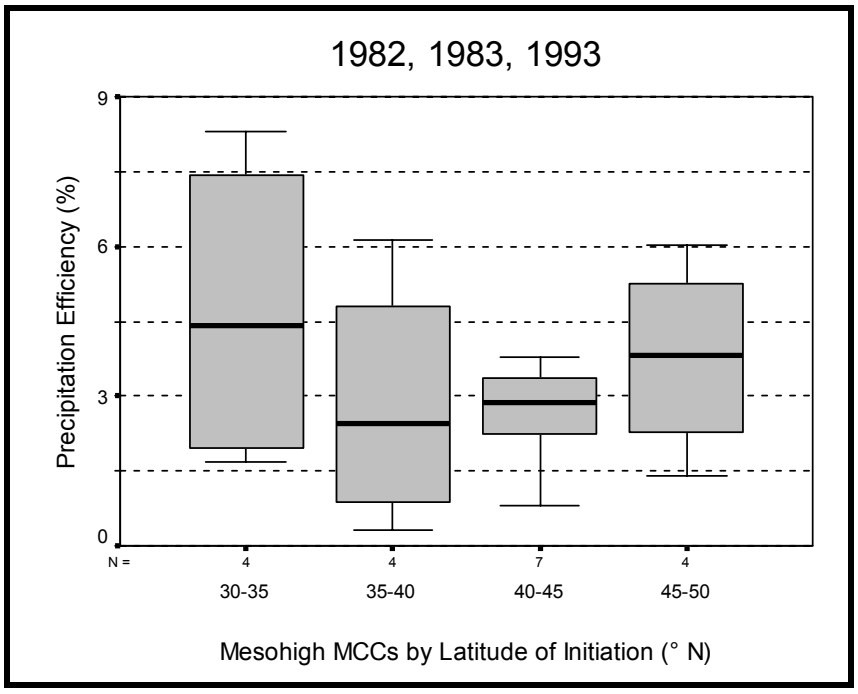

Figure 5.1.5. Box-and-whisker plot for all *mesohigh* precipitation efficiency in each latitude band during 1982, 1983, and 1993.

Frontal MCCs occurred at a mean latitude of 40.2°N with a mean efficiency of 3.26%. Mean *frontal* precipitation efficiency showed the greatest latitudinal variation. The latitudinal range for *frontal* events was 25-50°N. The most efficient *frontal* MCCs (5.22%) occurred between 45-50°N, followed by 30-35°N (4.05%) and between 25-30°N (3.96%) (Figure 5.1.6). The independent t-test showed that *frontal* precipitation efficiency between 25-30°N was significantly higher than that for *frontal* events that occurred between 35-45°N (Table 5.1.6). The monthly *frontal* analysis showed that April, May, and July precipitation efficiency decreased as latitude decreased. Conversely, mean August *frontal* precipitation efficiency increased from 1.92% to 4.89% between 35-50°N. During June, a time when *frontal* MCCs most often occur, the highest mean

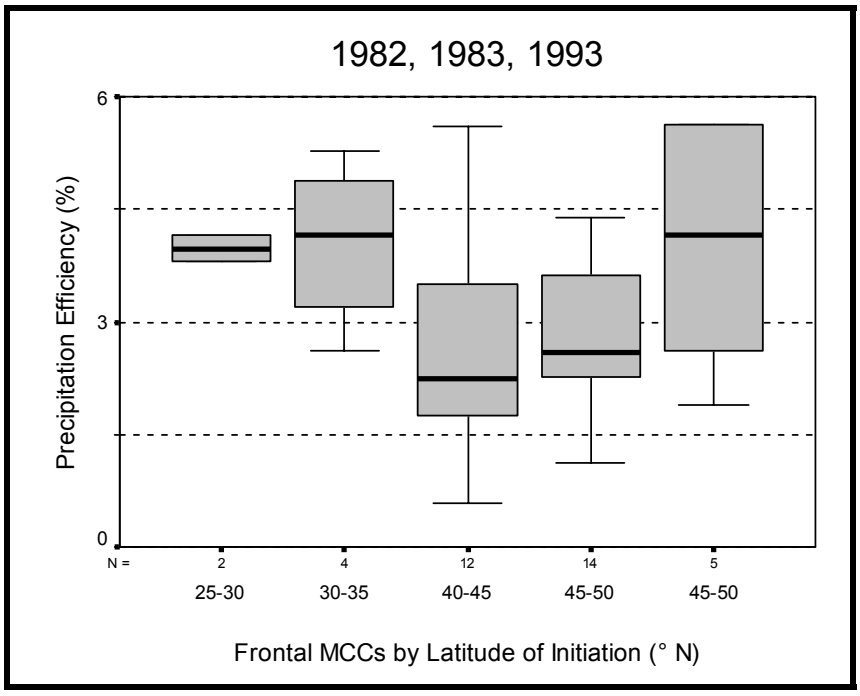

Figure 5.1.6. Box-and-whisker plot for all *frontal* precipitation efficiency in each latitude band during 1982, 1983, and 1993.

Table 5.1.6. Independent t-test results showing the number of *frontal* MCCs in the latitude bands of 25-30°N, 30-35°N, and 40-45°N (N), mean precipitation efficiency in each latitude band (PE), significance (two-tailed) (sig.), and t-score (t) with a 95% confidence interval.

Latitude Band	N	mean PE	t	sig.
25-30°N	2	3.98	3.10	.010
30-35°N	12	2.62		

Latitude Band	N	mean PE	t	sig.
25-30°N	2	3.98	3.01	.004
40-45°N	14	2.77		

Table 5.1.7. Linear regression results showing the significant relationship of *synoptic* MCC precipitation efficiency with latitude (Lat) and *mesohigh* efficiency with time of year (Month). Parameters include total number of events (N), coefficient of determination (R^2), slope coefficient (B), t-score (t), and significance (two-tailed) (sig.) with a 95% confidence interval.

Synoptic	**N**	**R^2**	**B**	**t**	**sig.**
Lat	31	.29	-.26	-3.37	.002
Mesohigh	**N**	**R^2**	**B**	**t**	**sig.**
Month	19	.23	-3.79E-7	19.06	.000

efficiency was 7.20% between 45-50°N. However, no latitudinal pattern in *frontal* efficiency was evident.

The linear regression analysis for each subset showed that latitude predicts 28.9% of the variance in, and is negatively correlated with *synoptic* MCC precipitation efficiency. In contrast, the time of year predicts 23.4% of the variance in, and is negatively correlated with *mesohigh* MCC precipitation efficiency (Table 5.1.7). Neither latitude, nor the time of year could predict a significant proportion of the variance in *frontal* MCC precipitation efficiency. These results suggest that higher *synoptic* precipitation efficiency is related to strong baroclinic zones with ample moisture supply in close proximity to the Gulf of Mexico.

5.2 Latitudinal Analysis By Year

5.2.1 Frequency

During the "normal" year of 1982, the peak MCC frequency by latitude band was 13 events between 35-40°N (Figure 5.2.1). Although the highest frequency of MCCs during 1983 occurred between 40-50°N, there was no clear clustering by latitude band (Figure 5.2.2). The highest frequency during 1993 occurred between 40-45°N with 11 events (Figure 5.2.3). The lowest frequency in 1983 and 1993 was between 25-30°N, whereas during 1982, the lowest frequency occurred between 45-50°N.

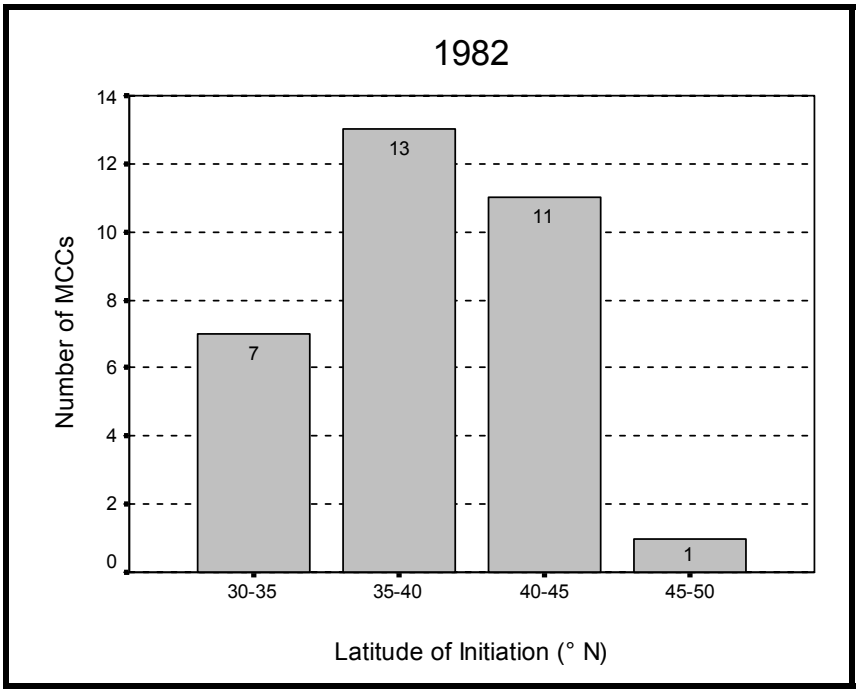

Figure 5.2.1. Bar graph of the storm frequency in each latitude band during 1982.

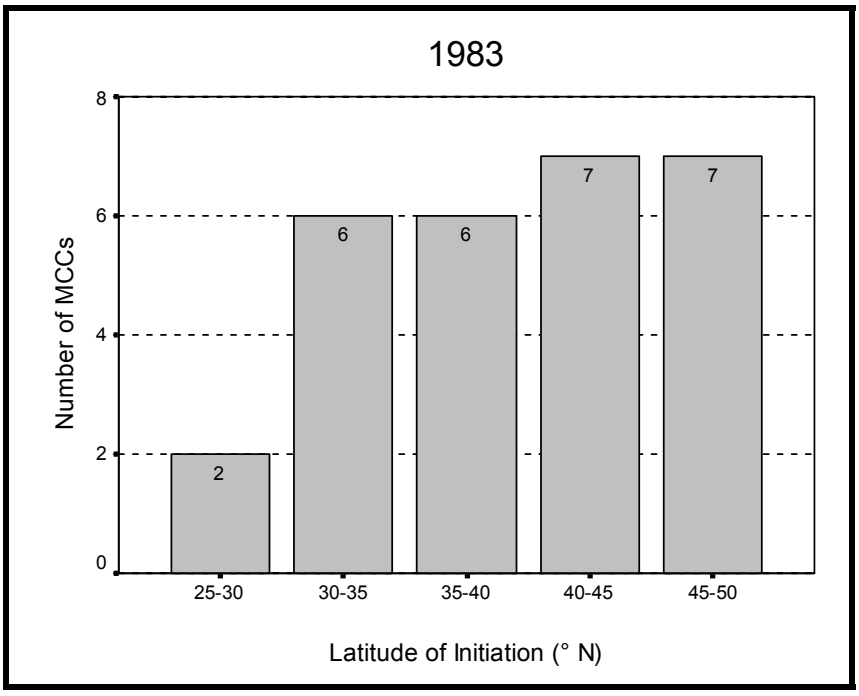

Figure 5.2.2. Bar graph of the storm frequency in each latitude band during 1983.

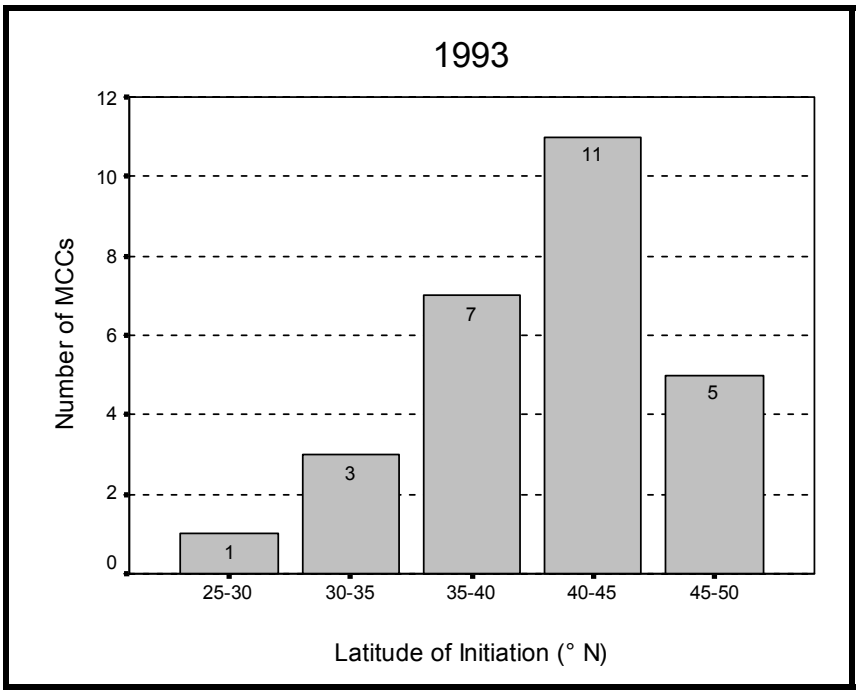

Figure 5.2.3. Bar graph of the storm frequency in each latitude band during 1993.

5.2.2 Precipitation Efficiency

An examination of mean precipitation efficiency during 1982 showed a decrease from 4.55% to 2.56% between 30-50°N (Figure 5.2.4). The monthly analysis showed a decrease from 7.13% to 2.26% between 35-45°N in May. No pattern was evident for June. During July, mean precipitation efficiency decreased from 3.24% to 2.56% between 35-50°N. In contrast, mean precipitation efficiency increased from 1.54% to 3.17% during August. The three MCCs in April during 1982 occurred on the same latitude band.

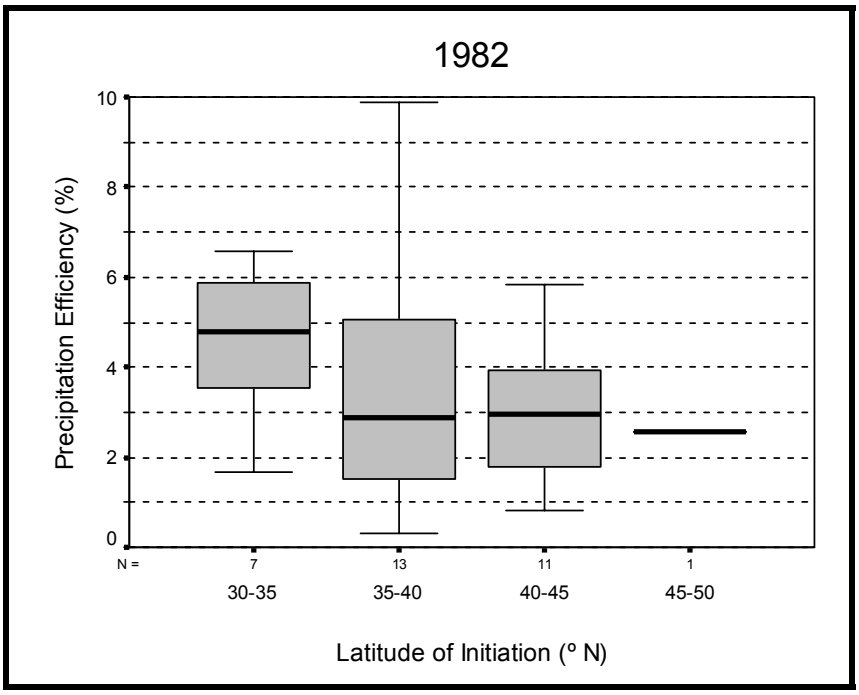

Figure 5.2.4. Box-and-whisker plot of the precipitation efficiency in each latitude band during 1982.

The highest mean efficiency in 1983 was 5.70% between 30-35°N, followed by 3.39% between 35-40°N and 3.28% between 45-50°N (Figure 5.2.5). The monthly

analysis showed a decreased from 6.53% to 2.63% between 30-40°N in April. No pattern was evident for May, June, or July. During August, the mean precipitation efficiency increased from 2.26% to 3.0% between 30-45°N.

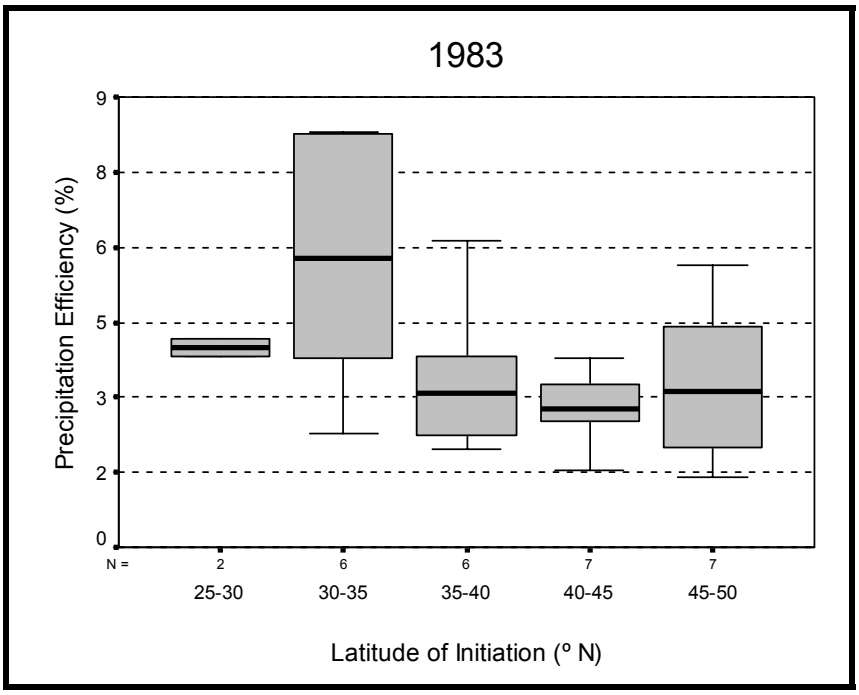

Figure 5.2.5. Box-and-whisker plot of the precipitation efficiency in each latitude band during 1983.

During 1993, the mean precipitation efficiency decreased from 6.21% to 2.65% between 25-45°N. However, the second highest mean precipitation efficiency occurred between 45-50°N (Figure 5.2.6). During the early warm season (April-May), precipitation efficiency decreased with increasing latitude. However, precipitation efficiency during June and July increased with increasing latitude. No pattern could be determined for July.

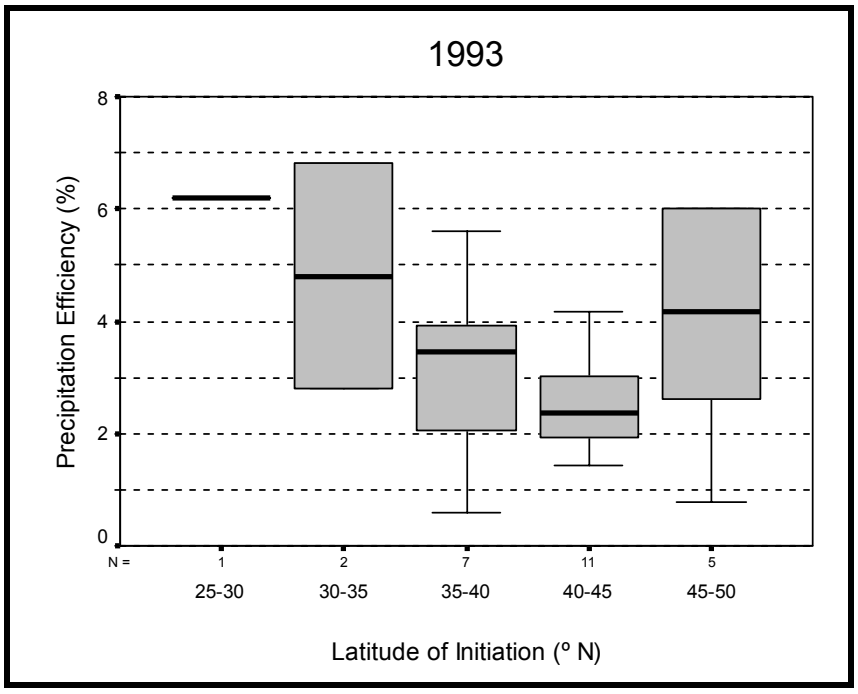

Figure 5.2.6. Box-and-whisker plot of the precipitation efficiency in each latitude band during 1993.

5.2.3 Storm-Type Precipitation Efficiency

The analysis of storm-type precipitation efficiency during each year showed that efficiency did not vary according to latitude in each type. For example, on average, *synoptic* MCCs all occurred near 38.5°N during 1982, 1983, and 1993. However, the highest mean *synoptic* precipitation efficiency occurred in 1982 (5.97%), followed by 1983 (4.28%) and 1993 (3.03%). Despite the similar latitude of *synoptic* occurrences during each year, the mean *synoptic* efficiencies between each year were dissimilar (i.e., no pattern was evident efficiency by storm type).

5.3 Summary

The spatio-temporal analysis illustrated that as the mean latitude for MCC development increased throughout the warm season, precipitation efficiency decreased. However, the most notable characteristic of the latitudinal analysis occurred between 45-50°N, where MCCs were more efficient than storms that occurred between 35-45°N. The analysis of the latitudinal distribution of MCC precipitation efficiency by month showed that early warm season efficiencies did not increase as storms developed further from the Gulf of Mexico. During the mid-to-late warm season, more efficient MCCs occurred between 45-50°N. These results suggest that storm types played a roll in precipitation efficiency and the dynamics of each storm type corresponded to the efficiencies for MCCs at given locations for a certain time of year.

The MCC storm-type analysis further illustrated storm types that generally occurred at lower (higher) latitudes (e.g., *synoptic* MCCs) had higher (lower) mean precipitation efficiencies. Each storm type illustrated an increase in latitude and decrease in precipitation efficiency throughout the warm season. The storm-type analysis by latitude demonstrated that *synoptic* MCCs had higher (lower) mean precipitation efficiencies at lower (higher) latitudes. *Mesohigh* MCCs straddled the latitudinal range with peak mean precipitation efficiency at both low and high latitudes. *Frontal* MCCs shared a similar latitudinal efficiency pattern as *mesohigh* events, except for a distinct peak in efficiency at higher latitudes.

The latitudinal storm-type analysis showed that on average, during the early warm season, each MCC storm type became less efficient as they developed further from the Gulf of Mexico. However, during the mid-to-late warm season, storm-type efficiency

became more variable with latitude and showed a general increase at higher latitudes – particularly *mesohigh* and *frontal* MCCs.

These results indicate that the relationship between *synoptic* precipitation efficiency and latitude may be accounted for by stronger baroclinicity at lower latitudes during the early warm season. *Synoptic* MCCs that develop further north during the early warm season may be spawned by weaker dynamics (e.g., a less amplified upper-level long and short-wave pattern and/or an area of weaker upper-level diffluence). Likewise, *mesohigh* and *frontal* MCCs generally occurred at higher latitudes during the mid-to-late warm season. Mean *mesohigh* and *frontal* precipitation efficiencies were generally higher at higher latitudes during the latter portion of the warm season. In other words, as a given storm type develops further away from their conducive environments, the storm's internal dynamics become weaker, lowering the overall efficiency of the storm.

The linear regression analysis suggests that the time of year had a greater influence on the overall MCC precipitation efficiency. Nevertheless, the time of year played a significant roll in where MCCs typically developed. The regression analysis for each storm type does not suggest that latitude or the time of year is more or less influential on all storm types. Rather, these results suggest that latitude influences *synoptic* MCC precipitation efficiency and the time of year influences *mesohigh* MCC precipitation efficiency. Further, *frontal* efficiency is neither influenced by latitude nor the time of year.

The spatio-temporal analysis suggests that precipitation efficiency is co-dependent upon latitude and storm type. For example, on average, if three MCCs (one of each storm type) occurred between 30-35°N during the early warm season, it is likely that

the *synoptic* event would be the most efficient system. If the same example were applied between 40-45°N during the late warm season, the *synoptic* event would be the least efficient system. Based on this reasoning, the underlying factor that MCC precipitation efficiency is most dependent on is the time of year. Ultimately, the time of year generally determines what type of MCC will develop where and thus, how efficient the storm will be at producing precipitation and the intensity of the rainfall.

The yearly comparative analysis illustrated that the precipitation efficiency between the "normal" year of 1982, drought year of 1983, and anomalously wet year of 1993 was statistically the same. The latitudinal analysis for MCC development in each year showed that the mean monthly latitude of initiation during 1983 was highly variable. The mean monthly latitude of initiation during 1993 was more consistent. In fact, 86% of all MCCs during 1993 occurred between 39.8-42.8°N. In other words, MCCs during 1993 were developing over the same area, resulting in flooding. Interestingly, an additional analysis of MCC duration showed that 1993 MCCs were significantly longer-lived than both 1982 and 1983 MCCs. The results also showed that the precipitation efficiency characteristics between each storm type were generally the same between each year. Therefore, the spatial storm density became an even more likely reason for explaining how MCCs during both a drought year and anomalously wet year can be generally equally efficient at producing precipitation.

Figure 5.3.1 illustrates the spatial storm density (i.e., the concentration of MCC occurrences based on storm duration) between each year. There was a clear difference between the spatial density pattern between 1983 and 1993. The northerly displacement of MCCs during 1993 is a likely reason for the lower mean precipitation efficiency.

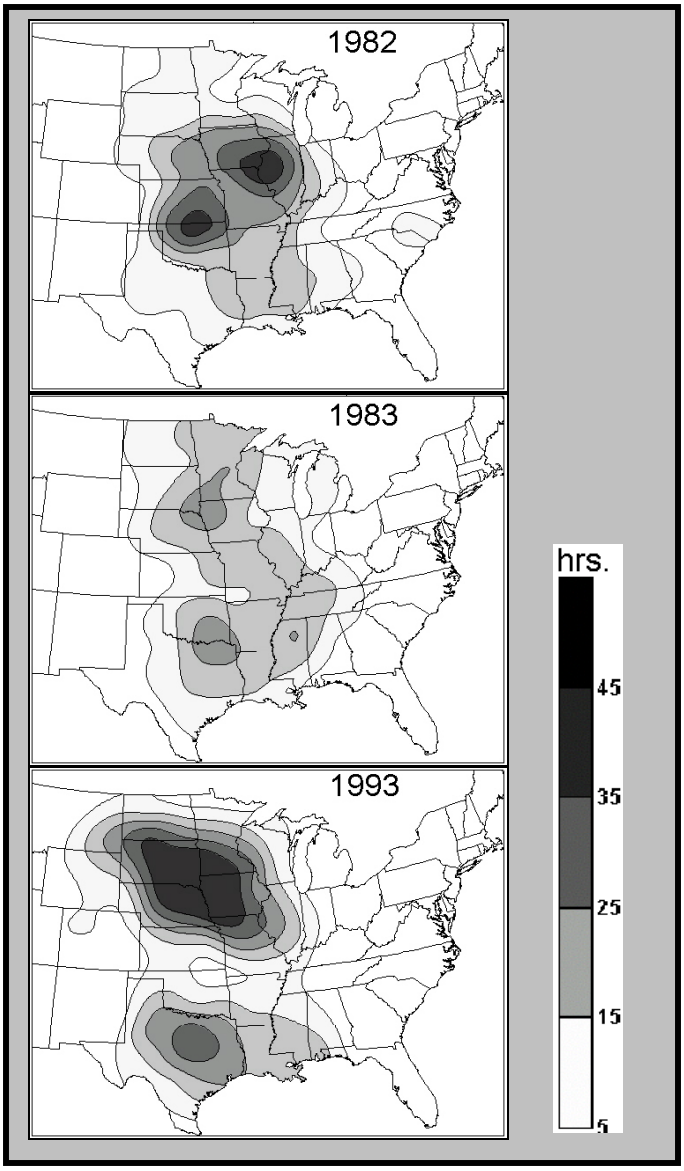

Figure 5.3.1. MCC densities derived from the total number of hours of -32°C cloud shield coverage for the years 1982, 1983, and 1993. From Ashley et al. (in press).

However, Figure 5.3.1 shows that MCCs occurred over the same area throughout most of the warm season. During 1983, MCC occurrences were more widely distributed. Therefore, the precipitation efficiency pattern for the anomalously wet and/or dry periods could not alone explain the anomalous conditions. Rather a combination of precipitation

efficiency, precipitation rate, storm frequency, and especially storm density were more suggestive of the anomalous moisture patterns during 1983 and 1993.

CHAPTER 6

SUMMARY AND CONCLUSIONS

This study is an examination of warm-season Mesoscale Convective Complex precipitation efficiency. Specifically, this study illustrates the spatio-temporal patterns and determines the significance of MCC precipitation efficiency during 1982 ("normal" year), 1983 (drought year), and 1993 (anomalously wet year) in the central United States. The monthly MCC frequency distribution for the three years is representative of the 15-year MCC climatology frequency distribution derived by Ashley et al. (in press). MCC frequency increased and peaked in June with 23 events. July marked the initial decline in storm frequency with 21 events.

6.1 Precipitation Efficiency Characteristics

MCC precipitation efficiency was determined by spatially averaging both precipitable water vapor and precipitation totals beneath the -32°C anvil cloud shield for each hour during the storm's lifecycle. By taking the ratio of precipitation to available water vapor for each hour, average precipitation efficiency for each MCC was calculated.

The highest mean efficiency occurred in April and decreased each month throughout the warm season. Similarly, the mean MCC precipitation rate and precipitation totals for each month followed the same pattern. These results showed a significant linear relationship that a higher (lower) precipitation efficiency leads to a

higher (lower) precipitation rate and higher (lower) precipitation amount. Therefore, on average, MCCs during the early warm season will be more efficient at producing copious amounts of precipitation with greater intensity. Progressively throughout the warm season, MCCs will become less efficient and thus, produce less amounts of precipitation at a lower precipitation rate.

The mean MCC precipitation efficiency pattern illustrated a significant spatial pattern. MCCs migrated poleward from approximately 35.0-43.0°N during April-August. The mean precipitation efficiency from the lowest (25-30°N) to the highest (45-50°N) latitude band did not a show a distinct poleward decrease. The highest and the lowest latitude band had the second and third highest mean precipitation efficiency. However, from 30-45°N (where 80% of MCCs occurred), precipitation efficiency significantly decreased.

Upon interpreting the spatial and temporal dependency of MCC precipitation efficiency, an examination of how the atmospheric synoptic patterns influenced precipitation efficiency was conducted. MCCs were stratified into three storm types: *synoptic*, *mesohigh*, and *frontal*. This procedure enabled an analysis of precipitation efficiency and its relationship with atmospheric dynamics, and ultimately, of space and time.

On average, *synoptic* MCCs mostly occurred early in the warm season at lower latitudes. *Synoptic* MCCs were the largest, longest-lived systems with the highest precipitation efficiencies, precipitation rates, and rain totals. *Frontal* events were the most frequent storm type which occurred all throughout the warm season, but clearly peaked in June. *Mesohigh* events were the least frequent system which occurred mainly during the

late warm season. Both the mean latitude of initiation and mean precipitation efficiency were similar for *mesohigh* and *frontal* MCCs. Although *mesohigh* systems had slightly higher precipitation rates, *frontal* MCCs were substantially larger, longer-lived systems which produced higher amounts of precipitation.

6.2 Precipitation Efficiency By Year

There was no significant difference in mean precipitation efficiency between 1982, 1983, and 1993. However, 1993 MCCs had a higher mean duration and precipitation total which likely contributed to the anomalous wet period during that time. The years 1983 and 1993 had similar storm frequencies and precipitation efficiencies in the central United States and yet the former is remembered as a drought year, while the latter a flood year. If MCCs with higher precipitation efficiencies occur over a broad geographic region (e.g. central United States), the chance of producing anything other than a localized flash flood is less than if the same frequency were to occur over a much smaller region (e.g., central-northern Plains). Such was the case between 1983 and 1993.

MCCs were widely scattered between Texas and Minnesota and from Tennessee to Nebraska during 1983. During 1993, MCCs repeatedly occurred over the eastern half of South Dakota and Nebraska, western half of Iowa, southeast Minnesota, and northwest Missouri. In other words, MCC precipitation likely contributed to the anomalously wet period during 1993 due to reoccurring heavy rainfall episodes (i.e., Series of Convective - Complexes (SCCs)) (Kane 1985) over the same general area. This resulted in reoccurring moisture pooling which acted to increase the precipitation total and precipitation rate. Based on the results in this study, the lower mean efficiency during 1993 may be

attributed to the significantly more northerly displaced mean latitude of initiation during May (compared to 1983).

MCC precipitation efficiency is dependent on the synoptic patterns in which the MCC develops, and the latitude of its occurrence. But ultimately, based on this research, MCC precipitation efficiency is most significantly dependent upon the time of year. The time of year is the underlying factor that affects where MCCs will generally occur, what dynamics will be involved in its occurrence, and thus, how efficient the storm will be at producing precipitation.

6.3 Further Research

Newton (1966) suggested that higher precipitation efficiencies could be expected from larger storms due to longer life-cycles (in concurrence with McAnelly and Cotton 1989) accompanied by a higher water vapor mass flux, upper-level divergence at lower pressures with smaller mixing ratios, and less entrainment leading to minimal evaporative loss near cloud edges. The results presented in this study are particularly low (mean MCC precipitation efficiency = 4%) compared to previous precipitation efficiency research (Table 6.3.1). Specifically, Allen's (2002) study of MCS precipitation efficiency found results nearly eight times that of this research (4% vs. 25%). In Allen's (2002) study, MCS precipitation was outlined from radar mosaics across a numbered grid template. A likely reason for lower than average efficiencies found in this study was due to the spatial averaging of precipitation totals beneath the -32°C anvil cloud shield. In this case, areas of heavier precipitation are likely underestimated and precipitation efficiency is lowered.

Table 6.3.1 A comparison of average precipitation efficiencies for various types of storms (e.g., air-mass thunderstorms, squall lines, etc.).

Average Precipitation Efficiency for Various Storm Types		
Author	**Storm Type**	**PE**
Braham (1952)	Air-Mass Thunderstorm	11%
Newton (1966)	Squall Line	50%
Auer and Marwitz (1968)	8 Hailstorms	21-20%
Foote and Fankhauser (1973)	1 Hailstorm	15%
Fankhauser (1988)	7 Mature-Phase Thunderstorms	19-47%
Sellers (1965)	Mean 30-40°N	19%
Sellers (1965)	Mean 40-50°N	15%
Allen (2002)	Mesoscale Convective System (MCSs)	25 %
This Study	Mesoscale Convective Complexes (MCCs)	4%

McAnelly and Cotton (1989) and Kane et al. (1987) found that the heaviest precipitation produced by MCCs is generally found on the right flank and particularly, the southeast quadrant of the anvil cloud shield relative to the storm's motion. By spatial averaging MCC precipitation beneath the cloud shield, it is likely that average precipitation totals are decreased substantially. To better compare MCC precipitation efficiency with other published work, future research may account for those areas only receiving precipitation.

Additional research may also examine MCC precipitation efficiency by flank and quadrant. However, although this study reveals below average efficiencies, the results are still reflective of the spatial and temporal efficiency patterns.

This study only considers three factors in which MCC precipitation efficiency is dependent on: time, space, and atmospheric dynamics. However, the most significant factor, the time of year, only explains nearly 10% of the variance in MCC precipitation efficiency. This indicates that other factors (e.g., environmental factors –wind shear, sub-cloud base moisture, evapotranspiration, convective inhibition, cloud base mixing ratio, sea surface temperatures in the Gulf of Mexico and moisture transfer, and the location of the Bermuda High) may play a larger roll in determining MCC precipitation efficiency.

Additional research on MCC precipitation efficiency should include a larger dataset for more reliable statistical analyses. The comparison of the difference of means between each MCC characteristic was not employed as a causal analysis. Therefore, correlations between MCC precipitation efficiency, and space and time were interpreted based on the independent t-test results. Based on the interpretation of the various differences of means, a linear regression analysis was used to determine which variable had a greater influence on MCC precipitation efficiency. Since there is strong evidence of covariance among latitude and the time of year, additional statistical support should include colinearity diagnostics to determine how strong the correlation is between the two independent variables. Finally, this study used a low precipitable water grid resolution. Higher resolution precipitable water data may be retrieved by initializing the water vapor fields within a mesoscale model (e.g., MM5).

The Mesoscale Convective Complex is an important rain-producing event within the meteorological and agricultural communities, as well as the general public. MCCs often produce the number one weather-related fatalities –flash flooding (Doswell 1996). MCCs also produce substantial amounts of precipitation required during the wheat and corn-growing season (Kane et al. 1987). Understanding MCC precipitation efficiency can further enhance our knowledge of how these large rain-producing events behave, and may be beneficial for those affected by MCC occurrences.

REFERENCES

Allen, S. N., (2002): The prediction of warm-season mesoscale convective system precipitation efficiency based on *GOES* sounding parameters. M. S. thesis, University of Missouri-Columbia, 43pp.

Anderson, C. J., and R. W. Arritt, 1998: Mesoscale convective complexes and persistent elongated convective systems over the United States during 1992 and 1993. *Mon. Wea. Rev.*, **126**, 578–599.

_____, and _____, 2001: Mesoscale convective systems over the United States during the 1997-1998 El Niño. *Mon. Wea. Rev.*, **129**, 2443-2457.

Ashley, W.S., T.L. Mote, P.G. Dixon, S.L. Trotter, J.D. Durkee, E.J. Powell, and A.J. Grundstein, 2003: Effects of Mesoscale Convective Complex Rainfall on the Distribution of Precipitation in the United States. *Mon. Wea. Rev.*, in press.

Auer, A. H., and J. D. Marwitz, 1968: Estimates of air and moisture flux into hailstorms on the High Plains. *J. Appl. Met*., **7**, 196-198.

Augustine, J. A., and K. W. Howard, 1988: Mesoscale convective complexes over the United States during 1985. *Mon. Wea. Rev.*, **116**, 685-701.

_____, and _____, 1991: Mesoscale convective complexes over the United States during 1986 and 1987. *Mon. Wea. Rev.,* **119**, 1575-1589.

Braham, R. R., 1952: The water and energy budgets of the thunderstorm and their relation to thunderstorm development. *J. Met*., **9**, 227-242.

Brooks, H. E., and D. J. Stensrud, 2000: Climatology of heavy rain events in United States from hourly precipitation observations. *Mon. Wea. Rev.*, **128**, 1194-1201.

Collander, R. S., and E. I. Tollerud, 1993: Characteristics of extreme rainfall in mesoscale convective complexes: a phenomenological study. Preprints, *13th Conference on Weather Analysis and Forecasting*, August 2-6, 1993: Vienna, Virginia, 393-396.

Corfidi, Stephen F., 1994: On the movement of mid-latitude mesoscale convective complexes. M.S. Thesis, The Pennsylvania State University, 123 pp.

Doswell, C. A., H. E. Brooks, and R. A. Maddox, 1996: Flash flood forecasting: An Ingredients-based methodology. *Wea. Forecasting*, **11**, 560-581.

Fankhauser, J. C., 1988: Estimates of thunderstorm precipitation efficiency from field measurements in CCOPE. *Mon. Wea. Rev*., **116**, 663-684.

Foote, G. B., and J. C. Fankhauser, 1973: Airflow and moisture budget beneath a northeast Colorado hailstorm. *J. Appl. Met*., **12**, 1330-1353.

Fritsch, J. M., R. J. Kane, and C. R. Chelius, 1986: The contribution of mesoscale convective weather systems to the warm-season precipitation in the United States. *J. Appl. Meteor.*, **25**, 1333-1345.

Geerts, B., 1998: Mesoscale convective systems in the Southeast United States during 1994-1995: A survey. *Wea. Forecasting*, **13**, 860-869.

Groisman, P. Y., and D. R. Legates, 1994: The accuracy of United States precipitation data. *Bull. Amer. Meteor. Soc*., **75**, 215-227.

Guttman, N. B., and R. G. Quayle, 1996: A historical perspective of U.S. climate divisions. *Bull. Amer. Met. Soc.* **77**, 293-303.

Hammer, G., and P. Steurer, 2000: Data documentation for hourly precipitation data TD-3240. National Climatic Data Center, Asheville, NC. [Available online ftp://ftp.ncdc.noaa.gov/pub/data/documentlibrary/tddoc/td3240.doc]

Kane, R. J., 1985: The temporal and spatial characteristics of precipitation from mesoscale convective weather systems. M.S. thesis, The Pennsylvania State University, 152 pp.

_____, C. R. Chelius, and J. M. Fritsch, 1987: Precipitation characteristics of mesoscale convective weather systems. *J. Appl. Meteor.*, **26**, 1345–1357.

Kunkel, K. E., S. A. Chagnon, and J. R. Angel, 1994: Climatic aspects of the 1993 upper Mississippi River basin flood. *Bull. Amer. Meteor. Soc.*, **75**, 811-822.

Ludlum, D. M., 1983: Weatherwatch –July 1983. *Weatherwise*, **36**, 262-269.

Maddox, R. A., 1979: A methodology for forecasting heavy convective precipitation and flash flooding. *Nat. Wea. Digest*, **4:4**.

_____, 1980: Mesoscale convective complexes. *Bull. Amer. Meteor. Soc.*, **61**, 1374-1387.

_____, D. M. Rodgers, and K. W. Howard, 1982: Mesoscale convective complexes over the United States during 1981 – Annual summary. *Mon. Wea. Rev.*, **110**, 1501-1514.

Marwitz, J. D., 1972: Precipitation efficiency of thunderstorms on the High Plains. *J. Res. Atmos*., **6**, 367-370.

McAnelly, R. L., W. R. Cotton, 1989: The precipitation life cycle of mesoscale convective complexes over the central United States. *Mon. Wea. Rev.*, **117**, 784–808.

Merritt, J. H., and J. M. Fritsch, 1984: On the movement of the heavy precipitation areas of mid-latitude mesoscale convective complexes. Preprints, *10th Conf. Weather Forecasting and Analysis,* AMS, Tampa, FL, 529, 536.

NOAA-CIRES Climate Diagnostics Center, 2003: NCEP Reanalysis Data, Boulder, CO., [Available online http://www.cdc.noaa.gov/]

Newton, C. W., 1966: Circulations in large sheared cumulonimbus. *Tellus*, **18**, 699-712.

Rodgers, D. M., K. W. Howard, and E. C. Johnston, 1983: Mesoscale convective complexes over the United States during 1982. *Mon. Wea. Rev.*, **111**, 2363-2369.

_____, M. J. Magnano, and J. H. Arns, 1985: Mesoscale convective complexes over the United States during 1983. *Mon. Wea. Rev.*, **113**, 888-901.

Sellers, W. D., 1965: *Physical Climatology*. The University of Chicago Press, Chicago, IL, 272pp.

Tollerud, E. I., and D. M. Rodgers, 1991: The seasonal and diurnal cycle of mesoscale convection and precipitation in the central United States: Interpreting a 10-year satellite-based climatology of mesoscale convective complexes. Preprints, *7th Conf. on Applied Meteorology*, Salt Lake City, Utah.

Tollerud, E. I., and R. S. Collander, 1993: Mesoscale convective systems and extreme rainfall in the central United States. *Extreme Hydrological Events: Precipitation, Floods and Droughts, Int. Assoc. Hydro. Sci. Publ. No. 213*, 11-19.

Tollerud, E. I., D. Rodgers, and K. Brown, 1987: Seasonal, diurnal, and geographic variations in the characteristics of heavy-rain-producing mesoscale convective complexes: A synthesis of eight years of MCC summaries. Preprints, *11th Conf. Weather Modification*. Edmonton, Alta., Canada, 143-146.

Wagner, A. J., 1983: Seasonal climate summary, the climate of summer 1982- A season with increasingly anomalous circulation over the equatorial Pacific Ocean. *Mon. Wea. Rev.,* **111**, 117-133.